DEVELOPMENT AND APPLICATIONS OF CARBOXYMETHYL TAMARIND KERNEL GUM BASED HYDROGELS

A THESIS

Submitted to the Delhi Technological University

For the award of the degree of

DOCTOR OF PHILOSOPHY

By

KHUSHBU

2K17/PhD/AC/13

DEPARTMENT OF APPLIED CHEMISTRY

DELHI TECHNOLOGICAL UNIVERSITY

DELHI- 110042 (INDIA)

September 2021

DELHI TECHNOLOGICAL UNIVERSITY

(*Formerly Delhi College of Engineering*)

Department of Applied Chemistry

Shahbad Daulatpur, Bawana Road Delhi- 110042, India

DECLARATION

This is to declare that the work presented in this thesis entitled of **"Development and Applications of Carboxymethyl Tamarind Kernel Gum based Hydrogels" is original and has been carried out by me for the degree of Doctor of Philosophy** under the supervision of **Dr. Sudhir Warkar**, **Professor**, Department of Applied Chemistry. This thesis is a contribution to my original research work. Wherever research contribution of others is involved, every effort has been made to clearly indicate the same. To the best of my Knowledge, this research work has not been submitted in part or full for the award of any degree or diploma in Delhi Technological University or in any other university/institution.

Date

KHUSHBU
Research Scholar
Reg. No. 2K17/PhD/AC/13

DELHI TECHNOLOGICAL UNIVERSITY

(***Formerly Delhi College of Engineering***)

Department of Applied Chemistry

Shahbad Daulatpur, Bawana Road Delhi- 110042, India

CERTIFICATE

This is to certify that the thesis entitled **"Development and Applications of Carboxymethyl Tamarind Kernel Gum based Hydrogels"** submitted to the Delhi Technological University, Delhi-110042, in fulfilment of the requirement for the award of the degree of **Doctor of Philosophy** by the candidate **Ms. KHUSHBU**, (Reg. No. 2K17/PhD/AC/13) under the supervision of **Dr. Sudhir Warkar**, **Professor**, Department of Applied Chemistry. It is further certified that the work embodied in this thesis has been neither partially nor fully submitted to any other university or institution for the award of any degree or diploma.

(Prof. Sudhir Warkar)
Supervisor
DRC Chairman
Head of the Department
Department of Applied Chemistry
Delhi Technological University, Delhi.

Research says that the most beautiful word to most people is the word "MOTHER".

नास्ति मातृसमा छाया नास्ति मातृसमा गतिः।
नास्ति मातृसमं त्राणं नास्ति मातृसमा प्रपा॥

There is no shade like a mother, no resort-like a mother, no security like a mother, no other ever-giving fountain of life!

Dedicated to

My beloved Mom

ॐ माँ ॐ

ACKNOWLEDGMENTS

"Creating a life that reflects your values and satisfies your soul is the real success."

It fills my heart with unspeakable joy to express my gratitude to everybody who contributed in the successful accomplishment of my Ph.D. thesis.

First and foremost, I desire to offer this endeavor to **GOD Almighty** for the determination showered upon me, tranquility of my mind, and great wellbeing to have been able to complete this research.

With profoundest gratitude and great humility, I extend my sincere respect, appreciation and honor to my supervisor **Professor Sudhir Warkar** for his valuable offering in molding the base of my research profession. His advice, encouragement, constructive criticism, and his truly scientific intuition enriched my growth as a student. Above all, i found him a great human being with kind and exemplary heart. I cannot be more thankful to him for being a blessing to me and constantly inspiring with his kindness and the way he maintains his dignity and integrity. I am indebted to him more than he knows. I feel myself extremely fortunate to have been trained and introduced into the fascinating world of hydrogels under his able guidance and giving me full freedom in every aspect one could ever think of. He has been there all the time motivating, encouraging and inspiring me. He is a person of gem and I feel blessed to have crossed paths with him.

It is my pleasure to express my deepest gratitude and heartfelt thanks to **Dr. Nandkishore Thombare** (Scientist, ICAR, Ranchi), for always being so gracious, helpful

and full of positive vibes. He was always available every time I ran into a trouble spot. He helped me throughout from resolving my research queries.

No words and no language are ever adequate to express my heartfelt admiration for my lovely family, **Mrs. Sheela Khatri** (Mother), **Mr. Balbir Singh** (Father), **Mr. Deepak Khatri** (Brother) who have been pillars of inspiration for my academic expedition and for their blessings and unconditional love, without which I would have failed to complete this work.

For efficaciously accomplishing a project, a healthy environment is a must.

- My sisters for life, Dr. Shivani Jain, Dr. Sarika Gupta and Dr. Neha Singh, for their distinct engrossment in me at each phase of my Ph.D. Their genuine love, motherly care, and enlightenment showed me always the best path to follow.
- My friends for life, Ms. Deeksha Rana, Ms. Lalita Bisht, Ms. Divya Vashitha, Ms. Asha Goyal, Ms. Upasana Swami, for their kind love and affection which always made me feel special and kept me going in adverse times.
- My colleagues and especially lab-mates of Delhi Technological University for their support, inspiring discussions and for fun, we had during the course of Ph.D.
- My deepest thanks to **Mr. Mange Ram Mangyan and Mr. Lakhan Kumar** for their generous help whenever needed and for being such good well wishers and motivators all the time.
- I thank all the non-teaching (special mention to Mr. Raju) and official staff of the Department of Applied Chemistry, DTU, for their obligatory help whenever needed.
- I must also thank ICAR-NBSS and ICAR-SS&AC, Indian Agricultural Research Institute, Delhi, special mention to Mr. Kuldeep Singh and Mr. Gowardhan for providing instrumentation facilities (AAS, UV-VIS spectrophotometer, Pressure

Plate Apparatus), and the instrumentation facilities at DTU for FTIR and TGA analysis.

- I want to offer my gratitude to Dr. R.L. Ray, Head of R&D, Hindustan Gums Pvt. Ltd. for always providing me with CMTKG.
- I am grateful to Prof. Yogesh Singh, Vice Chancellor, Delhi Technological University, for giving me this opportunity to conduct my research work.
- I also want to thank all those whom I have failed to mention specifically and personally, but they have helped me in various ways during this work.

Thank you so much!!!!!

(KHUSHBU)

ABSTRACT

The solely goal is to help Indian farmers to grow more food with less water. Keeping in perspective the fact that there's a need of an irrigation system that is reliable and requires less investment, low water supply, and low maintenance. Henceforth, the objective has been kept to synthesize a biodegradable biopolymer based superabsorbent hydrogel that can sustain the crops for longer period of time even with lesser irrigation, supporting the cause of water conservation along with acting as a soil conditioner by being the carrier vehicle of micro-nutrients.

The novel superabsorbent hydrogels were fabricated by interpenetrating carboxymethyl tamarind kernel gum with sodium-acrylate. The synthesis of SAH was verified by characterization using Fourier-transform infrared spectroscopy, thermo-gravimetric analysis, scanning electron microscopy and swelling studies under various solutions. The hydrogel formed was found out to be bio-degradable (soil burial biodegradation test). Maximum water holding capacity, bulk density, porosity and water retention capacity of soil were evaluated to see the effects on soil by the hydrogel treatment. The synthesized SAH was then tested to display promising potential as soil conditioner for agricultural applications.

The novel Boron and Zinc micronutrients loaded separate superabsorbent hydrogels were synthesized via *in-situ* mechanism having carboxymethyl tamarind kernel gum as its principle component. The synthesis was established by TGA examination, SEM micrographs studies, and FTIR analysis which further also confirmed the interaction between micronutrients and tri-dimensional network of superabsorbent hydrogels to be entirely physical. The influence of various solvents, such as standard saline solution, different pH solutions (4, 9, 12), and distilled water on the swelling index of both set of hydrogels were examined. These micronutrients loaded hydrogels were also examined for the agricultural application to assess the release of the micronutrients. It was established by studying and calculating the release behavior pattern along with the release kinetics of BSH in water, and as well in soil. The half-life and time period for release of 95 % and 99 % of micronutrients were calculated as per the Olson's single exponential model, to predict the pattern of boron and zinc release from developed superabsorbent hydrogel formulation.

THESIS ORGANIZATION

The thesis has been divided into six chapters. The background of the work as well as the relevant literature survey including several reported applications and forms for the Carboxymethyl Tamarind Kernel Gum is summarized in ***Chapter 1***. The synthesis, optimization, characterization, and swelling studies of superabsorbent hydrogel developed using Carboxymethyl Tamarind Kernel Gum along with sodium acrylate by free radical mechanism has been reported in ***Chapter 2***. The ***Chapter 3*** deals with the evaluation of the synthesized superabsorbent hydrogel for the agricultural application as a potent soil conditioner. The ***Chapter 4*** describes the synthesis of boron micronutrient loaded superabsorbent hydrogel and to further examine for controlled release and release kinetics studies in both cases of water and the soil. Another CMTKG based superabsorbent hydrogel was prepared and to utilize it as a zinc carrier along with water and soil studies is described in ***Chapter 5***. The conclusions and the future scope of the work have been presented in the ***Chapter 6*** of the thesis.

LIST OF PUBLICATIONS AND CONFERENCES

Journal Articles:

1. **Khushbu**, Sudhir G. Warkar and Anil Kumar, Synthesis and Assessment of Carboxymethyl Tamarind Kernel Gum based Novel Superabsorbent Hydrogels for Agricultural Applications. *Polymer.* **2019**, 182**,** 121823.
2. **Khushbu** and Sudhir G. Warkar, Potential Applications and Various Aspects of Polyfunctional Macromolecule- Carboxymethyl Tamarind Kernel Gum. *European Polymer Journal.* **2020**, 140**,** 110042.
3. **Khushbu**, Sudhir G. Warkar and Nandkishore Thombare, Controlled Release and Release Kinetics Studies of Boron through the Functional Formulation of Superabsorbent Hydrogels. *Polymer Bulletin*. **2021**.
4. **Khushbu**, Sudhir G. Warkar and Nandkishore Thombare, Zinc Micronutrient loaded Superabsorbent Hydrogels: Controlled Release and Release Kinetics Studies for Agricultural Applications. Colliod and Polymer Science. **2021**.
5. Divya Balodhi, **Khushbu**, Sudhir G. Warkar, Archana Rani, and Rajinder K. Gupta, Novel Natural Gums Based Hydrogels. Indian Journal of Chemical Technology. **2021**.
6. **Khushbu** and Sudhir G. Warkar, Carboxymethyl Tamarind Kernel Gum based Drug Delivery Excipients: A Review. (Accepted).
7. Sudhir G. Warkar, **Khushbu** and Anil Kumar, Adsorption of Basic Dye by Poly(Acrylamide)/Carboxymethyl Guar Gum Hydrogel for Wastewater Treatment: Kinetics and Isotherm Studies. (Under review).
8. Divya Balodhi, **Khushbu**, Sudhir G. Warkar, Archana Rani, and Rajinder K. Gupta, A Review on Biopolymer Based Hydrogels. (Under review).

9. **Khushbu**, Ashank Upadhaya and Sudhir G. Warkar, Synthesis and Study of Novel Carboxymethyl Guar Gum/ Polyacrylate Polymeric Structured Hydrogel For Agriculture Application. *Springer.* Book Chapter, 2020.

Publications in conference/workshop proceeding:

1. **Khushbu** and Sudhir G. Warkar, Synthesis and study of novel biodegradable biopolymer-polysaccharide semi interpenetrating polymeric structured hydrogel application in agriculture. *3rd International Conference on Advanced Production and Industrial Engineering Research (ICAPIE'18) October 5th-6th, 2018, 5 Star Hotel, Delhi, India*. (Oral Presentation)
2. **Khushbu** and Sudhir G. Warkar, Biopolymer based hydrogels for soil conditioning .*Indian Analytic Congress (IAC-2019) December 12th -14th*, *2019*, Amity University, Noida, India. (Poster Presentation)
3. Participated in the *International Conference on Atomic, Molecular, Optical and Nano Physics with Applications* (*CAMNP-2019*) Organized by Delhi Technological University, Delhi, India, *December 18th -20th*, *2019*.
4. **Khushbu** and Sudhir G. Warkar, Application of novel biodegradable biopolymer based hydrogel in the sphere of agriculture. *4th International Conference on Advanced Production and Industrial Engineering Research (ICAPIE'19) December 5th-6th, 2019, Delhi Polytechnique College, Delhi, India*. (Oral Presentation)
5. **Khushbu** and Sudhir G. Warkar, CMTKG based drug delivery carrier. *5th International Conference on Advanced Production and Industrial Engineering Research (ICAPIE'21) June 18th-19th, 2021, WEBINAR, India*. (Oral Presentation)

INDEX

LIST OF FIGURES

LIST OF TABLES

LIST OF ABBREVIATIONS

CMTKG	Carboxymethyl Tamarind Kernel Gum
KPS	Potassium per sulphate
MBA	N,N'-methylenebis(acrylamide)
SA	Sodium Acrylate
PSA	Poly (Sodium Acrylate)
SAH	Superabsorbent Hydrogel
SEM	Scanning Electron Microscopy
FTIR	Fourier Transform Infrared
TGA	Thermogravimetric Analysis
BSH	Boron loaded Superabsorbent Hydrogel
ZSAH	Zinc loaded Super Absorbent Hydrogel
AAS	Atomic Absorption Spectrophotometer
BA	Boric acid
ZC	Zinc Chloride
SH	Superabsorbent Hydrogel

Chapter 1

INTRODUCTION AND LITERATURE REVIEW

1.1 Introduction

One of the most important inputs in agriculture is water. In rain fed agriculture, the sustainability of crop production majorly depends on availability of water. Even if a drought tolerant trait is introduced, water is not accessible to crops. Irrigation through dams, wells and other ground water sources is still not possible in many areas due to scarcity of groundwater and cost effectiveness.

Most of the 852 million poor people in the world live in the developing countries of Asia and Africa, more so in drylands/rainfed areas. These rainfed areas are hotbeds of poverty, malnutrition, water scarcity, severe land degradation and poor physical and social infrastructure. Rainfed agriculture constitutes 80% of global agriculture and hence, plays a crucial role in achieving food security, increasing water scarcity and climate change threaten to affect rainfed areas and their peoples owing to their vulnerability to drought during the crop-growing season [1]. Globally, only half of the nutrients that crops take from the soil are replaced. This depletion of soil nutrients often leads to fertility levels that limit production and severely reduce water productivity. Shorter fallow periods do not compensate for losses in soil organic matter and nutrients, leading to the deficiency of soil nutrients. Recent characterization of 4000 farmers' fields in different states across India revealed a widespread (80–100% fields) deficiency of zinc and boron, causing productivity declines and affecting human nutrition, acidification and salinization [2].

Rain is a free and first source of water but rainfall itself is becoming more and more unpredictable. This variability greatly affects soil which imposes crop production risks, especially on rain fed subsistence cultivation systems on marginal land. Since we know that world faces water and food

crises which means a growing population means more food to feed. Climate change is causing massive droughts and is expected to get much worse. Top soil erosion makes it harder to grow food and food scarcity leads to high prices which leads to social unrest [3]. To enhance the water utility competency in agriculture, a lot of methods are being implemented. There are primarily four ways through which irrigation have been done over the years namely, surface, sprinkler, drip, and subsurface irrigation. Surface irrigation consists of a method in which water is distributed over the surface of the soil by virtue of gravity. The irrigation water is introduced into level or graded furrows or basins, using siphons, gated pipe, or turnout structures, and is allowed to advance across the field. Surface irrigation is best suited to flat land slopes and medium to fine-textured soil types which promote the lateral spread of water down the furrowed row or across the basin. In Sprinkler irrigation method water is sprinkled, or sprayed in the air in rain like drops. The spray and sprinkling devices can be permanently set in place (solid set), temporarily set and then moved after a given amount of water has been applied (portable set or intermittent mechanical move), or they can be mounted on booms and pipelines that continuously travel across the land surface (wheel roll, linear move, center pivot). Drip/trickle irrigation systems are methods of micro-irrigation where water is supplied through emitters to the surface of the soil as small streams or drops. The release rate of the emitters is low so this irrigation method can be used on all soil types. Subsurface irrigation consists of methods whereby irrigation water is supplied below the surface soil. The specific type of irrigation method varies depending on the depth of the water table. When the water table is well below the surface, drip or trickle irrigation emission devices can be buried below the soil surface (usually within the plant root zone).

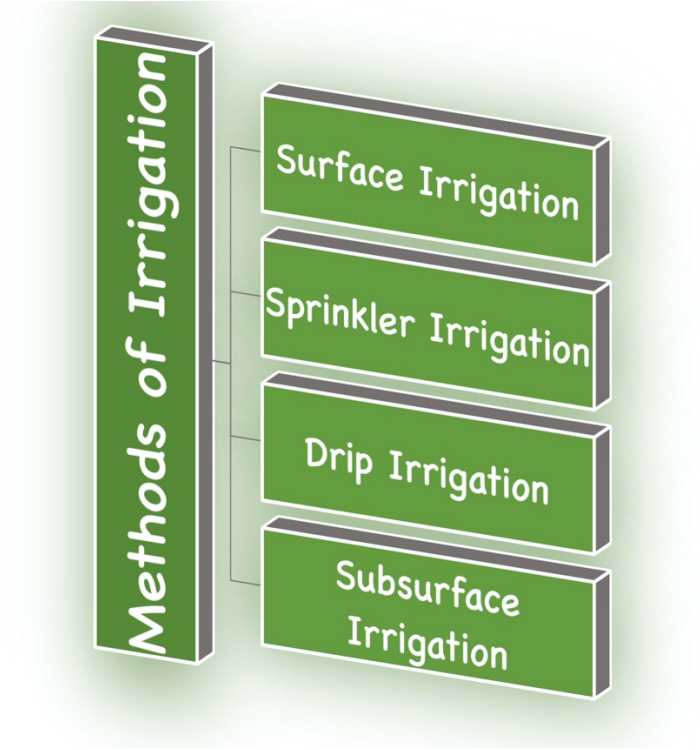

Figure 1.1 Different methods of irrigation

Proof from water balance examinations on farmers' fields show that just a little part, for the most part under 30% of rainfall is utilized as profitable green water stream supporting plant development [4]. Fig. 1.2 explains the status of rainfall water in the farming system wherein most of the water seemed to have got wasted as drainage water, non-productive evaporation and as surface run-off. For an enhanced production in rainfed/dryland ecosystems, a large fraction of the precipitation ought to be stored in the soil and the stored water must be utilized all the more proficiently to its maximum capacity. Hence, there is need of a scientific system where the rainfall water could be made trapped for the crops for the time even when rainfall won't happen.

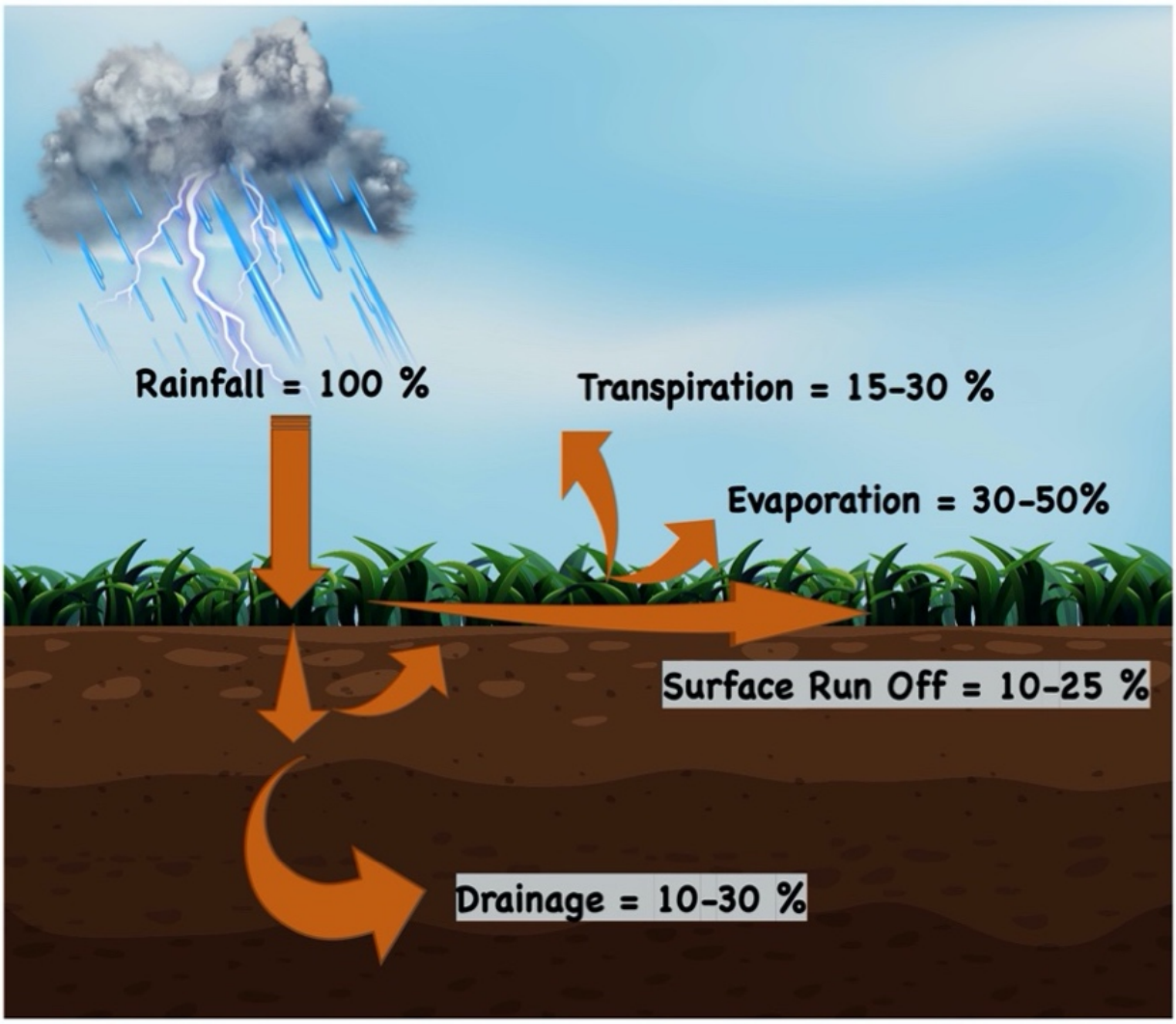

Figure 1.2 Overview of rainfall status in farming system in hot weathers [4]

The major need of the hour for rainfed agriculture for food security is that the vast untapped potential of rainfed agriculture needs to be tapped as the current farmers' crop yields are lower by two- to five fold than the potential, based on the clear documented evidence [5]. There is a critical need to build up a new paradigm for soil and water management. We have to have a converging

approach dependent on uniting all the important aspects of conserving natural resource, their effective utilization, good production, and income-enhancement avenues.

Hydrogels are being explored for soil conditioning and water retention in agriculture because of its special properties[6,7]. All this led to hydrogels as they enhance the growth of the plant, harmless to flora and fauna and have good water intake and retain capacity.

1.1.1 Hydrogels

Technically, hydrogels are tridimensional cross-linked hydrophilic polymers which possess the ability to assimilate a substantial volume of waters or other fluids and can swell without being dissolved off. While more practically, they are superabsorbent material that can hold hundreds of times its weight in water [8]. Reason being for their special properties are the hydrophilic functional groups that are connected to the polymeric backbone whereas their insolubility springs up from cross-links between network trails. The hydrogels which can absorb water up to 95% of their initial completely dry weight are usually known to be superabsorbent hydrogels (SAH) [9,10].

Due to their remarkable hydrophilic properties, bio-compatibility and high swelling index, hydrogels have been used extensively in the field of drug delivery [11], wastewater treatment [12], bio-sensors [13], tissue engineering [14], agriculture [15] and cosmetics [16]. It is important to mention here about the very first hydrogel which was synthesized by Wichterle and Professor Lim of Prague (Czech Republic). This hydrogel was used for preparing contact lenses for eyes which was made up of poly-2-hydroxyethylmethacrylate with 40-50 % of swelling percentage, in the year of 1960 [17]. However, it took a decade in synthesizing the very first commercial superabsorbent hydrogel. It was synthesized by alkaline hydrolysis of starch grafted polyacrylonitrile in the year 1970 [18]. Moreover, this hydrogel couldn't succeed as a result of its high cost and poor mechanical

properties. The polymeric material utilized for hydrogel synthesis influences its biodegradability and hydrophilicity. Polyacrylates and acrylamides have been broadly utilized throughout the years for the fabrication of exceptionally hydrophilic hydrogels [19].

1.1.1.1 Classification of hydrogels

The hydrogels can conveniently be classified in many ways depending on their nature of swelling, origin, sources, physical properties, method of preparation, ionic charges, nature of cross-linking and rate of biodegradation [20]. The structural strength of hydrogels depends upon the nature of bonds, either chemical or physical, between the cross-linker and the biopolymers [21]. Fig. 1.3 systematically covers all the possible grouping of hydrogels in which hydrogels are segregated into following basis and groups:

- Source: natural, synthetic and hybrid
- Degradability: degradable or non-degradable
- Cross-linking: chemical or physical cross-linking
- Preparation: homo polymeric, copolymeric and interpenetrating network
- Response: chemically responsive (pH, glucose)
  biochemical responsive (enzymes, ligands)
  physically responsive (temperature, pressure, electric and magnetic field)
- Physical properties: smart or conventional hydrogels
- Ionic charge: neutral or ionic (anionic or cationic)

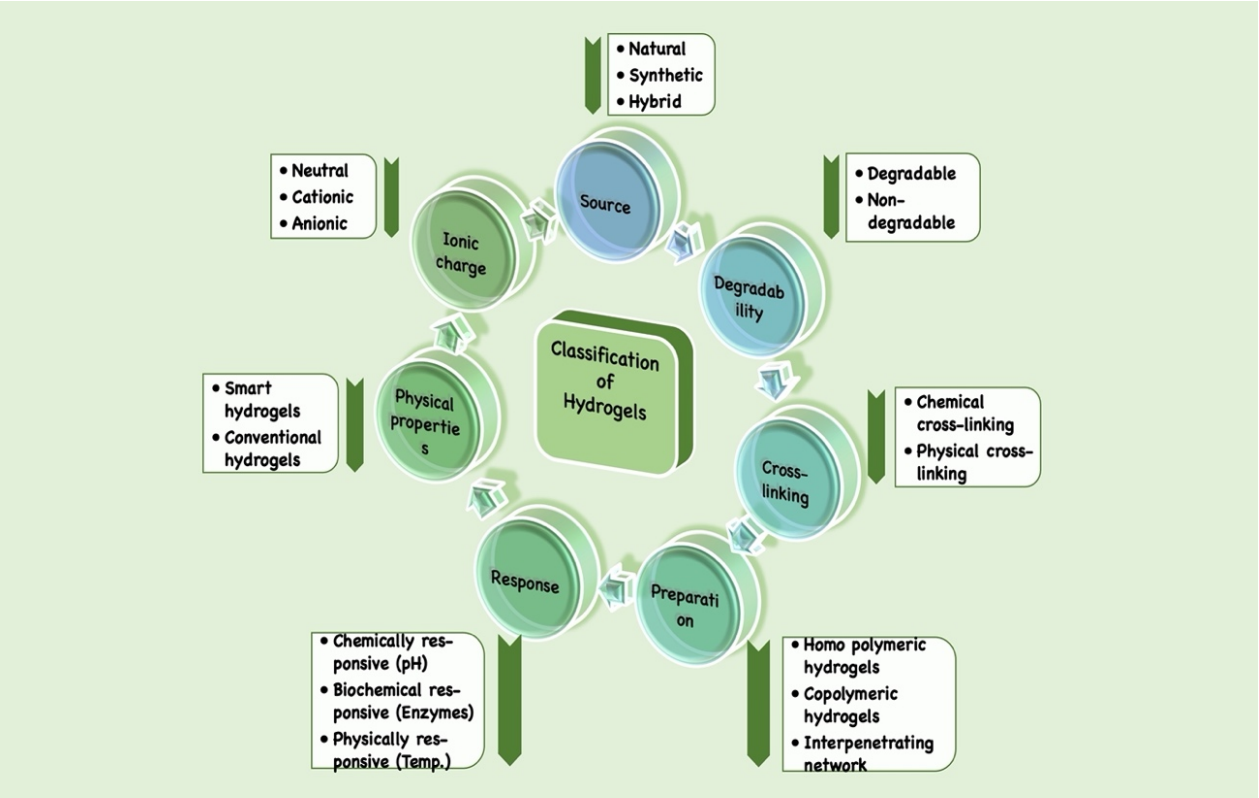

Figure 1.3 Classification of hydrogels on the basis of their properties

1.1.2 Agriculture

1.1.2.1 Hydrogels: Solution for present and future agriculture

Over the years, an upsurge has been observed in the studies of the utilization of biopolymer-based hydrogels in agriculture as they are financially and ecologically feasible options for conditioning of the soil in terms of providing water and various macro-micro nutrients [22]. Moreover, the bio-polymer based hydrogels are suitable for agricultural purposes because of the certain desirable properties for agriculture based hydrogels like they are non-toxic, widely available, stable in the soil and most importantly, they can be made into cost effective [23]. Also, the hydrogels are

susceptible to degradation by microbial , chemical and physical agents [24,25]. Nowadays, most of the commercial hydrogels are made up of synthetic polymers, thus non-degradable and considered as pollutant for the soil. Due to alarming attention towards the environmental protection, development of natural polymers and hence biopolymer based SAH has become deal of great interest because of their environmental and commercial advantages. Presently, a lot of natural polymers based SAH have been synthesized using biopolymers and their derivatives such as chitosan [26], starch [27], xanthan [28], cellulose [29] and guar gum etc. [30–34].

Many commercials superabsorbent hydrogels like Stockosorb™ (acrylamide cross-linked with potassium/sodium acylate), Aqualic™ (sodium acrylate cross-linked with acrylic acid), Luquasorb™ (potassium acrylate cross-linked with acrylic acid), and so forth are being utilized in agriculture these days [35]. Despite the fact that the synthetic polymer-based hydrogels are more famous because of their durability and high water retention limit, the utilization of bio/natural polymer-based hydrogels is prospering because of their non-toxicity and degradability factors [35].

Hydrogels are identified as one of the most potential candidate for trapping the rainfall water in the soil which will made available to crops in drought conditions as hydrogels have many advantages. Some of the many advantages are listed in the fig. 1.4 [36].

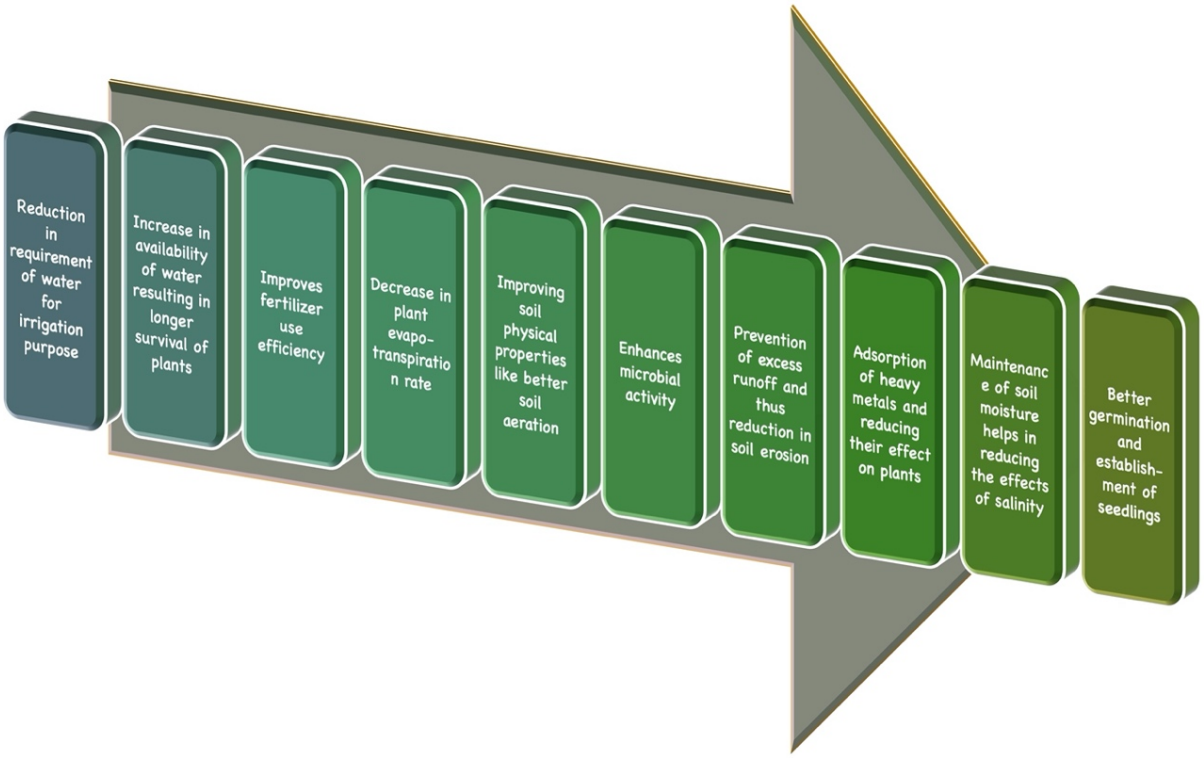

Figure 1.4 Advantages of hydrogel in agriculture

1.1.2.2 Soil conditioners

It helps to retain water in the soil by dispersing the absorbed water slowly, thus soil gets hydrated which capacitates the plant to sustain longer under water stress which consequently enhances the crop production. Henceforth, SAH can act as a personal underground reservoir which encapsulates all the water that evaporates and helps in crop production in cases of drought [37]. In short, it can supplement rainfall to supply crop water needs [30]. These substances can be called as artificial humus because of the presence of carboxylic groups and their hydrophilicity. In comparison to humus, SAH have a higher density of hydrophilic cation binding groups and contains non aromatic moieties. Since SAH are more pronounced per weight with respect to humus which consequently lowers down the chances of becoming hydrophobic, as humus does become the same in drought

conditions [38]. Consequently, along with water retention, the hydrogels also enhances the various physical and chemical properties of the soil such as density, permeability, soil structure, texture, water infiltration and porosity. They lessen irrigation need, decrease soil erosion, and upgrade micro-flora activity and aeration [39]. Hydrogels have been effectively used as soil conditioners in agricultural harvests for expanding water and supplement maintenance in sandy soils [40]. Fig. 1.5 tries to explain that how a hydrogel works in favor of plants/seeds.

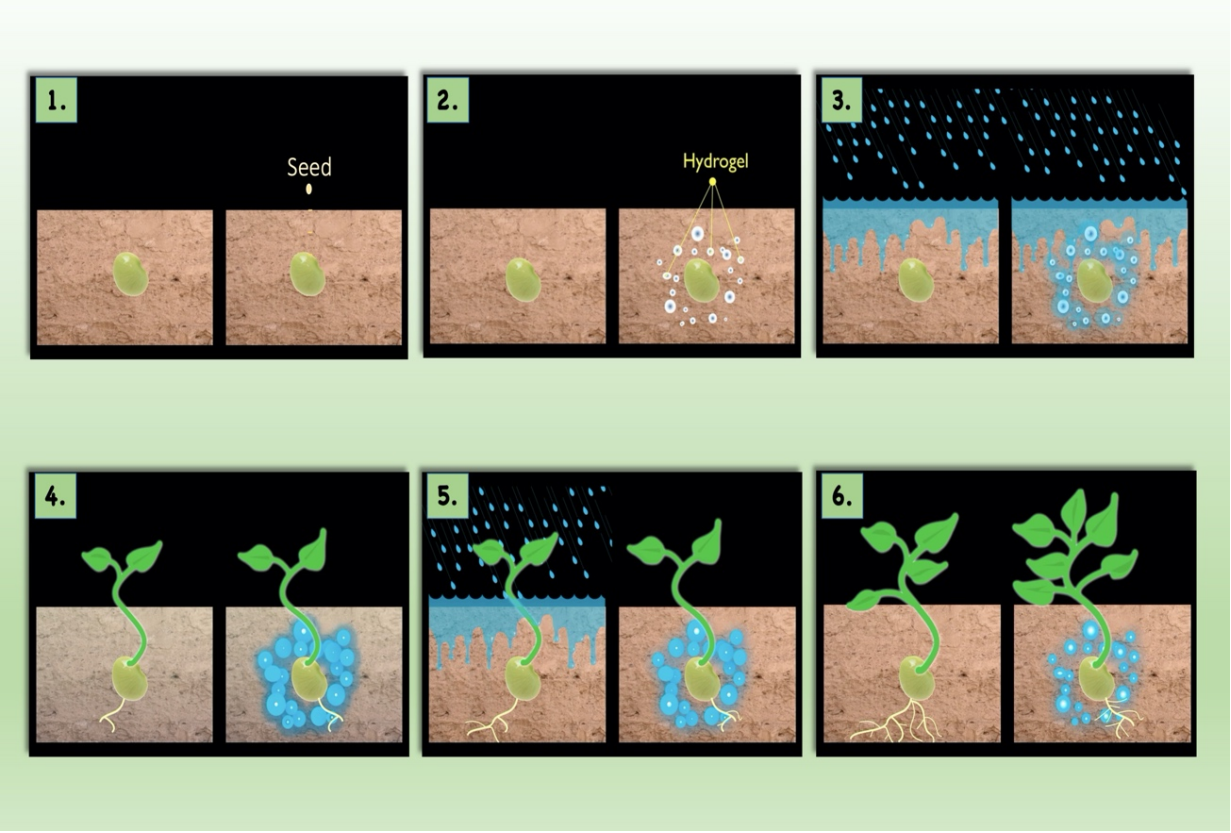

Figure 1.5 How do hydrogels work?!!

The hydrogel can go about as a recovery operator for light sandy soils and for substrates in aquaculture as it imparts different soil properties that are available in ordinary arable land. The ideal concentration of the use of hydrogel relies upon different factors, for example, age and nature

of the plant as well as soil properties and ecological conditions [41]. In general, 0.05 to 0.1% dry hydrogel is utilized with seeds during planting [42]. The hydrogel can also be utilized during transplantation in any case of forestry. The hydrogel can be applied over the roots of plants/trees when they are moved for transplantation to keep them away from drying. Hydrogels have been utilized in dry territories of China to develop soybean, sugar beet, rice, and so on. It was discovered that the hydrogels expanded the yield of soybean, sugar beet, and rice crops [43–45].

1.1.2.3 Micro-nutrients delivery

Plant micro-nutrients (Zinc (Zn), Boron (B), Copper (Cu), Chlorine (Cl), Iron (Fe), Manganese (Mn) and Molybdenum (Mo)) when applied to the soil are dependent upon different types of losses, for example, runoff, volatilization, leaching, and so on. Along these lines, just a bit, around 20-25 % of applied supplements are accessible to crops, and the loss of supplements in the runoff, chemical processes, leaching, and excess rain additionally brings about eutrophication of surface water bodies and contamination of ground-water. An elective methodology that has been latest examined includes the controlled release of micro-nutrients as well macro-nutrients from the fertilizer loaded hydrogels [46–51].

A controlled release system is planned for ensuring the reserve of active micro-nutrient for releasing it at a moderate controlled rate so as to maintain the concentration in the system at ideal levels for a broadened timeframe without influencing the efficiency. Controlled release utilization of agrochemicals is useful in conserving their concentration in the soil at an optimum level and furthermore lessens the runoff losses [52]. An assortment of biopolymers, for example, guar gum , chitin, cellulose, tragacanth gum, etc. have been utilized for the controlled release of nutrients as

they enhance the efficiency of nutrients by lowering their cost, environmental pollution and toxicity [53].

The loading of nutrients in a hydrogel can be in done by adopting two methodologies, viz. *in-situ* loading and post-synthesis loading. *In-situ* loading is done during the synthesis of hydrogel while in case of post-synthesis, loading is done once the synthesis of hydrogel gets completed. In the *in-situ* approach, incorporation of nutrient in to the hydrogel composition takes place during the synthesis process only and stays in the dried form prior adding to the soil. The release of nutrient gets activated once the hydrogel starts swelling under the influence of rain or irrigation water. The water present in the hydrogel dissolves the nutrient which gets delivered/released in the surrounding either by osmosis or diffusion (fig. 1.6).

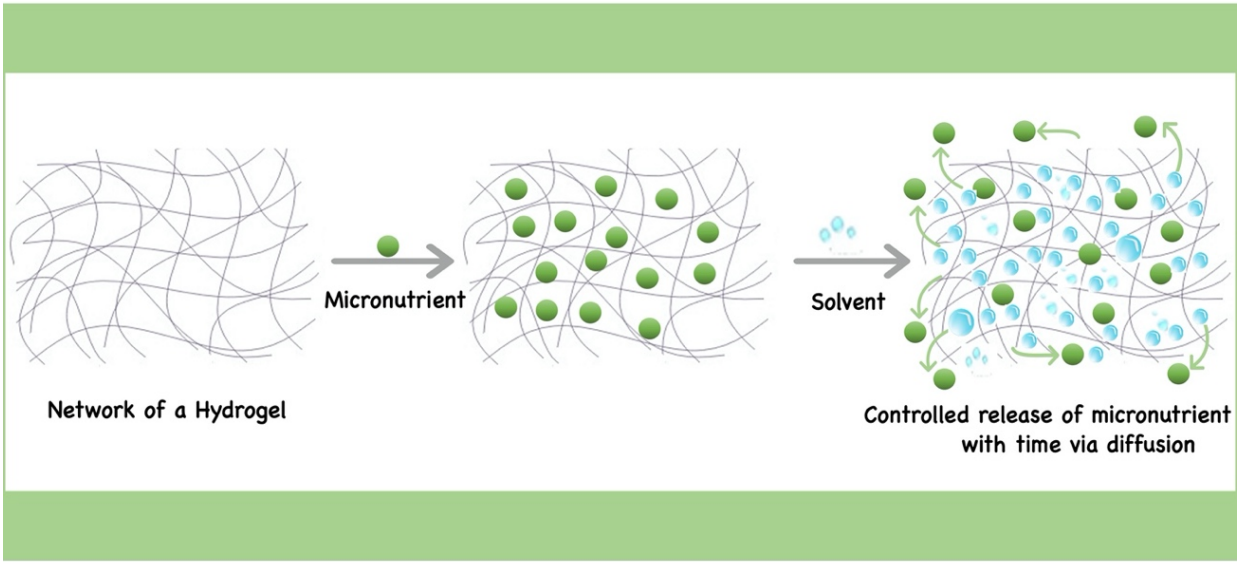

Figure 1.6 Entrapping of micronutrients and its controlled release via hydrogels

In case of post-synthesis loading, the hydrogel is first swelled up in a concentrated nutrient's solution wherein the nutrient gets diffused inside the swollen hydrogel matrix by the simple phenomenon of absorption. The adequacy of this approach relies on the chemical and physical affinity of nutrients for the polymeric system of hydrogel. However, the in situ methodology is considered far better than the post-synthesis loading approach as the former has higher loading efficiency with better controlled-release [54]. This way, the expense of application could also be reduced as more than one nutrient (each one of the nutrient having specific separate release rate and uses) can be easily loaded to a single hydrogel. The entire amount of nutrients present in the lattice isn't released and a bit of it stays as a reserve during drier periods. At the point when rain or irrigation water comes again in the contact of the hydrogel, the release mechanism gets activated again. Consequently, furnishing an elongated supply of nutrients with least leaching losses. Fig. 1.7 showcases the nutrient and water release through hydrogels and absorption of the same by the roots of a plant.

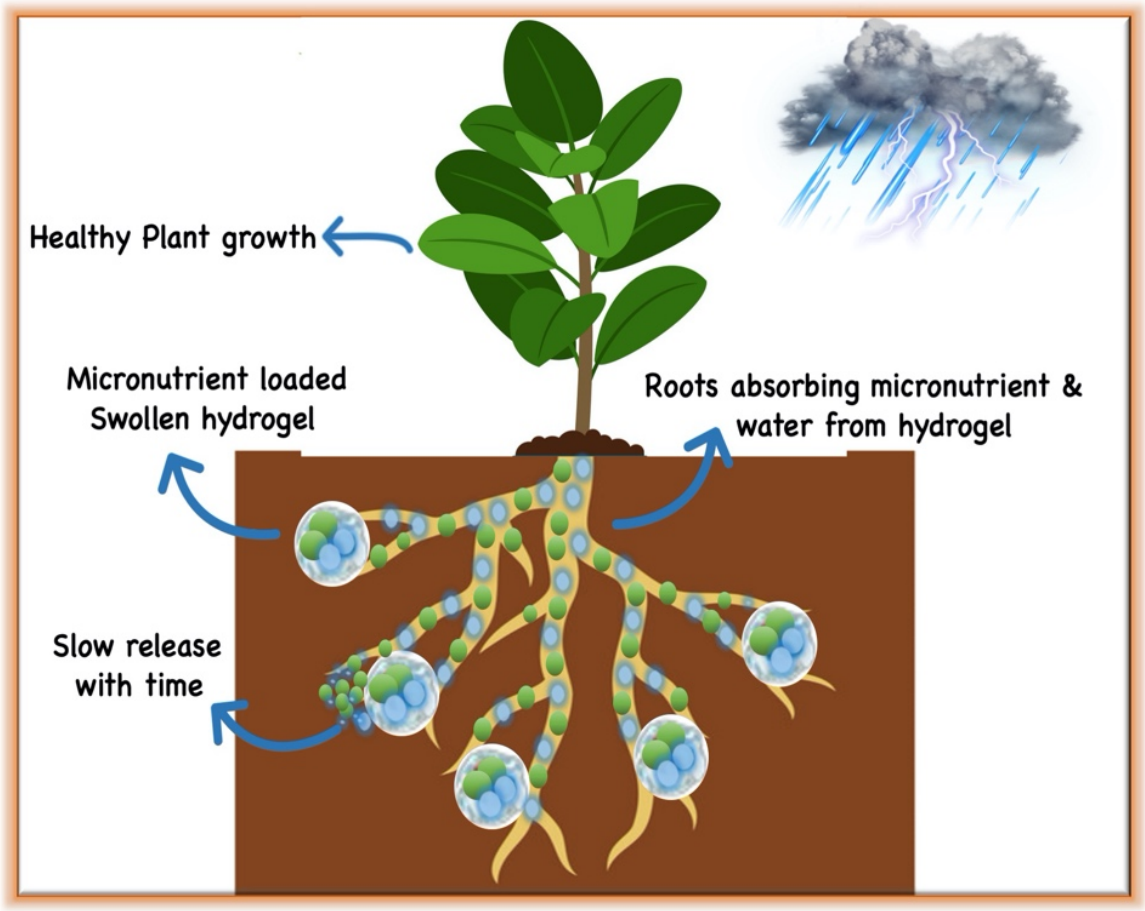

Figure 1.7 Micronutrient and water absorption by roots through hydrogels

1.2 Literature Review

1.2.1 Introduction

The generally known facts about polymers in respect to their broad area of applications and specific properties in the global market is enhancing day by day [55]. Over the last few decades, there has been a huge demand for natural polymers over synthetic polymers due to the alarming attention towards environmental protection. In recent years, polymers derived from plants have captivated

an impressive interest in the varied field of areas. Hence, natural polymers are being considered over synthetic polymers due to their non-toxicity, ease of availability, the flexibility of chemical modification, and degradability as compared to synthetic polymers with long synthesis times, environment-related issues and toxicity problems [56]. Natural polymers possess diversified applications because of the two major properties namely, biocompatibility and biodegradability [57]. Polysaccharides are the most copiously available natural polymers and more importantly, they are renewable, economical, hydrophilic, easily modifiable, and stable. Polysaccharides secluded from natural-sources are drawing in expanding consideration from pharmaceutical and food businesses, since some of them display some biological related activities, for an instance, antiviral, anticancer, immunostimulatory and anti-inflammatory activities. In contrast with synthetic based food and medications supplements, these bioactive polysaccharides from consumable materials are commonly more secure, more effective with negligible side-effects, and all the more promptly accessible and less expensive [58]. Among commonly used natural polymers are guar gum [33,59,60], chitosan [61], sodium alginate [62], xanthan gum [63], cellulose [64], to name a few.

The chemical modification of biopolymers has received significant attention in the last decade as this simultaneously maintains the natural polymers to their potential and imparts desirable properties on to them without influencing the basic architecture of the polymer backbone [65]. Carboxymethyl tamarind kernel gum (CMTKG) is one such fine example of chemical modification that comes from Tamarind kernel gum. It is composed of D-xylose, D-galactose, and D-glucose in the molar ratio of 1:2:3 [66]. This polysaccharide consists of carboxymethylated chain of β-D-(1→4) linked glucopyranosyl units (main chain) along with a side chain of having single xylopyranosyl unit which are further attached to every 2nd, 3rd and 4th D-glucopyranosyl unit via

α-D-(1→6) linkage whereas one xylopyranosyl unit is attached to one of the D-galactopyranosyl unit with a β-D-(1→2) linkage. Fig. 1.8 shows the chemical structure of CMTKG.

Tamarind kernel gum (TKG), one of the cheapest gum and a natural polysaccharide of food-grade, is extracted from the seeds of *Tamarindus Indica* L; a prevalent tree of South East Asia and Africa [67]. It is composed of xylose, galactose, and glucose in the molar ratio of 1:2:3 [66]. The seeds contain xyloglucans which are being used extensively as gelling agents and food thickeners [68]. Its major use has remained as a wet end additive in the paper industry which is also an alternative to galactomannas and starches. However, unpleasant odor, very fast biodegradability, low solubility in cold water, and dull color are few of the several drawbacks which TKG possesses [69]. Hence, this arises the need to modify TKG so as to alter and improve its pharmaceutical and physicochemical characteristics for better action and consequently broader application for CMTKG in addition to those of TKG by carboxymethylation of TKG [70]. Carboxymethylation of TKG disrupts the polysaccharide structure, hence revealing the network of hydration and imparting an anionic nature to the polysaccharide. This chemical modification results in lower biodegradability than TKG and thus enhancing the life shell, swell ability, mucoadhesivity, *in situ* gelation, broad pH tolerance, high drug loading capacity, hydrophilicity, stability and release kinetics. In addition to all the above stated properties, CMTKG also shows antibacterial properties like that of TKG. In fig. 1.9, special properties of CMTKG and their significance has been highlighted.

This literature review tried to include all the possible data published till date regarding the synthesis, mechanism, and different applications and forms of CMTKG. Fig. 1.10 covers all the aspect of hydrogels studied till date.

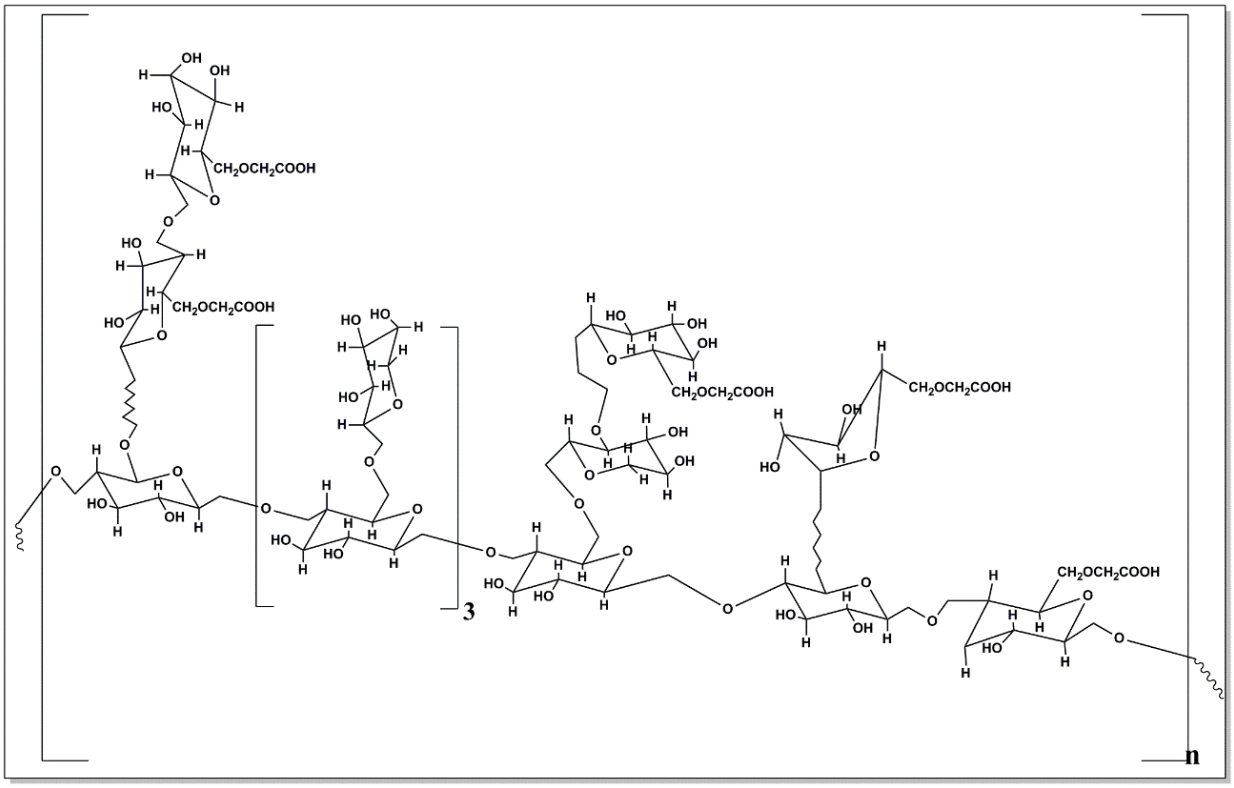

Figure 1.8 Structure of CMTKG [71]

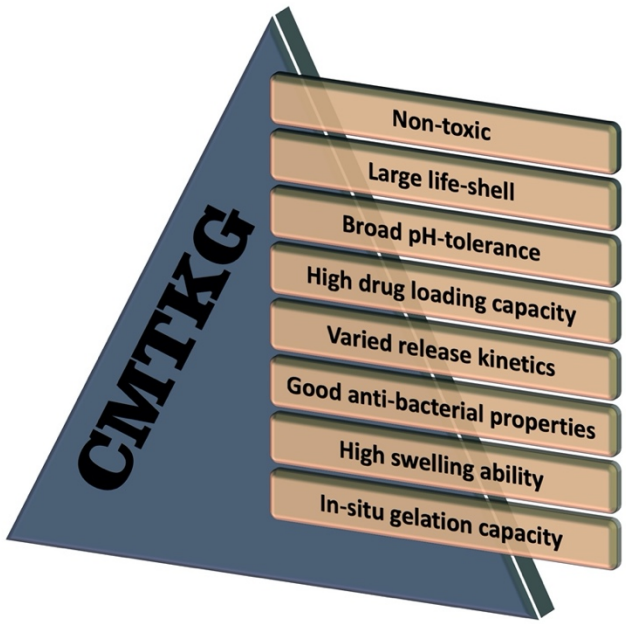

Figure 1.9 Highlights of CMTKG

Figure 1.10 Overview of the literature review

1.2.2 Synthesis and Mechanism

The synthesis or derivatization of CMTKG from TKG has been carried out by a single methodology which is also shown in fig.1.11. In brief, the carboxymethylation of TKG (0.05 mol) can be done by dispersing TKG in alkaline aqueous methanol (0.16 mol of NaOH) followed by the addition of monochloroacetic acid (MCA) (0.16 mol). The solution is then required to be kept in a hot water bath at 70˚C for 60 min. Filter the reaction product on a G-3 sintered glass crucible followed by dissolving the filtered product in water and neutralizing the same with dilute HCl (1:1 v/v). Precipitate it with ethanol and wash it further with aqueous methanol (H_2O:Methanol:: 20:80) followed by pure methanol. Dry the product, initially at room temperature, and finally drying at

vacuum oven maintained at 40˚C for 4h [69]. However, the degree of substitution of CMTKG can be determined by the titrimetric method [72].

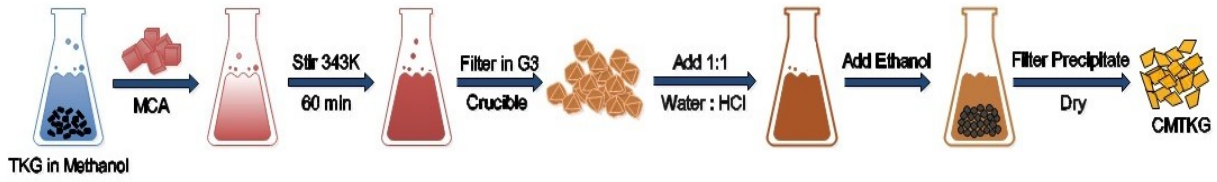

Figure 1.11 Schematic for the development of CMTKG via TKG

The mechanism for the carboxymethylation of TKG can be understood by a 2-step consecutive reaction (fig.1.12). The reaction starts with sodium hydroxide attacking the hydroxyl groups of TKG to give alkoxides groups. SN_2 reaction takes place to form carboxymethylation groups between TKG-alkoxide and MCA [69] (fig.1.12a).

$$TKG\text{-}OH + NaOH \rightarrow TKG\text{-}ONa + H_2O$$

$$TKG\text{-}ONa + ClCH_2COOH \rightarrow TKG\text{-}OCH_2COONa + NaCl$$

(CMTKG)

Another route for carboxymethylation of CMTKG can be done by using sodium salt of MCA which is shown below [70](fig.1.12b).

$$TKG\text{-}CH_2OH + NaOH \rightarrow TKG\text{-}O\text{-}CH_2ONa + H_2O$$

$$TKG\text{-}CH_2ONa + ClCH_2COONa \rightarrow TKG\text{-}O\text{-}CH_2COONa + NaCl$$

(CMTKG)

The side reaction also takes place which results from the reaction between sodium hydroxide and MCA to form sodium glycolate [73].

$$NaOH + ClCH_2COONa \rightarrow HOCH_2COONa + NaCl$$

The process of carboxymethylation can be easily optimized varying the various process parameter such as duration of reaction, temperature, methanol-water ratio, the concentration of MCA, and sodium hydroxide.

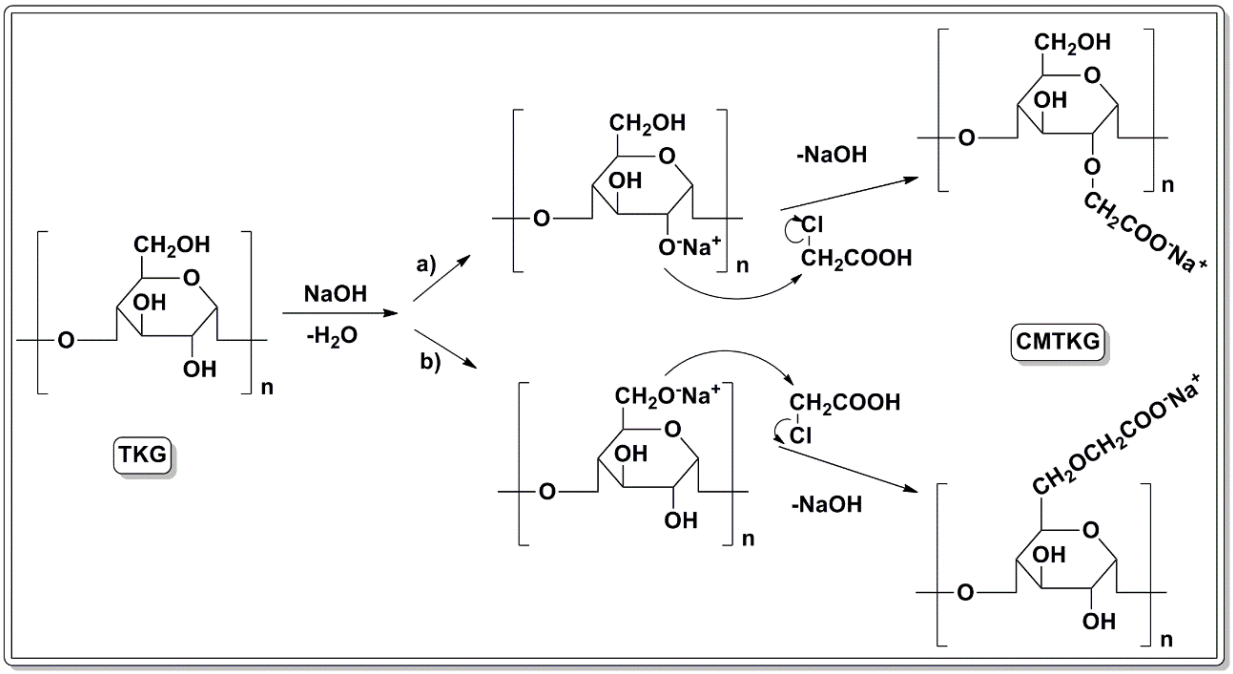

Figure 1.12 Possible Mechanism of CMTKG

Table 1.1 Applications of CMTKG

Area of application	Principle of application	Polymer constituents(s)	Form of CMTKG	Method of fabrication	Highlights	Ref
Agriculture	water-conserving agent and soil conditioner	poly(sodium-acrylate)	hydrogel	free-radical polymerization	superabsorbent hydrogel with 648 g/g swelling index	[74]
Wastewater treatment	recycling waste water	polyacrylamide	flocculant	grafting	surpassed most of the available commercial flocculant's performance wise	[75]
	flocculant and dye removal	silicon dioxide nanofiller	nanocomposite	*in situ* mechanism	followed pseudo-second-order kinetics and Langmuir equations	[76]
	to remove Cu^{+2}	tamarind kernel gum	gel	free-radical mechanism	maximum adsorption capacity for Cu^{+2} was 68.03 mg/g	[77]
Thickener	thickener in pharmaceutical and cosmetics formulation	carboxymethyl guar gum & PEPO	injectable	grafting	can also be explored as a smart injectable in controlled release technology	[78]

	double-sided printing of georgette fabric	carboxymethyl starch	paste	blending	CMTKG:CMS::4:6 showed the highest surface color, and penetration	[79]
	analyzing rheological behaviors of as thickener on georgette printing	-	paste	blending	obtained excellent levelness, hand double-sided printings, and color fastness	[80]
	printing of cellulosic cotton	-	paste	blending	eco-friendly with a low-cost printing process with improved quality	[81]
Tissue Engineering	bone tissue engineering	poly(2-Hydroxyethyl methacrylate)	hydrogel	grafting	Successful attachment and growth of HUVEC cells on the surface of hydrogel and hence can be used in humans	[82]
		tamarind kernel gum & gelatin	films	blending	improved the proliferation of the HaCaT cells and	[83]

	skin tissue engineering applications.				further can be explored for controlled drug delivery	
	controlling human's skin tissue damage	poly(hydroxyethyl methacrylate)	hydrogel	grafting	Non-allergic and non-toxic material for skin wound healing and suitable for *ex-vivo* skin disorder	[84]
Urine Adsorbent	diapers	poly(acrylonitrile)	hydrogel	grafting	obeyed second-order kinetics in various swelling media like NaCl, $CaCl_2$, and $AlCl_3$, and simulated urine (SU)	[71]

1.2.3. Application of CMTKG in various sectors

Over the years, CMTKG has been used in making hydrogels, composites, films, pellets, etc. which further been tested in various fields of application like agriculture, drug delivery, wastewater treatment, tissue engineering, etc. The more in detail has been discussed and summarized in Table 1.1 and Table 1.2 and broadly shown in fig. 1.13.

Figure 1.13 Various applications and forms of CMTKG

1.2.3.1 Wastewater treatment

A polymeric flocculant for recycling wastewater was synthesized by Sen et al. [75]. For the development of this novel flocculant, polyacrylamide (PAM) was grafted onto the backbone of CMTKG. Turbidity tests and settling tests were carried out for the flocculation studies. This optimized CMTKG-g-PAM flocculant prepared was then compared with a few other commercial flocculants available in the international and national markets. The authors concluded that their synthesized flocculant surpassed most of the available commercial flocculants' performance-wise.

A new CMTKG based nanocomposite with nanofiller (SiO_2) was synthesized and has shown excellent dye adsorption and flocculation efficiency which followed pseudo-second-order kinetics and Langmuir equations [76]. The concentration of SiO_2 greatly affected the adsorption as well as

flocculation capacity. Nanocomposite at 1.5 wt% of SiO_2, showed a maximum of 43.859 mg/g adsorption capacity. A higher hydrodynamic radius as well as higher hydrodynamic volume were quoted as the reasons for high adsorption and flocculation capacity of the nanocomposite.

C. Niu et al. showed that crosslinked CMTKG (prepared through reaction of sodium monochloroacetic acid, epichlorohydrin and tamarind kernel polysaccharide) can effectively be used to remove Cu^{+2} from wastewater. Interestingly, crosslinked CMTKG could be repeatedly used without changing their adsorption capacities as suggested by their regeneration study. The suitable pH range was 2-6. Adsorption followed Langmuir isotherm adsorption under the concentration range and second-order kinetic model. The Q_m (maximum adsorption capacity) for Cu^{+2} was found out to be 68.03 mg/g. The crosslinked CMTKG equilibrium of adsorption capacity was reported to reach in just 15 mins [77].

1.2.3.2 Thickener

A new thermo associating polymers have been designed and synthesized by grafting amino terminated poly(ethylene oxide-co-propylene oxide) (PEPO) onto CMTKG and carboxymethyl guar gum (CMG). The grafting was done by coupling reaction between COOH groups of CMG and CMTKG and NH_2 groups of PEPO using coupling agents, EDC/NHS [1-(3-(dimethylamino) propyl)-3-ethyl carbodiimide hydrochloride/*N*-hydroxysuccinimide]. By studying and observing various parameters like, fluorescence and rheological measurements, the authors concluded these thermo associating polymers with biodegradable nature of CMTKG and CMG could be used as a smart injectable in controlled release technology and as thickeners in pharmaceutical and cosmetics formulation [78].

Printability and rheology of the different mixture ratio from CMTKG and carboxymethyl starch (CMS) were studied by Wang et al., to explore the availability of the mixture on double-sided printing of georgette fabric [79]. The viscoelasticity and flowability of the mixture gradually increase with the increase of CMS and hence the deviation from Cox-Merz rule became much larger. In comparison to just CMTKG or CMS, the mixture of both showed better double sided printing effects on georgette fabric, including higher penetration (more than 90%), better colour yield (enhanced by 3-26%), good levelness, colour fastness, handle and outline sharpness. Out of all the combination prepared, CMTKG:CMS::40:60 showed the highest surface color, and penetration and hence this ratio was nominated by the authors to have great potential for the double-sided printing of georgette fabric.

Authors [80] also investigated rheological behaviors of CMTKG as a thickener on georgette printing with disperse dyes. For printing performances, the rheological behavior of CMTKG was compared with sodium alginate (SA) with respect to oscillatory tests, steady shear tests, and transient tests. In comparison to SA, CMTKG was found to have better penetrability and screen ability in screen printing. Also, the printed georgette fabrics using CMTKG paste obtained excellent levelness, hand double-sided printings, outline sharpness, and color fastness. Hence, the authors concluded that CMTKG could be very well used as a thickener in disperse printing of georgette fabrics instead of SA.

In order to develop eco-friendly with a low-cost printing process, a thickener with improved properties was made by taking a modified recipe with 6% CMTKG, 4% trichloroacetic acid and 2% PEG-400. The results were observed by taking two different reactive dyes, reactive violet 01 and reactive Blue 21. They aimed to replace sodium bicarbonate, urea, and sodium alginate in

the conventional reactive printing of cotton with trichloroacetic acid, polyethylene glycol 400, and CMTKG respectively. Results showed that the fabric softness, sharpness of edges, light fastness, perspiration fastness, washing fastness, rubbing fastness (dry and wet), shade strength, dye penetration, staining on a white ground of the fabric, and the Sum K/S (Kubelka Munk Ratio) all got improved in the modified CMTKG version (Majeed et al. [81]).

1.2.3.3 Tissue Engineering

Sanyasi et al. [82], reported a hydrogel made up of chemically grafted CMTKG with hydroxyethyl methacrylate in the ratio of 1:10. They proved it to be non-toxic and observed its utility in commercial as well as clinical applications in the field of bone tissue engineering as the surface of their hydrogel successfully did the attachment and favored the growth of three cells namely, HUVEC, Neuro2a, and RAW264.7.

The synthesis and evaluation of gelatin-TKG/CMTKG based phase-separated films for the application of skin tissue engineering were discussed by Shaw et al. [83] which showed that the agglomeration was lower in the CMTKG films as compared to TKG films which in turn was attributed to the high hydrophilicity of the CMTKG molecules. The drug (ciprofloxacin) loaded films were made with the same composition which showed good antimicrobial properties against *E. coli*. By adding CMTKG/TKG within the gelatin films improved the proliferation of the HaCaT cells.

Choudhury et al. [84], studied CMTKG based hydrogels with hydroxyethyl methacrylate, synthesized by Sanyasi et al. [82], as a scaffold for skin tissue engineering. The hydrogels were proved to be biocompatible as confirmed from the biocompatible studies with NIH-3T3, Mouse dermal fibroblasts and HaCaT. The authors proved it to be safe and free from cytotoxicity through

assay of mitochondrial functionality such as ATP assay and mitochondrial reactive oxygen generation. Acute skin irritation test and hemolytic assay with red blood cells on SD rats confirmed this hydrogel is suitable for ex-vivo applications in the future.

1.2.3.4 Drug delivery

The potential application of CMTKG based formulation in the pharmaceutical field has been reported through oral, nasal, colon, ophthalmic, pulmonary routes. In the present review, CMTKG based drug delivery systems and its applications has been discussed in detail and has also been summarized in Table 1.2.

Table 1.2. Applications of CMTKG in drug-delivery

Principle of application	Co-Polymer constituents(s)	Form of CMTKG	Method of fabrication	Highlights	Ref.
loading (*ex-situ*) and estimating the release of metronidazole	poly(vinyl alcohol)	hydrogel	Freeze thaw-treatment	released 75% of metronidazole for a period of 6h following the Higuchi's release kinetics	[85]

ciprofloxacin *in vitro* release in intestinal pHs and gastric pHs	tamarind gum & gelatin	hydrogel	mixing	high proliferation of the MG63 cells for the CMTKG based hydrogels	[86]
monitoring delivery of acyclovir by in vitro analysis	sodium alginate	hydrogel	gelation	CMTKG could retard drug release when used with sodium alginate at an optimized mass ratio	[87]
aceclofenac for site specific controlled delivery	chitosan	hydrogel	crosslinking	drug release showed slow release of aceclofenac up to 12h in comparison to 8h for the same commercial formulation	[88]
be used for loading drug moxifloxacin hydrochloride	citric acid	hydrogel	crosslinking	citric acid can be successfully used as crosslinking agent for CMTKG and in preparing hydrogel	[89]
to optimized the composite using 4-factor, 3-level central	poly(acrylonitrile)	composite	Microwave assisted graft copolymerization	Increasing the concentration of acrylonitrile	[90]

composite experimental design				decreased the grafting efficiency	
controlling the delivery of aceclofenac	gelatin	composite	crosslinking	anti-inflammatory activity of aceclofenac-loaded composite in albino rats lasted for 7 h	[91]
Erlotinib-loaded composite for NSCLC therapy	poly(N-isopropylacrylamide)	composite	free-radical polymerization	efficiently suppressed promoted apoptosis and A549 cell proliferation	[92]
colon release of budesonide	chitosan	film	mixing	Release of drug was done for 19h by mimicking large intestine	[93]
bio adhesive strength	TKG	film	solvent casting method	cationic and anionic derivatives could be utilized for drug delivery systems.	[94]
be used for improving PVA films' bio-logical	poly(vinyl alcohol)	film	casting method	a potent candidate in sphere of wound dressings and other skin diseases	[95]

be adopted to see the effect on properties of film by graphene oxide	poly(vinyl alcohol)	film	crosslinking	amount of drug release was inversely proportional to graphene oxide concentration	[96]
vitro drug (methelene blue) release studies	poly(vinylpyrrolidone)	pellet	mixing	United States Pharmacopeia (USP) rotating paddle method was used to study release	[97]
Lornoxicam loaded drug delivery system	Microcrystalline cellulose	pellet	Extrusion/spheronization technique	tested the influence of compression force on pellet	[98]
overcome the constraint of the conventional floating matrix pellet	Hydroxypropyl methyl cellulose	pellet	wet granulation method	exhibited a potential to control and retain the release of drug (verapamil hydrochloride) in stomach for 12 h	[99]
synthesizing Lansoprazole pellets	microcrystalline cellulose	pellet	extrusion-spheronization technique	Drug release of the synthesized pellet found higher than LANZOL cap	[100]

				(marketed formulation)	
to release oral pellets into the colon region and intestine	curcumin	pellet	extrusion spheronization technique	absorption and dissolution of curcumin were found to be increased by 2 and 1.5 fold, respectively	[101]
controlled-release agents for Diclofenac sodium	*Cassia fistula*	pellet	direct compression technique	the drug release mechanism followed super case II transport	[102]
targeted colon drug (Ibuprofen) delivery	microcrystalline cellulose	pellet	extrusion spheronization technique	Drug delivery was achieved without incorporation of any coating technique	[103]
ocular delivery from Tropicamide-loaded nanoparticle	Dioctyl sodium sulfosuccinate	nanoparticle	ionotropic gelation	showed ex vivo corneal permeation of tropicamide comparable to its aqueous solution	[104]
analyses of ciprofloxacin-loaded nanoparticles	-	nanoparticle	ionotropic gelation	was studied its effect on Vero cell lines	[105]

eliminates multi-drug resistant bacteria	silver nanoparticles	film	*in situ* mechanism and capping	very low cytotoxicity towards mammalian cells	[106]
effective immobilization of amylase	tetramethoxysilane	nanohybrid matrix	sol-gel polymerization	enzyme activity not changed even after 90 days (4˚C)	[107]
mucoadhesive *in situ* nasal gel	sodium-acrylate	gel	*in situ* mechanism	safe to be used using histopathological evaluation	[108]

1.2.4 Novel drug delivery systems of CMTKG

1.2.4.1 Hydrogels

J.H. Trivedi in 2013 synthesized, characterized, and studied swelling behavior of CMTKG based hydrogel in combination with polyacrylonitrile [71]. The superabsorbent hydrogel was synthesized by grafting acrylonitrile on to partially carboxymethylated TKG followed by alkaline hydrolysis of the grafted copolymer to obtain an *in-situ* crosslinked network of the hydrogel. The data showed this hydrogel obeyed second-order kinetics in various swelling media like NaCl, $CaCl_2$, and $AlCl_3$, low conductivity water, and simulated urine (SU). The maximum swelling capacity was exhibited by SU. The authors proposed their hydrogel to be suitable for use as diapers along with an adsorbent material.

In 2014, Meenakshi & Ahuja [85] prepared hydrogels of CMTKG and PVA using freeze-thaw treatment and further evaluated for release behavior. CMTKG-PVA hydrogels loaded with

metronidazole (an antibacterial agent used as model drug) was optimized employing central composite experimental design. The optimization study revealed that high proportions of PVA favored the sustained release of metronidazole while higher proportions of CMTKG favored the faster release of metronidazole. Equilibrium swelling of 600% was found for optimized CMTKG-PVA hydrogel. It released 75% of metronidazole for a period of 6h following the Higuchi's release kinetics.

Gelatin based phase-separated hydrogels with CMTKG were developed by Shaw et al. [86] whose swelling property, biocompatibility, and muco-adhesivity were evaluated. They studied the antimicrobial efficiency of their hydrogels loaded with ciprofloxacin (an antimicrobial drug) against *E. coli* and carried out in vitro drug release in both intestinal pHs and gastric pHs. The research documented a high proliferation of the MG63 cells for the CMTKG based hydrogels as compared to the controls.

An interpenetrating hydrogel network was constructed by using alginate and CMTKG by induced gelation method using Ca^{+2} ions [87]. The combination of two natural polymers appeared best at CMTKG: Alginate ratio of 1:3 with respect to their drug entrapment efficiency, morphological characteristics, and drug delivery properties. The authors reported swelling of polymeric chains and diffusion as the controlling factor for drug release.

Drug loaded interpenetrating networks of CMTKG and chitosan with glutaraldehyde as a crosslinking agent was reported by Mali et al. and in vivo study was conducted for the confirmation of synthesized hydrogel for oral drug delivery. The entrapment efficiency of hydrogels was found to be directly proportional to the concentration of CMTKG and the concentration of crosslinker.

The results were concluded by comparing the sustained release of aceclofenac up to 12h from the hydrogel while fast release for commercial formulation [88].

The authors have also projected the drug delivery application of low-cost cum biodegradable based products in the form of CMTKG hydrogel films using citric acid [89]. The authors claimed the controlled release of a drug by their hydrogel films as drug release followed the non-Fickian release mechanism. They studied drug release at PH 7.4 using moxifloxacin hydrochloride as a model drug.

1.2.4.2 Composites

Meenakshi et al. [90] used 4 factor, 3-level central composite experimental design for studying composite made up of microwave-assisted graft copolymer of CMTKG and polyacrylonitrile. Response surface methodology showed a synergic influence by varying the concentration of ammonium persulfate whereas the grafting efficiency decreased when the concentration of acrylonitrile increased. The grafting efficiency was reported to be 96% with optimal calculated parameters like microwave exposure time (99.48 s), the concentration of ammonium persulfate (40 mmol/l), microwave exposure power (160 W) and concentration of acrylonitrile (0.10% (w/v)). The authors concluded its usefulness in designing pH-responsive applications as the grafting improved the thermal stability, imparted pH-dependent swelling characteristics, and enhanced the crystallinity.

Interpenetrating network (IPN) biocomposite of gelatin and CMTKG could be beneficial for the application of controlled drug delivery using aceclofenac as a model drug. CMTKG in biocomposites suppressed the rate of drug release in HCl solution (pH=1.2), though the same increased in phosphate buffer solution (pH=6.8). Simple diffusion in vitro and polymeric chain

relaxation were quoted as the reasons for controlled drug release. The drug entrapment efficiency was found out to be above 90%. The authors suggested their drug-loaded biocomposites has the potential as an anti-inflammatory therapeutics as its anti-inflammatory activity lasted over 7h in albino rats [91].

Bera et al. [92] synthesized Erlotinib-loaded semi-interpenetrating network nanocomposites for which CMTKG along with poly (N-isopropyl acrylamide) and montmorillonite were used. This nanocomposite was demonstrated for ERL (erlotinib HCl) delivery for non-small-cell lung cancer (NSCLC) treatment. These nanocomposites were made by *in situ* free-radical polymerization and subsequently, ERL was loaded via probe sonication-assisted self-assembly protocol. The synthesized optimized formulation showed outstanding mucin adsorption ability and exhibited cytotoxic activity and induced apoptosis against A549 cells, which were higher than that of native ERL. Hence this nano formulation is a great therapeutic strategy for NSCLC therapy.

1.2.4.3 Films

The possible use of films made from chitosan (CH) and CMTKG for colon release of budesonide for the period of 19h by mimicking large intestine in the fashion of zero-order was evaluated and the reason for the release was provided in terms of the stability of these complexes in acidic medium and the ability of films with $–NH_3$ groups of CH to form complexes with $–COO^-$ groups of CMTKG [93].

In 2013, the same group prepared CMTKG based polysaccharide films by solvent casting method. For this to happen, they first synthesized carboxymethylated, sulfated, and aminated derivatives of TKP, whose degree of substitution was reported to be lying between 0.1 and 0.2. The authors proposed these synthesized films for the application as bioadhesive polymer for drug delivery and

proved these derivatized films depicted higher force of detachment in comparison to TKP. Out of three derivatized films, aminated films required a maximum force of detachment from porcine cheek mucosa [94].

Yadav et al. [95] showed that properties of polyvinyl alcohol (PVA), in terms of biological as well as physicochemical properties, could be effectively improved by adding CMTKG as co-ingredient. The presence of CMTKG significantly enhanced the biological, thermal, and mechanical properties of the (PVA-CMTKG) films. The authors too used this film in drug loading of ciprofloxacin which showed good antimicrobial property against *E. coli.* Better cell proliferation observed in the CMTKG containing films in comparison to PVA only films by using human keratinocytes for the study. Based on these observations, authors suggested CMTKG based films can also be further used in wound dressings and other skin diseases where a typical drug is required.

They have also prepared films having CMTKG, PVA, and graphene oxide (GO) and used it for the application of drug delivery, using ciprofloxacin hydrochloride [96]. The drug release reported following Fickian diffusion law. The amount of drug released appeared to be inversely proportional to the concentration of GO. It was also observed that the films having a low proportion of GO, showed better proliferation of the human skin keratinocytes whereas, at higher concentrations, it was found to be cytotoxic.

1.2.4.4 Pellets

In 2008, Pal et al. synthesized CMTKG pellets by derivatizing TKG [97]. The formed CMTKG was confirmed by using various techniques, namely FTIR spectroscopy, TGA, DTA, ^{13}C NMR spectroscopy, intrinsic viscosity measurement, and static light scattering technique (SLS). This

pellet was used for the controlled delivery of methylene blue drug. The authors used United States Pharmacopeia (USP) rotating paddle method for controlled release studies and further studied the kinetics of the same, where it was observed that up to 30% of drug release, the pellet obeyed zero-order release kinetics while at 60% of drug release non-Fickian release behavior was dominated.

A blend of CMTKG with microcrystalline cellulose was used to form sustained-release pellets/spheroids of lornoxicam (a non-steroidal anti-inflammatory drug) through spheronization/extrusion technique and the effect of compression force on the same was evaluated [98]. The pellets synthesized were found to sustain the drug release for a period of 12h. The authors claimed the employed method is simple, economical, and rapid. The drug-loaded pellets were in spherical shape which was evident in SEM photomicrographs. The rate of drug release can be varied by varying the concentration of polymer used in the formulation.

A floating-bioadhesive tablet using wet granulation method was designed and a central composite design was employed for optimization. These tablets were prepared using CMTKG, hydroxypropyl methylcellulose (HPMC), and sodium bicarbonate and they were further loaded with verapamil hydrochloride (VH). The tablets showed 17-30% of burst release in the 1st hour and showed control release for a period of 12h. The authors concluded by mentioning that these tablets exhibit the potential to retain and control the release of VH in the stomach for more than 12h. However further in vivo studies are required to validate the in vitro results [99].

Muley et al. [100] prepared Lansoprazole pellets employing CMTKG using the extrusion-spheronization technique. The pellets were evaluated for hardness (0.307 kg/cm^2), yield (93.53%), drug content (90.46%), and disintegration time (292 sec). Drug release of the marketed formulation and the optimized batch was found to be 80.07% and 82.33% respectively.

Curcumin pellets of CMTKG were formulated by Kshirsagar & Pandit [101] for the application of colon drug delivery. The pellets were prepared using CMTKG and curcumin solid dispersion using the extrusion spheronization technique. Absorption and dissolution of curcumin were observed to be increased by 2 and 1.5 fold, respectively. Everted rat intestine segments were used to do in vitro studies which showed enhanced oral bioavailability of solid dispersion curcumin pellets. The authors concluded that CMTKG pellets with solid dispersion of curcumin were found out to be a better candidate for colon drug delivery.

Huanbutta & Sittikijyothin [102] demonstrated the matrix tablet form from CMTKG and carboxymethylated gum of *Cassia fistula* in order to achieve the controlled release of diclofenac sodium. *In vitro,* drug release studies and drug content estimation were done to evaluate the matrix tablets. Compression time and hardness got increased while thickness found to be decreased as and when the concentration of gums increased. The results were well fitted with the Korsmeyer-Peppas model while the diclofenac sodium tablets were observed to release the drug by super case II transport (relaxation).

Ibuprofen loaded CMTKG pellets were prepared by extrusion spheronization technique using 3-level 2-factor full factorial design [103]. These pellets were specially designed targeting colonic disease via colon drug delivery. Scanning electron microscopy verified small pore openings at the surface of pellets for the drug release. *In vitro* dissolution test of the drug-loaded CMTKG pellets were done at different pHs (1.2, 6.8, 7.4) phosphate buffer solutions which showed drug release within 10h while extended drug release of 9h in presence of rat caecal content was observed.

1.2.4.5 Nanoparticles

Kaur et al. in 2011, CMTKG nanoparticles loaded with Tropicamide were prepared and studied for ocular delivery [104]. The CMTKG nanoparticles were synthesized via ionotropic gelation technique and further optimized using 3-levels, 2-factor central composite design. The results revealed that the concentration of polymer (CMTKG) and crosslinker (Calcium Chloride) had a synergistic effect on 5 encapsulation efficiency and particle size. The non-irritant and mucoadhesive nature of CMTKG nanoparticles proved their suitability as an ocular delivery system.

Ciprofloxacin loaded CMTKG nanoparticles were prepared using the ionotropic gelation method. The results confirmed the concentration of CMTKG and magnesium chloride showed synergistic effect on the efficiency of encapsulation while the concentration of CMTKG had a significant effect on particle size. The antibacterial assay results revealed the greatest zone of inhibition by these nanoparticles in Micrococcus luteus. Minimum toxicity was also confirmed of the prepared nanoparticles using Vero cell lines via resazurin assay [105].

1.2.4.6 Miscellaneous

Sanyasi et al. [106] synthesized nanoparticles doing a green synthesis of an efficient silver nanoparticle (AgNP) by *in-situ* reduction and capping with CMTKG (SIZE ~20-40 nm). These AgNPs inhibit biofilm formation and growth of both Gram-positive and Gram-negative bacterial strains even at much low concentration than the MIC (minimum inhibitory concentration) breakpoints of antibiotics but showed no cytotoxicity against mammalian cells. CMTKG-capped AgNPs also blocked the growth of several clinical isolates and hence capable of resisting multiple antibiotics belonging to various classes. Therefore, the authors proposed CMTKG-capped AgNPs

to have strong potential bio-medical applications against multi drug-resistant microbes with very low cytotoxicity towards mammalian cells.

A promising application of enzyme (amylase) in immobilized stage on a nanohybrid support CMTKG initiated and catalyzed sol-gel polymerization of TMOS (tetramethoxysilane) was demonstrated to produce monolithic silica nanohybrids and they were found to be efficient in immobilizing amylase for starch hydrolysis along with the improvement of the affinity and catalytic properties of amylase. The authors reported the stability of the enzyme in the nanohybrid matrix (CMTKG-Silica) as the activity of the enzyme did not change even after 90 days at 4˚C [107].

Mali et al. developed a mucoadhesive *in situ* gel of Granisetron hydrochloride (GH) with reduced nasal mucocillary clearance [108]. Thermogelling Pluronic flake 127 (PF 127) was used for the *in situ* gelation upon contact with nasal mucosa. To modulate mucoadhesion, CMTKG along with SA and Moringa gum was used. 0.3% polyethylene glycol 6000 (PEG 6000) was used for the modification of drug release for optimized formulation. The formulation with the highest order of CMTKG showed optimum results and further, the formulation is safe for use (tested using histopathological evaluation). To the same above formulation, drug diffusion increased with the addition of PEG 6000. Hence, this study concluded the potential use of CMTKG as mucoadhesive *in situ* nasal gel.

1.3 Conclusion

The industrial utilization of natural polymers in place of synthetic polymers is of great importance for more continual progress in the time to come. The flexibility of chemical modification of TKG

into CMTKG with improved functional properties makes it a strong candidate in the sector of agriculture, drug delivery, tissue engineering, papers, and cloth industry.

Due to the availability of sound information on the excellent pharmaceutical and physicochemical properties of CMTKG, the last decade did an extensive investigation of CMTKG as a drug delivery vehicle. However, it is notable that none of the CMTKG based formulations have found a way to the commercial market of pharmaceuticals due to the unattainability of safety data. CMTKG has effectively been exposed as a drug delivery vehicle but its commercialization and benefits to the world are still a matter of investigation. The utility and versatility of CMTKG would help to meet the expectations of researchers and particularly regulatory authorities of the pharmaceutical sector so that CMTKG based products will be in the service to meet the therapeutic needs globally soon.

Interestingly, CMTKG possesses strong candidature in the agriculture field but it is yet to be exploited for its usage in the agricultural field. As per the research gap and capacity of carboxymethyl tamarind kernel gum (CMTKG), to the best of our knowledge, it is being used for the first time with sodium acrylate and for the application of agriculture as a soil conditioner and as well as boron and zinc micro-nutrients carrier vehicle. Hence, all the applications related to agriculture namely, soil conditioning and micronutrients carrier, have been reported for the very first time with the synthesized novel superabsorbent hydrogel.

1.4 Aims and objectives

The solely aim of this research is to help farmers in achieving high agricultural productivity with less water keeping in mind the alarming situation of our environment. Hence, prime focus of this study was to synthesize biodegradable chemically cross-linked CMTKG based hydrogels and to

further explored its applications in agriculture sphere. In order to achieve the objectives following methodology was adopted:

1. A series of biopolymer based hydrogel were planned to be synthesized. The best candidate hydrogel was chosen based on its maximum swelling capacity for meeting other objectives of proposed research.
2. The synthesized hydrogel was subjected to the following characterization techniques:
    - FTIR spectroscopy
    - Surface morphology through SEM
    - Thermal studies like TGA
3. Equilibrium swelling studies were conducted for the synthesized hydrogel. Effect of cross-linker and biopolymer used was monitored. Percent swelling as a function of temperature, pH and influence of salt solutions was also investigated.
4. Degradation experiments of optimized hydrogel was carried out by the soil burial method.
5. Synthesized hydrogel was evaluated for the application in the field of agriculture as soil conditioners by observing and calculating its effect on various physical properties of soil.
    - maximum water holding capacity
    - particle density
    - bulk density
    - porosity
    - water retention capacity at different pressures.

6. Furthermore, two different loaded hydrogel was also evaluated as a Boron and Zinc carrier vehicle. Their release kinetics studies using different mathematical models was studied and analyzed in detail.

1.5 References

1. Food and Agriculture Organization of the United Nations, R. *No Title*. 2004.
2. Pathak, P.; K.L., S.; S.P., W.; *et al.* Opportunities for Water Harvesting and Supplemental Irrigation for Improving Rainfed Agriculture in Semi-arid Areas. *Rainfed Agriculture: Unlocking the Potential*; 2009: 197–221.
3. S. P. wani, Piara Singh, K.B. and K.L.S. Climate Change and Sustainable Rain-fed agriculture : Challengea and Opportunities:221–39; 2009.
4. Rockström, J.; Barron, J.; Fox, P. Rainwater management for increased productivity among small-holder farmers in drought prone environments. *Phys. Chem. Earth* **27**(11–22):949–59; 2002. Doi: 10.1016/S1474-7065(02)00098-0.
5. Kijne, J.W.; Barker, R.; Molden, D.; *et al. Comprehensive Assessment of Water Management in Agriculture Series Titles Available Volume 1. Water Productivity in Agriculture: Limits and Opportunities for Improvement Edited by Volume 2. Environment and Livelihoods in Tropical Coastal Zones: Managing Agriculture-Fishery-Aquaculture Conflicts Edited Volume 5. Community-based Water Law and Water Resource Management Reform in Developing Countries Edited*. 2009.
6. Xie, L.; Liu, M.; Ni, B.; *et al.* Slow-release nitrogen and boron fertilizer from a functional superabsorbent formulation based on wheat straw and attapulgite. *Chem. Eng. J.* **167**(1):342–8; 2011. Doi: 10.1016/j.cej.2010.12.082.

7. Ni, B.; Liu, M.; Lü, S.; *et al.* Multifunctional Slow-Release Organic−Inorganic Compound Fertilizer. *J. Agric. Food Chem.* **58**(23):12373–8; 2010. Doi: 10.1021/jf1029306.

8. Guilherme, M.R.; Aouada, F.A.; Fajardo, A.R.; *et al.* Superabsorbent hydrogels based on polysaccharides for application in agriculture as soil conditioner and nutrient carrier: A review. *Eur. Polym. J.*; 2015. Doi: 10.1016/j.eurpolymj.2015.04.017.

9. Kuang, J.; Yuk, K.Y.; Huh, K.M. Polysaccharide-based superporous hydrogels with fast swelling and superabsorbent properties. *Carbohydr. Polym.* **83**(1):284–90; 2011. Doi: 10.1016/j.carbpol.2010.07.052.

10. Batista, R.A.; Espitia, P.J.P.; Quintans, J. de S.S.; *et al.* Hydrogel as an alternative structure for food packaging systems. *Carbohydr. Polym.* **205**(October 2018):106–16; 2019. Doi: 10.1016/j.carbpol.2018.10.006.

11. Zhang, X.Z.; Yang, Y.Y.; Chung, T.S. The influence of cold treatment on properties of temperature-sensitive poly(N-isopropylacrylamide) hydrogels. *J. Colloid Interface Sci.* **246**(1):105–11; 2002. Doi: 10.1006/jcis.2001.8063.

12. Guilherme, M.R.; Reis, A. V.; Paulino, A.T.; *et al.* Superabsorbent hydrogel based on modified polysaccharide for removal of Pb2+ and Cu2+ from water with excellent performance. *J. Appl. Polym. Sci.* **105**(5):2903–9; 2007. Doi: 10.1002/app.26287.

13. Adhikari, B.; Majumdar, S. Polymers in sensor applications. *Prog. Polym. Sci.* **29**(7):699–766; 2004. Doi: 10.1016/j.progpolymsci.2004.03.002.

14. Kim, J.; Lee, K.W.; Hefferan, T.E.; *et al.* Synthesis and evaluation of novel biodegradable hydrogels based on poly(ethylene glycol) and sebacic acid as tissue engineering scaffolds. *Biomacromolecules* **9**(1):149–57; 2008. Doi: 10.1021/bm700924n.

15. Pourjavadi, A.; Ghasemzadeh, H.; Soleyman, R. Synthesis, characterization, and swelling

behavior of alginate-g-poly(sodium acrylate)/kaolin superabsorbent hydrogel composites. *J. Appl. Polym. Sci.* **105**(5):2631–9; 2007. Doi: 10.1002/app.26345.

16. Johnson, W.; Heldreth, B.; Bergfeld, W.F.; *et al.* Safety Assessment of Galactomannans as Used in Cosmetics. *Int. J. Toxicol.* **34**:355–655; 2015. Doi: 10.1177/1091581815586798.
17. Wichterle, O.; Lím, D. Hydrophilic Gels for Biological Use. *Nature* **185**(4706):117–8; 1960. Doi: 10.1038/185117a0.
18. Buchholz, F.L.; Peppas, N.A. *Superabsorbent Polymers*. vol. 573. Washington, DC: American Chemical Society.; 1994.
19. Laftah, W.A.; Hashim, S.; Ibrahim, A.N. Polymer hydrogels: A review. *Polym. - Plast. Technol. Eng.*:1475–86; 2011. Doi: 10.1080/03602559.2011.593082.
20. Qiu, Y.; Park, K. Environment-sensitive hydrogels for drug delivery. *Adv. Drug Deliv. Rev.*:321–39; 2001. Doi: 10.1016/S0169-409X(01)00203-4.
21. Kamath, K.R.; Park, K. Biodegradable hydrogels in drug delivery. *Adv. Drug Deliv. Rev.* **11**(1–2):59–84; 1993. Doi: 10.1016/0169-409X(93)90027-2.
22. Kazanskii, K.S.; Dubrovskii, S.A. Chemistry and physics of "agricultural" hydrogels. *Adv. Polym. Sci.* **104**:97–133; 1992. Doi: 10.1007/3-540-55109-3_3.
23. Pillai, C.K.S. Challenges for Natural Monomers and Polymers: Novel Design Strategies and Engineering to Develop Advanced Polymers. *Des. Monomers Polym.* **13**(2):87–121; 2010. Doi: 10.1163/138577210X12634696333190.
24. Baldrian, P.; Valášková, V. Degradation of cellulose by basidiomycetous fungi. *FEMS Microbiol. Rev.*:501–21; 2008. Doi: 10.1111/j.1574-6976.2008.00106.x.
25. Villay, A.; Lakkis de Filippis, F.; Picton, L.; *et al.* Comparison of polysaccharide degradations by dynamic high-pressure homogenization. *Food Hydrocoll.* **27**(2):278–86;

2012. Doi: 10.1016/j.foodhyd.2011.10.003.

26. Wu, L.; Liu, M. Preparation and properties of chitosan-coated NPK compound fertilizer with controlled-release and water-retention. *Carbohydr. Polym.* **72**(2):240–7; 2008. Doi: 10.1016/j.carbpol.2007.08.020.

27. Guo, M.; Liu, M.; Hu, Z.; *et al.* Preparation and properties of a slow release NP compound fertilizer with superabsorbent and moisture preservation. *J. Appl. Polym. Sci.* **96**(6):2132–8; 2005. Doi: 10.1002/app.21140.

28. Melaj, M.A.; Daraio, M.E. Preparation and characterization of potassium nitrate controlled-release fertilizers based on chitosan and xanthan layered tablets. *J. Appl. Polym. Sci.* **130**(4):2422–8; 2013. Doi: 10.1002/app.39452.

29. Wu, L.; Liu, M. Preparation and characterization of cellulose acetate-coated compound fertilizer with controlled-release and water-retention. *Polym. Adv. Technol.* **19**(7):785–92; 2008. Doi: 10.1002/pat.1034.

30. Hemvichian, K.; Chanthawong, A.; Suwanmala, P. Synthesis and characterization of superabsorbent polymer prepared by radiation-induced graft copolymerization of acrylamide onto carboxymethyl cellulose for controlled release of agrochemicals. *Radiat. Phys. Chem.* **103**:167–71; 2014. Doi: 10.1016/j.radphyschem.2014.05.064.

31. Bhattacharyya, R.; Ray, S.K.; Mandal, B. A systematic method of synthesizing composite superabsorbent hydrogels from crosslink copolymer for removal of textile dyes from water. *J. Ind. Eng. Chem.* **19**(4):1191–203; 2013. Doi: 10.1016/j.jiec.2012.12.017.

32. Zhou, Y.; Fu, S.; Zhang, L.; *et al.* Superabsorbent nanocomposite hydrogels made of carboxylated cellulose nanofibrils and CMC-g-p(AA-co-AM). *Carbohydr. Polym.* **97**(2):429–35; 2013. Doi: 10.1016/j.carbpol.2013.04.088.

33. Thombare, N.; Jha, U.; Mishra, S.; *et al.* Guar gum as a promising starting material for diverse applications: A review. *Int. J. Biol. Macromol.* **88**:361–72; 2016. Doi: 10.1016/j.ijbiomac.2016.04.001.

34. Wang, W.B.; Wang, A.Q. Preparation, Swelling and Water-Retention Properties of Crosslinked Superabsorbent Hydrogels Based on Guar Gum. *Adv. Mater. Res.* **96**(11):177–82; 2010. Doi: 10.4028/www.scientific.net/AMR.96.177.

35. Hüttermann, A.; Orikiriza, L.J.B.; Agaba, H. Application of superabsorbent polymers for improving the ecological chemistry of degraded or polluted lands. *Clean - Soil, Air, Water* **37**(7):517–26; 2009. Doi: 10.1002/clen.200900048.

36. Mishra, S.; Thombare, N.; Ali, M.; *et al.* Applications of Biopolymeric Gels in Agricultural Sector. In: Thakur, V.K., Thakur, M.K., and Voicu, S.I., editors. *Polymer Gels: Perspectives and Applications*; Singapore: Springer Singapore; 2018: 185–228.

37. Zhong, K.; Zheng, X.-L.; Mao, X.-Y.; *et al.* Sugarcane bagasse derivative-based superabsorbent containing phosphate rock with water–fertilizer integration. *Carbohydr. Polym.* **90**(2):820–6; 2012. Doi: 10.1016/j.carbpol.2012.06.006.

38. Hüttermann, A.; Orikiriza, L.J.B.; Agaba, H. Application of Superabsorbent Polymers for Improving the Ecological Chemistry of Degraded or Polluted Lands. *CLEAN - Soil, Air, Water* **37**(7):517–26; 2009. Doi: 10.1002/clen.200900048.

39. El-Rehim, H.A.A.; Hegazy, E.-S.A.; El-Mohdy, H.L.A. Radiation synthesis of hydrogels to enhance sandy soils water retention and increase plant performance. *J. Appl. Polym. Sci.* **93**(3):1360–71; 2004. Doi: 10.1002/app.20571.

40. Bouranis, D.L.; Theodoropoulos, A.G.; Drossopoulos, J.B. Designing synthetic polymers as soil conditioners. *Commun. Soil Sci. Plant Anal.* **26**(9–10):1455–80; 1995. Doi:

10.1080/00103629509369384.

41. Azzam, R.A.I. Tailoring Polymeric Gels For Soil Reclamation And Hydroponics. *Commun. Soil Sci. Plant Anal.* **16**(10):1123–38; 1985. Doi: 10.1080/00103628509367670.

42. Zohuriaan-Mehr, M.J.; Motazedi, Z.; Kabiri, K.; *et al.* Gum arabic–acrylic superabsorbing hydrogel hybrids: Studies on swelling rate and environmental responsiveness. *J. Appl. Polym. Sci.* **102**(6):5667–74; 2006. Doi: 10.1002/app.25033.

43. Jena, B.; Bandita Jena, C.; Mohapatra, S.; *et al.* Effect of boron fertilization on fate of soil boron pool under a rice-vegetable cropping system grown in an Inceptisols of Odisha. ~ *74 ~ Int. J. Chem. Stud.* **5**(1):74–8; 2017.

44. Toor, G.S.; Bahl, G.S. Kinetics of phosphate desorption from different soils as influenced by application of poultry manure and fertilizer phosphorus and its uptake by soybean. *Bioresour. Technol.* **69**(2):117–21; 1999. Doi: 10.1016/S0960-8524(98)00179-5.

45. Narayan, D.; Chandeli, A.S.; Singh, G.R. *EFFECT OF BORON FERTILIZATIQNON YIELD AND QUALITY OF SUGARBEET (BET A VULGARIS L.)*. vol. XXXII. No. 1989.

46. Wenlin, Z.; Yunsheng, L.; Lixuan, R.; *et al.* Application of controlled-release nitrogen fertilizer decreased methane emission in transgenic rice from a paddy soil. *Water. Air. Soil Pollut.* **225**(3); 2014. Doi: 10.1007/s11270-014-1897-x.

47. Aouada, F.A.; De Moura, M.R.; De Abreu Menezes, E.; *et al.* Hydrogel synthesis and kinetics of ammonium and potassium release. *Rev. Bras. Cienc. Do Solo* **32**(4):1643–9; 2008. Doi: 10.1590/s0100-06832008000400029.

48. Davidson, D.W.; Verma, M.S.; Gu, F.X. Controlled root targeted delivery of fertilizer using an ionically crosslinked carboxymethyl cellulose hydrogel matrix. *Springerplus* **2**(1):1–9; 2013. Doi: 10.1186/2193-1801-2-318.

49. Ni, B.; Liu, M.; Lü, S.; *et al.* Environmentally friendly slow-release nitrogen fertilizer. *J. Agric. Food Chem.* **59**(18):10169–75; 2011. Doi: 10.1021/jf202131z.

50. Guilherme, M.R.; Reis, A. V.; Paulino, A.T.; *et al.* Pectin-based polymer hydrogel as a carrier for release of agricultural nutrients and removal of heavy metals from wastewater. *J. Appl. Polym. Sci.* **117**(6):3146–54; 2010. Doi: 10.1002/app.32123.

51. Ni, B.; Liu, M.; Lü, S. Multifunctional slow-release urea fertilizer from ethylcellulose and superabsorbent coated formulations. *Chem. Eng. J.* **155**(3):892–8; 2009. Doi: 10.1016/j.cej.2009.08.025.

52. Ahmad, F.; de Moura, M.R.; Capparelli Mattoso, L.H. Biodegradable Hydrogel as Delivery Vehicle for the Controlled Release of Pesticide. *Pesticides - Formulations, Effects, Fate*; InTech; 2011.

53. Noppakundilograt, S.; Pheatcharat, N.; Kiatkamjornwong, S. Multilayer-coated NPK compound fertilizer hydrogel with controlled nutrient release and water absorbency. *J. Appl. Polym. Sci.* **132**(2); 2015. Doi: 10.1002/app.41249.

54. Zheng, Y.; Li, P.; Zhang, J.; *et al.* Study on superabsorbent composite XVI. Synthesis, characterization and swelling behaviors of poly(sodium acrylate)/vermiculite superabsorbent composites. *Eur. Polym. J.* **43**(5):1691–8; 2007. Doi: 10.1016/j.eurpolymj.2007.02.023.

55. Kumar, M.N.V.R.; Kumar, N. Polymeric controlled drug-delivery systems: Perspective issues and opportunities. *Drug Dev. Ind. Pharm.* **27**(1):1–30; 2001. Doi: 10.1081/DDC-100000124.

56. Kulkarni, A.D.; Joshi, A.A.; Patil, C.L.; *et al.* Xyloglucan: A functional biomacromolecule for drug delivery applications. *Int. J. Biol. Macromol.* **104**:799–812;

2017. Doi: 10.1016/j.ijbiomac.2017.06.088.

57. Racovita, S.; Vasiliu, S.; Popa, M.; *et al.* Polysaccharides based on micro- and nanoparticles obtained by ionic gelation and their applications as drug delivery systems. *Rev. Roum. Chim.* **54**:709–18; 2009.

58. Han, Q. Bin Critical Problems Stalling Progress in Natural Bioactive Polysaccharide Research and Development. *J. Agric. Food Chem.* **66**(18):4581–3; 2018. Doi: 10.1021/acs.jafc.8b00493.

59. Thombare, N.; Jha, U.; Mishra, S.; *et al.* Borax cross-linked guar gum hydrogels as potential adsorbents for water purification. *Carbohydr. Polym.* **168**(12):274–81; 2017. Doi: 10.1016/j.carbpol.2017.03.086.

60. Warkar S.G.; A.P., G. Synthesis, characterization and swelling properties of poly (Acrylamide-cl-carboxymethylguargum) hydrogels. *Int. J. Pharma Bio Sci.* **6**(1):516–29; 2015.

61. Nangia, S.; Warkar, S.; Katyal, D. Pure and Applied Chemistry A review on environmental applications of chitosan biopolymeric hydrogel based composites **1325**; 2019. Doi: 10.1080/10601325.2018.1526041.

62. Abd El-Rehim, H.A. Characterization and possible agricultural application of polyacrylamide/sodium alginate crosslinked hydrogels prepared by ionizing radiation. *J. Appl. Polym. Sci.* **101**(6):3572–80; 2006. Doi: 10.1002/app.22487.

63. Pandey, S.; Senthilguru, K.; Uvanesh, K.; *et al.* Natural gum modified emulsion gel as single carrier for the oral delivery of probiotic-drug combination. *Int. J. Biol. Macromol.* **92**:504–14; 2016. Doi: 10.1016/j.ijbiomac.2016.07.053.

64. Chang, C.; Zhang, L. Cellulose-based hydrogels: Present status and application prospects.

Carbohydr. Polym.; 2011. Doi: 10.1016/j.carbpol.2010.12.023.

65. Giusti, P.; Lazzeri, L.; Barbani, N.; *et al.* Hydrogels of poly(vinyl alcohol) and collagen as new bioartificial materials - Part I Physical and morphological characterization. *J. Mater. Sci. Mater. Med.* **4**:538–46; 1993. Doi: 10.1007/BF00125590.

66. J., J.; S., K.; G., R.; *et al.* Tamarind seed polysaccharide: A promising natural excipient for pharmaceuticals. *Int. J. Green Pharm.*; 2012. Doi: 10.4103/0973-8258.108205 LK - http://sfx.library.uu.nl/utrecht?sid=EMBASE&issn=19984103&id=doi:10.4103%2F0973-8258.108205&atitle=Tamarind+seed+polysaccharide%3A+A+promising+natural+excipient+for+pharmaceuticals&stitle=Int.+J.+Green+Pharm.&title=International+Journal+of+Green+Pharmacy&volume=6&issue=4&spage=270&epage=278&aulast=Joseph&aufirst=Joshny&auinit=J.&aufull=Joseph+J.&coden=&isbn=&pages=270-278&date=2012&auinit1=J&auinitm=.

67. Kumar, C.S.; Bhattacharya, S. Tamarind seed: Properties, processing and utilization. *Crit. Rev. Food Sci. Nutr.* **48**:1–20; 2008. Doi: 10.1080/10408390600948600.

68. Gupta, V.; Jain, S.; Rao, G.; *et al.* Tamarind kernel gum: An upcoming natural polysaccharide. *Syst. Rev. Pharm.* **1**:50–4; 2010. Doi: 10.4103/0975-8453.59512.

69. Goyal, P.; Kumar, V.; Sharma, P. Carboxymethylation of Tamarind kernel powder. *Carbohydr. Polym.* **69**(2):251–5; 2007. Doi: 10.1016/j.carbpol.2006.10.001.

70. Pal, S.; Sen, G.; Mishra, S.; *et al.* Carboxymethyl tamarind: Synthesis, characterization and its application as novel drug-delivery agent. *J. Appl. Polym. Sci.* **110**(1):392–400; 2008. Doi: 10.1002/app.28455.

71. Trivedi, J.H. Synthesis, characterization, and swelling behavior of superabsorbent hydrogel from sodium salt of partially carboxymethylated tamarind kernel powder- g -

PAN. *J. Appl. Polym. Sci.* **129**(4):1992–2003; 2013. Doi: 10.1002/app.38910.

72. Ponnikornkit, B.; Ngamsalak, C.; Huanbutta, K.; *et al.* Swelling Behaviour of Carboxymethylated Tamarind Gum. *Adv. Mater. Res.*; 2014. Doi: 10.4028/www.scientific.net/amr.1060.137.

73. Tijsen, C.J.; Scherpenkate, H.J.; Stamhuis, E.J.; *et al.* Optimisation of the process conditions for the modification of starch. *Chem. Eng. Sci.* **54**:2765–72; 1999. Doi: 10.1016/S0009-2509(98)00321-2.

74. Khushbu; Warkar, S.G.; Kumar, A. Synthesis and assessment of carboxymethyl tamarind kernel gum based novel superabsorbent hydrogels for agricultural applications. *Polymer (Guildf).* **182**(September):121823; 2019. Doi: 10.1016/j.polymer.2019.121823.

75. Sen, G.; Pal, S. Polyacrylamide Grafted Carboxymethyl Tamarind (CMT-g-PAM): Development and Application of a Novel Polymeric Flocculant. *Macromol. Symp.* **277**(1):100–11; 2009. Doi: 10.1002/masy.200950313.

76. Pal, S.; Ghorai, S.; Das, C.; *et al.* Carboxymethyl Tamarind-g-poly(acrylamide)/Silica: A High Performance Hybrid Nanocomposite for Adsorption of Methylene Blue Dye. *Ind. Eng. Chem. Res.* **51**(48):15546–56; 2012. Doi: 10.1021/ie301134a.

77. Niu, C.M.; Li, S.Y.; Lan, F. Adsorption of Cu^{2+} from Aqueous Solution by Crosslinked Carboxymethyl Tamarind. *Adv. Mater. Res.* **781**–**784**(3):2100–5; 2013. Doi: 10.4028/www.scientific.net/AMR.781-784.2100.

78. Gupta, N.R.; Torris A. T, A.; Wadgaonkar, P.P.; *et al.* Synthesis and characterization of PEPO grafted carboxymethyl guar and carboxymethyl tamarind as new thermo-associating polymers. *Carbohydr. Polym.* **117**:331–8; 2014. Doi: 10.1016/j.carbpol.2014.09.073.

79. Wang, L.; Li, R.; Wang, C.; *et al.* Mixture from carboxymethyl tamarind gum and carboxymethyl starch on double-sided printing of georgette fabric. *Cellulose* **24**(8):3545–54; 2017. Doi: 10.1007/s10570-017-1346-2.

80. Wang, L.; Li, R.; Shao, J.; *et al.* Rheological behaviors of carboxymethyl tamarind gum as thickener on georgette printing with disperse dyes. *J. Appl. Polym. Sci.* **134**(26):1–7; 2017. Doi: 10.1002/app.45000.

81. Majeed, H.; Bhatti, H.N.; Bhatti, I.A. Replacement of sodium alginate polymer, urea and sodium bicarbonate in the conventional reactive printing of cellulosic cotton. *J. Polym. Eng.* **39**(7):661–70; 2019. Doi: 10.1515/polyeng-2019-0076.

82. Sanyasi, S.; Kumar, A.; Goswami, C.; *et al.* A carboxy methyl tamarind polysaccharide matrix for adhesion and growth of osteoclast-precursor cells. *Carbohydr. Polym.* **101**:1033–42; 2013. Doi: 10.1016/j.carbpol.2013.10.047.

83. Shaw, G.S.; Biswal, D.; B, A.; *et al.* Preparation, Characterization and Assessment of the Novel Gelatin–tamarind Gum/Carboxymethyl Tamarind Gum-Based Phase-Separated Films for Skin Tissue Engineering Applications. *Polym. Plast. Technol. Eng.* **56**(2):141–52; 2017. Doi: 10.1080/03602559.2016.1185621.

84. Choudhury, P.; Kumar, S.; Singh, A.; *et al.* Hydroxyethyl methacrylate grafted carboxy methyl tamarind (CMT-g-HEMA) polysaccharide based matrix as a suitable scaffold for skin tissue engineering. *Carbohydr. Polym.* **189**:87–98; 2018. Doi: 10.1016/j.carbpol.2018.01.079.

85. Meenakshi; Ahuja, M. Metronidazole loaded carboxymethyl tamarind kernel polysaccharide-polyvinyl alcohol cryogels: Preparation and characterization. *Int. J. Biol. Macromol.* **72**:931–8; 2014. Doi: 10.1016/j.ijbiomac.2014.09.040.

86. Shaw, G.S.; Uvanesh, K.; Gautham, S.N.; *et al.* Development and characterization of gelatin-tamarind gum/carboxymethyl tamarind gum based phase-separated hydrogels: a comparative study. *Des. Monomers Polym.* **18**(5):434–50; 2015. Doi: 10.1080/15685551.2015.1041075.

87. Jana, S.; Sharma, R.; Maiti, S.; *et al.* Interpenetrating hydrogels of O -carboxymethyl Tamarind gum and alginate for monitoring delivery of acyclovir. *Int. J. Biol. Macromol.* **92**:1034–9; 2016. Doi: 10.1016/j.ijbiomac.2016.08.017.

88. MALI, kailas krishnat; DHAWALE, S.C.; DIAS, R.J.; *et al.* Interpenetrating networks of carboxymethyl tamarind gum and chitosan for sustained delivery of aceclofenac. *Marmara Pharm. J.* **21**(4):771–82; 2017. Doi: 10.12991/mpj.2017.20.

89. Mali, K.K.; Dhawale, S.C.; Dias, R.J. Synthesis and characterization of hydrogel films of carboxymethyl tamarind gum using citric acid. *Int. J. Biol. Macromol.* **105**:463–70; 2017. Doi: 10.1016/j.ijbiomac.2017.07.058.

90. Meenkashi; Ahuja, M.; Verma, P. MW-assisted synthesis of carboxymethyl tamarind kernel polysaccharide-g- polyacrylonitrile: Optimization and characterization. *Carbohydr. Polym.* **113**:532–8; 2014. Doi: 10.1016/j.carbpol.2014.07.041.

91. Jana, S.; Banerjee, A.; Sen, K.K.; *et al.* Gelatin-carboxymethyl tamarind gum biocomposites: In vitro characterization & anti-inflammatory pharmacodynamics. *Mater. Sci. Eng. C* **69**:478–85; 2016. Doi: 10.1016/j.msec.2016.07.008.

92. Bera, H.; Abbasi, Y.F.; Lee Ping, L.; *et al.* Erlotinib-loaded carboxymethyl temarind gum semi-interpenetrating nanocomposites. *Carbohydr. Polym.* **230**:115664; 2019. Doi: 10.1016/j.carbpol.2019.115664.

93. Kaur, G. Chitosan-Carboxymethyl Tamarind Kernel Powder Interpolymer Complexation:

Investigations for Colon Drug Delivery. *Sci. Pharm.* **78**(1):57–78; 2009. Doi: 10.3797/scipharm.0908-10.

94. Kaur, G.; Mahajan, M.; Bassi, P. Derivatized polysaccharides: Preparation, characterization, and application as bioadhesive polymer for drug delivery. *Int. J. Polym. Mater. Polym. Biomater.* **62**:475–81; 2013. Doi: 10.1080/00914037.2012.734348.

95. Yadav, I.; Rathnam, V.S.S.; Yogalakshmi, Y.; *et al.* Synthesis and characterization of polyvinyl alcohol- carboxymethyl tamarind gum based composite films. *Carbohydr. Polym.* **165**:159–68; 2017. Doi: 10.1016/j.carbpol.2017.02.026.

96. Yadav, I.; Nayak, S.K.; Rathnam, V.S.S.; *et al.* Reinforcing effect of graphene oxide reinforcement on the properties of poly (vinyl alcohol) and carboxymethyl tamarind gum based phase-separated film. *J. Mech. Behav. Biomed. Mater.* **81**(November 2017):61–71; 2018. Doi: 10.1016/j.jmbbm.2018.02.021.

97. Pal, S.; Sen, G.; Mishra, S.; *et al.* Carboxymethyl tamarind: Synthesis, characterization and its application as novel drug-delivery agent. *J. Appl. Polym. Sci.* **110**:392–400; 2008. Doi: 10.1002/app.28455.

98. Gowda, D. V; Mahammed, N.; Vishnu Datta, M. Design and evaluation of carboxymethyl tamarind kernel polysaccharide (CMTKP) controlled release spheroids/pellets and investigating the influence of compression. *Int. J. Pharm. Pharm. Sci.* **6**(7):103–9; 2014.

99. Mali, K.K.; Dhawale, S.C. Design and Optimization of Modified Tamarind Gum-based Floating-bioadhesive Tablets of Verapamil Hydrochloride. *Asian J. Pharm.* **10**(4):239–50; 2016.

100. Muley, S.S.; Nandgude, T.; Poddar, S. Formulation and Optimization of Lansoprazole Pellets Using Factorial Design Prepared by Extrusion-Spheronization Technique Using

Carboxymethyl Tamarind Kernel Powder. *Recent Pat. Drug Deliv. Formul.* **11**(1):54–66; 2017. Doi: 10.2174/1872211311666170113150248.

101. Kshirsagar, S.; Pandit, A.P. Curcumin Pellets of Carboxymethylated Tamarind Seed Polysaccharide for the Treatment of Inflammatory Bowel Disease. *Drug Deliv. Lett.* **8**(1):29–40; 2017. Doi: 10.2174/2210303107666171106143357.

102. Huanbutta, K.; Sittikijyothin, W. Use of seed gums from Tamarindus indica and Cassia fistula as controlled-release agents. *Asian J. Pharm. Sci.* **13**:398–408; 2018. Doi: 10.1016/j.ajps.2018.02.006.

103. Pandit, A.P.; Waychal, P.D.; Sayare, A.S.; *et al.* Carboxymethyl tamarind seed kernel polysaccharide formulated into pellets to target at colon. *Indian J. Pharm. Educ. Res.* **52**:363–73; 2018. Doi: 10.5530/ijper.52.3.42.

104. Kaur, H.; Ahuja, M.; Kumar, S.; *et al.* Carboxymethyl tamarind kernel polysaccharide nanoparticles for ophthalmic drug delivery. *Int. J. Biol. Macromol.* **50**(3):833–9; 2011. Doi: 10.1016/j.ijbiomac.2011.11.017.

105. Dilbaghi, N.; Kaur, H.; Ahuja, M.; *et al.* Synthesis and evaluation of ciprofloxacin-loaded carboxymethyl tamarind kernel polysaccharide nanoparticles. *J. Exp. Nanosci.* **9**(10):1015–25; 2013. Doi: 10.1080/17458080.2013.771244.

106. Sanyasi, S.; Majhi, R.K.; Kumar, S.; *et al.* Polysaccharide-capped silver Nanoparticles inhibit biofilm formation and eliminate multi-drug-resistant bacteria by disrupting bacterial cytoskeleton with reduced cytotoxicity towards mammalian cells. *Sci. Rep.* **6**:24929; 2016. Doi: 10.1038/srep24929.

107. Singh, V.; Kumar, P. Carboxymethyl tamarind gum-silica nanohybrids for effective immobilization of amylase. *J. Mol. Catal. B Enzym.* **70**:67–73; 2011. Doi:

10.1016/j.molcatb.2011.02.006.

108. Mali, K.; Dhawale, S.; Dias, R.; *et al.* Nasal Mucoadhesive In Situ Gel of Granisetron Hydrochloride using Natural Polymers. *J. Appl. Pharm. Sci.* (July):084–93; 2015. Doi: 10.7324/JAPS.2015.50714.

Chapter 2

SYNTHESIS, OPTIMIZATION, SWELLING STUDIES, AND, CHARACTERIZATION OF (CMTKG-PSA) SUPERABSORBENT HYDROGELS

2.1 Introduction

As per thermodynamics, there are two forces which comes into play while the hydrogel swells and de-swells. These two forces are known as to be as elastic retractive forces and deformative forces. As the polymer framework swells due to the intake of the solvent, which leads to its deformation, an elastic retractive force is generated in opposition to the deformative force. When these two forces counter balance each other, swelling reaches a steady state of equilibrium [1]. It can be inferred from this fact that, if deformative forces are greater than elastic retractive forces then swelling would take place. On the other hand, de-swelling of hydrogel will take place if the elastic retractive forces happens to be greater than that of deformative forces.

Nowadays, most of the commercial hydrogels are made up of synthetic polymers, thus non-biodegradable and considered as pollutant for the soil. Due to alarming attention towards the environmental protection, development of natural polymers and hence biopolymer based superabsorbent hydrogels (SAH) has become deal of great interest because of their environmental and commercial advantages. Presently, a lot of natural polymers based SAH have been synthesized using biopolymers and their derivatives such as chitosan [2], starch, alginate, cellulose and guar gum etc. [3–7].

Tamarind kernel gum (TKG) is a natural polymer and one of the cheapest gums available as it is extracted from the seeds of tamarindus indica L. It is composed of xylose, galactose and glucose in the molar ratio of 1:2:3 [8]. TKG and its derivative have been used as a good alternative biopolymer to the synthetic polymers because of its biodegradability, varying solubility, non-toxicity and vulnerability to microbial degradation [9]. Number of TKG based modified products have been studied in various applications, such as textile, explosives, food industries, plywood and medical industries [4]. One such derivative of TKG is carboxymethyl tamarind kernel gum (CMTKG). It has better properties in comparison to TKG [10]. But very spare literature is handy on their utilization in the field of agriculture.

This chapter elucidates synthesis, swelling studies and characterization of carboxymethyl tamarind kernel gum (CMTKG) based novel SAH.

2.2 Experimental Section

2.2.1 Materials

CMTKG having 0.20 degree of substitution, was generously gifted by Hindustan Gum and chemicals ltd., Bhiwani, Haryana. Acrylic acid (AA, CDH, New Delhi), Potassium per sulfate (KPS, Fischer Scientific, Mumbai), N,N'-methylenebis(acrylamide) (MBA, Merck, Germany), Sodium hydroxide (Fischer Scientific, Mumbai) were used as received. Distilled water was used for the preparations of solutions.

2.2.2 Synthesis of CMTKG-PSA Superabsorbent Hydrogel

The novel superabsorbent cross-linked hydrogels of CMTKG and sodium acrylate (SA) were fabricated by free radical copolymerization using KPS as an initiator and MBA as a cross-linker.

In a typical procedure, this reaction was performed by dispersing desirable amount of CMTKG in 10 mL of distilled water. To this, a prefixed quantity of SA, MBA and KPS were mixed according to the desired ratios in a beaker and were stirred with the help of a magnetic stirrer. After 2 h, the resulting mixture was transferred into test tubes and kept in the hot water bath maintained at 60°C for 2h. The hydrogel then obtained were taken out by breaking the test tubes and cut into equal thin slices. Then, the hydrogels in the shape of small discs were immersed in distilled water for overnight so as to get rid of unreacted chemicals. Finally, the soaked hydrogel discs were first air dried and then in the oven at 50°C till the arrival of constant weight [11]. The schematic representation is shown in Figure 2.1.

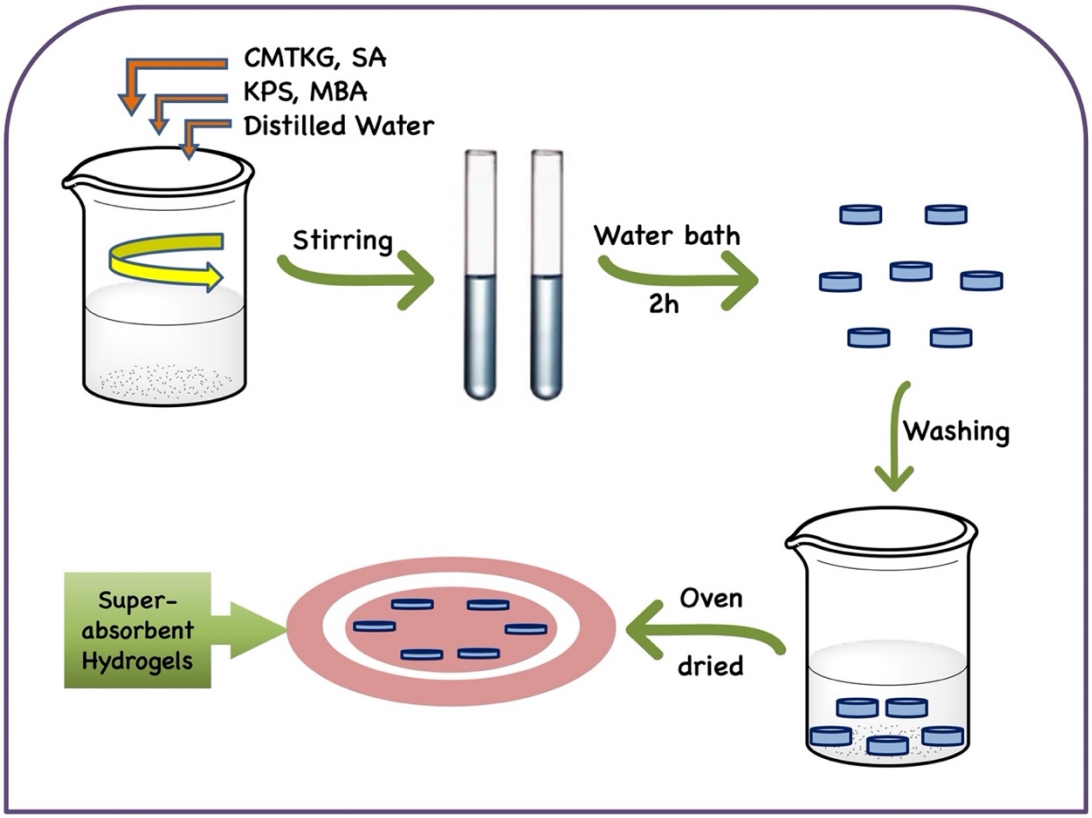

Figure 2.1 Schematic representation of CMTKG-PSA hydrogel synthesis

The exact ratios of the reactants of reaction are summarized in Table 2.1. The combination which was found out to be the best is shown in bold.

Table 2.1 Concentration of reactants used in synthesis and resultant swelling index

Formulation	CMTKG(g)/ distilled- water (mL)	Monomer (AA) (mL)	NaOH (g)	Distilled-water (mL)	Cross-linker (MBA) (mg)	Initiator (KPS) (g)	Swelling Index in distilled water (g/g)
H-1	0.1/10	7.1	4.2	13	17	0.1	359.20
H-2	0.2/10	7.1	4.2	13	17	0.1	414.33
H-3	**0.3/10**	**7.1**	**4.2**	**13**	**17**	**0.1**	**648.19**
H-4	0.1/10	7.1	4.2	13	26	0.1	320.27
H-5	0.2/10	7.1	4.2	13	26	0.1	396.22
H-6	0.3/10	7.1	4.2	13	26	0.1	531.39
H-7	0.1/10	7.1	4.2	13	35	0.05	153.10
H-8	0.1/10	7.1	4.2	13	35	0.1	227.32
H-9	0.1/10	7.1	4.2	13	35	0.4	200.07
H-10	0.1/10	7.1	4.2	13	35	0.8	158.41
H-11	0.2/10	7.1	4.2	13	35	0.1	318.45
H-12	0.3/10	7.1	4.2	13	35	0.1	429.74
H-13	0.3/10	7.1	4.2	13	44	0.1	341.11

H-14	0.3/10	7.1	4.2	13	53	0.1	223.31
H-15	0.15/10	7.1	4.2	13	17	0.1	387.29
H-16	0.25/10	7.1	4.2	13	17	0.1	503.34

2.2.3 Swelling Studies

Swelling studies of the fabricated hydrogels were conducted by gravimetric analysis. Fully dried hydrogel samples were accurately weighed and immersed in distilled water, solutions of pH 4, 9 and 12 (prepared by adding NaOH or HCl in their dilute version) and 0.9% NaCl.

After regular time interval, the swollen hydrogels were taken out and weighed after removing the surface water with filter paper (Figs. 2.2(a) & 2.2(b)). The swelling indexes were calculated using the given equation [12].

$$SI = (W_e - W_d) / W_d$$

where, SI is the swelling index of SAH, W_e is the weight of equilibrium swollen SAH while W_d is the initial weight of the dried SAH. All experiments were done in triplicate.

(a) (b)

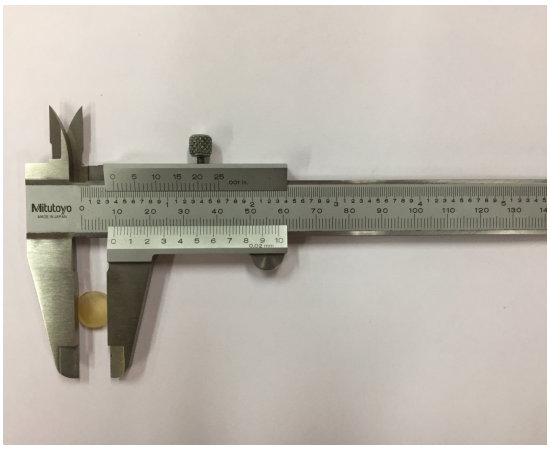

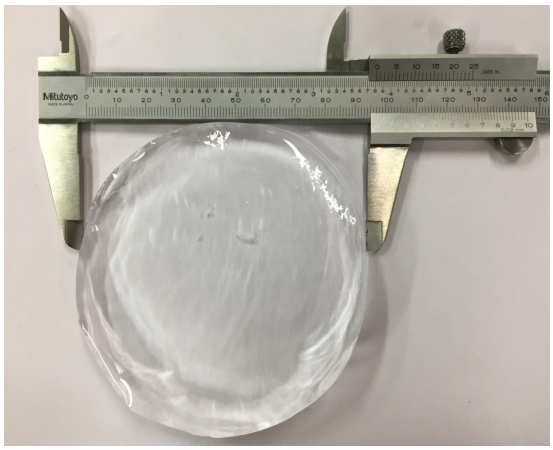

Figure 2.2 (a) Appearance of dry hydrogel (b) Appearance of swollen hydrogel

2.2.4 Characterization

2.2.4.1 Fourier-transform Infrared (FTIR) spectroscopy

The FTIR spectra of CMTKG based SAH were recorded using a FTIR spectrophotometer in a solid state by KBr pellet method (Model: PerkinElmer spectrum version 10.5.3).

2.2.4.2 Thermal Analysis

The thermo-gravimetric analysis (TGA) of CMTKG and its SAH were carried out using a PerkinElmer TGA by using N_2 atmosphere from 25°C to 900°C with 10°C/min of uniform heating rate.

2.2.4.3 Scanning electron microscopy (SEM)

Surface morphology of CMTKG and its SAH were analyzed by SEM (Model: JEOL JSM-6610LV).

2.3 Results and discussions

2.3.1 Mechanism of the formation of (CMTKG-PSA) SAH

In order to obtain SAH with maximum swelling index, different combinations of CMTKG, cross-linker (MBA), initiator (KPS) were tried during synthesis (Table 2.1).

The (CMTKG-PSA) SAH preparation scheme is depicted in figure 2.3. The initiator KPS was first decomposed at 60°C to generate persulphate anion radicals. These active free radicals attack on vinyl groups of SA and initiate the polymerization of SA with simultaneous generation of new monomeric radicals which further process propagation of chain to form poly sodium acrylate (PSA). Due to polyfunctionality of cross-linker, MBA (CH_2=CHCONHCH_2NHCOCH=CH_2), a macro radical with reactive sites was formed which can be utilized for cross-linking both the PSA and CMTKG through its –OH groups. This resulted into the formation of tri-dimensional network of CMTKG-PSA hydrogel. It is relevant to mention that the SAH preparation was attempted solely with CMTKG (keeping all the reaction conditions identical), but it came out to be a jelly like mass and hence no hydrogel formation was observed.

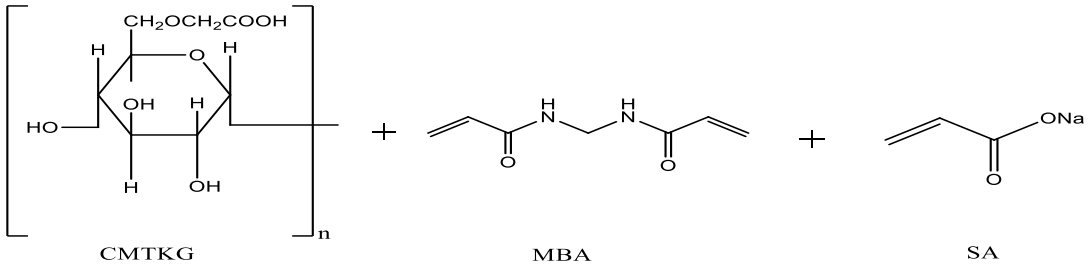

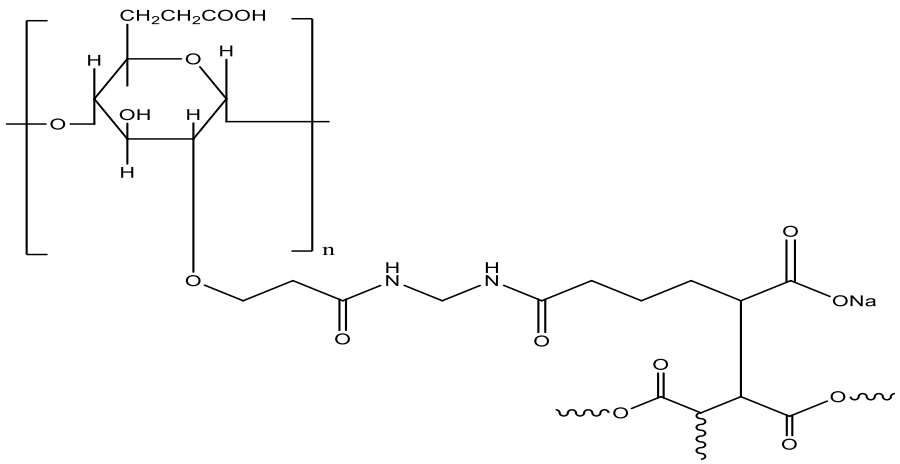

(CMTKG- PSA) Hydrogel

Figure 2.3 Synthesis mechanism of CMTKG-PSA Hydrogel.

2.3.2 Effect of biopolymer

The water absorption behavior of SAH was affected by the different concentration of the biopolymer, CMTKG. Different concentration of CMTKG showed significant effect on the capacity of water absorption (swelling index) of SAH is evident in fig. 2.4(a). This behavior may be due to the fact that as the concentration of CMTKG increased from 0.15 g to 0.3 g, the COO^- groups and the number of counter ions (Na^+) along the polymeric chains also got increased within the gel phase, resulting an amplification in the chain relaxation because of the repulsion among like charged COO^- groups. Furthermore, osmotic swelling pressure too got increased because of the increase in Na^+ (free counter ions) in the gel phase. Hence, these two factors play a significant part towards the increased swelling index of SAH with respect to the concentration of CMTKG [11]. Further, it can be noted that the synthesis of hydrogel with even higher concentration of biopolymer was also tried out but in that case the solution used to get very viscous and hence was very difficult to stir.

2.3.3 Effect of cross-linker

Cross-linking density is one of the important factors which affects swelling of SAH as explained by Flory's network theory [13]. SAH in terms of swelling undergo major changes even with a relatively small change in the concentration of cross-linker. In view of the swelling index of SAH, the relationship between the swelling index and the concentration of cross-linker, MBA was studied (fig. 2.4(b)).

As the concentration of MBA increased from 17mg to 53mg, the swelling index decreased significantly. It is known that the dosage of cross-linker determines the cross-linking density.

Hence, higher the concentration of MBA levels, more will be the cross-linking, which resulted in additional network formation. Consequently, the pore spaces among the frameworks of the tri-dimensional network would decrease which further reduced the free volume available inside the polymeric network of hydrogel, and restricting the water absorption rate. Hydrogels become harder and compact with excess cross-linking. It was observed that the hydrogel with even lesser concentration than 17mg, resulted into the formation of jelly like product. This can be attributed to the insignificant network formation between the chains of polymers.

2.3.4 Effect of initiator

Reaction initiator plays a notable role in preparation of SAH by creating lot of active sites on the chains of polymer. Keeping the amount of cross-linker fixed at 35mg, concentration of initiator, KPS, was varied and its outcome was studied in distilled water as shown in fig. 2.4(c).

Initially, the water absorption increased and then reduced with the increase in the dosage of initiator. At 0.1 g of initiator concentration, maximum water absorbency was observed which was about 227 g/g. For the concentration below 0.1 g, sharp decline in water absorbency was observed. This can be attributed to slow disintegration of the KPS at lower concentration. This results in sedate reaction of polymerization leading into more concentration of soluble monomer. This results in the formation of loose hydrogel network leading to give less swelling. Again, decrease in water absorbency was observed beyond 0.1 g amount of the initiator because of the elevated

collisions amid free-radicals and monomer due to fast velocity of reaction. This resulted in the increment of oligomer content in the network of hydrogel. It did not led to swelling because of the solubility of oligomeric part in water and hence swelling index of the SAH got decreased when concentration of initiator increased beyond 0.1 g [14].

(a)

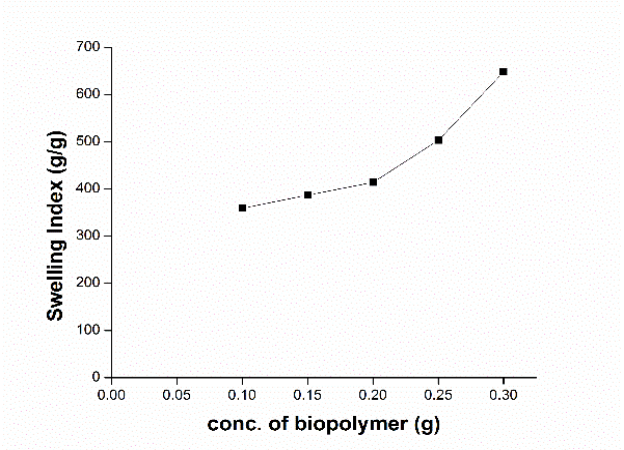

(b)

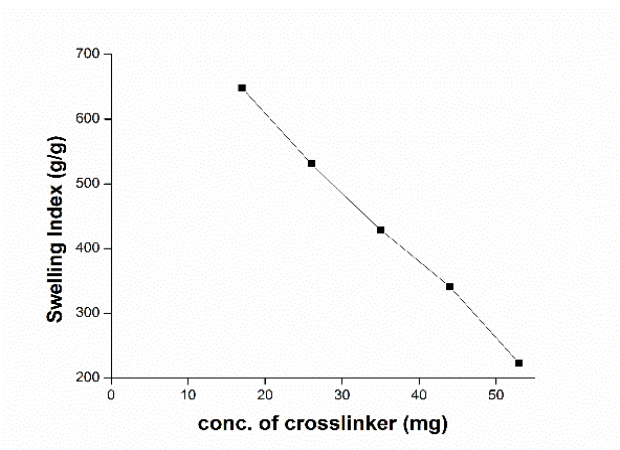

(c)

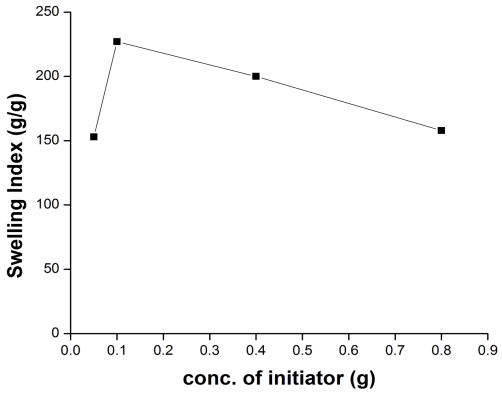

Figure 2.4 Effects of reagent concentration on swelling index of the hydrogel. (a) Effect of biopolymer (b) Effect of cross-linker (c) Effect of initiator

2.3.5 Swelling studies

Swelling study of (CMTKG-PSA) SAH showed its huge potential to swell by holding water into its sponge-like framework. The swollen and dry SAH are shown in fig. 2.2(a) (b). The swelling index of (CMTKG-PSA) SAH for various solvents viz., pH 4, 9 and 12, 0.9 % NaCl and distilled

water have shown in fig. 2.5. Swelling equilibrium was observed in about 46 hours (h). Amongst the different solvents used, the highest swelling index was shown by the distilled water, it absorbed 648 g/g of distilled water.

For solutions at various pHs, the water absorption capacity increased from pH 4-12. At pH 4, 141 g/g swelling index was shown by the hydogel which at pH 9 increased to 340 g/g and at pH 12 increased further to 452 g/g. Improper ionization of the cross-linked network may be attributed for the lower swelling in acidic medium. Hence, a collapsed state was obtained at low pH. Whereas, at alkaline conditions, increase in electrostatic repulsions produced by the carboxylate anions (COO^-) in hydrogel might had widened the space present in the networks of SAH [15]. Water absorbency of the SAH was observed to be dropped drastically in case of 0.9 % NaCl solution, where it absorbed 55 g/g of solvent. Significant reduction in the swelling capacity of hydrogel in the case of 0.9 % NaCl solution is due to presence of high ionic concentration in surrounding which decreases the difference in the osmotic pressure between outer and inner phases. Consequently, restricts free entry of any solvent inside the 3-D network of SAH [16].

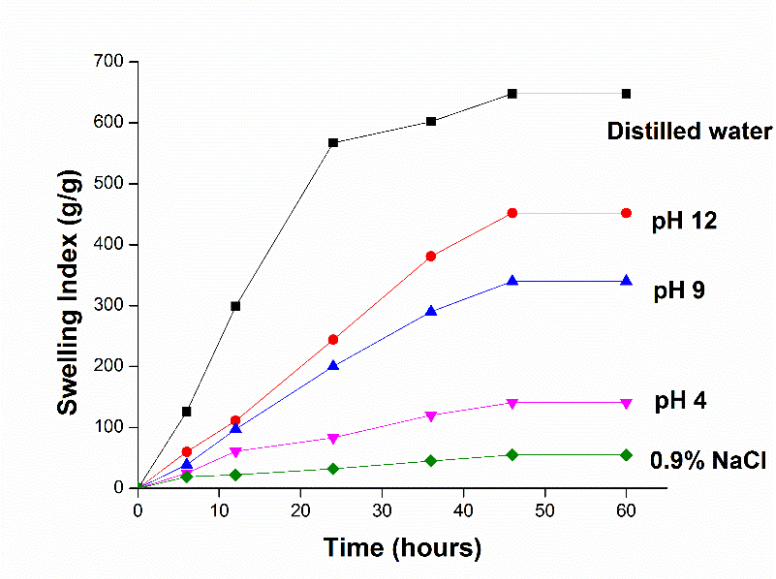

Fig. 2.5 Absorption dynamics in different solvents of CMTKG-PSA hydrogel

2.3.6 Characterization

2.3.6.1 FTIR spectroscopy

FTIR spectra of CMTKG and (CMTKG-PSA) SAH are as shown in fig. 2.6. CMTKG showed characteristic broad absorption peak at 3428 cm^{-1} for –OH stretching vibrations. The symmetric and asymmetric vibration of $–COO^-$ moiety are assigned to 1415 cm^{-1} and 1631 cm^{-1}, respectively [17]. For the spectrum of SAH, a broad absorption band at 3418 cm^{-1} corresponded to the –OH stretching vibration and $–COO^-$ symmetric and asymmetric vibrations at 1410 cm^{-1} and 1568 cm^{-1}, respectively. This strong transmittance peak at 1568 cm^{-1} was linked with stretching vibration of C=O of the polysodium acrylate, whereas the occurrence of bands at 1039 cm^{-1} and 627 cm^{-1} were characteristic of the CMTKG polysaccharide skeleton. The broad band at 627 cm^{-1} and a peak at 1317 cm^{-1} corresponded to the O=C-N and C-N groups of MBA [18]. This confirmed the presence of cross-linking. These together attributed to the successful cross-linking network between CMTKG chains and PSA.

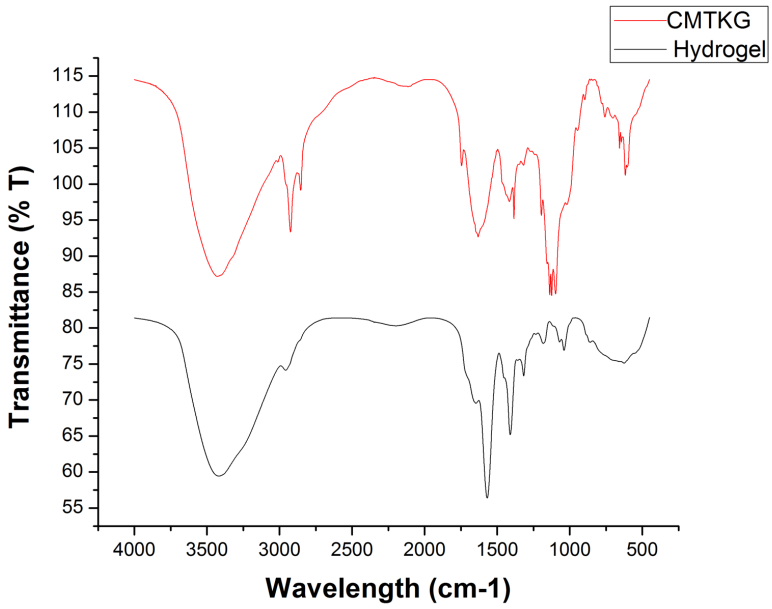

Figure 2.6 FTIR of CMTKG and synthesized CMTKG-PSA hydrogel

2.3.6.2 Thermal Analysis

Thermal stability of the SAH is expected to be more than its starting material, CMTKG. Hence, to confirm the same, comparative thermal studies were done. TGA thermograms of CMTKG and its cross-linked SAH are shown in fig. 2.7 (a),(b). Weight loss was observed in three distinct zones in the case of CMTKG. The weight loss of 5.66 %, at initial stage (30 - 155°C) is attributed to the removal of moisture from the polymer. The second zone of weight loss (192-422°C) could be because of the polymeric backbone degradation, i.e. decomposition of carboxymethyl and hydroxyl group of CMTKG [9,19] with 32.31 % weight loss. This was followed by third zone of degradation (652-723°C) with 3.80 % weight loss. The weight loss was recorded in three zones in the case of (CMTKG-PSA) SAH also. First region (196-346°C) was due to loss of unreacted cross-linker or monomers. The weight loss of 23.20 % for Second region (385-570°C) attributes to degradation of polymer backbone. The third region (679-863°C) was found out with 4.90 % of

weight loss. However, the SAH had a higher mass percentage of about 79 % until 400°C was observed as compared to about 43 % of the raw CMTKG at the same temperature. Similarly, at 850°C, the SAH recorded more than 40 % of residual mass in comparison to CMTKG with only 18 % of residual mass. Hence, thermal stability of SAH was found to be much improved than the biopolymer.

(a) **(b)**

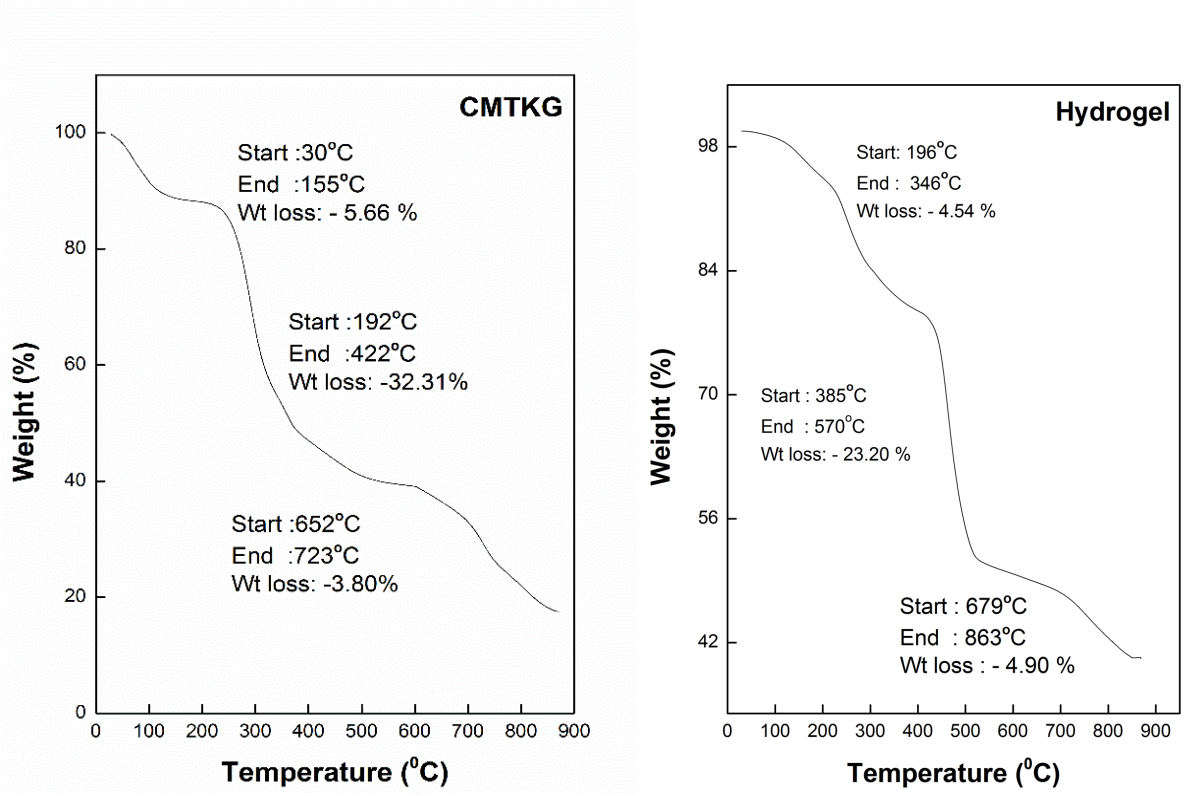

Figure 2.7 TGA (a) CMTKG and (b) synthesized CMTKG-PSA hydrogel

2.3.6.3 Scanning electron microscopy (SEM)

SEM micrographs of CMTKG and (CMTKG-PSA) SAH are shown in fig. 2.8. This analysis showed the morphology of (CMTKG-PSA) SAH having lots of interspatial voids and spongy surface. It showed distinct and clear boundaries in a conventional network fashion whereas CMTKG exhibited a compact and non-porous surface. At higher magnification, the gel network was observed that comprised both micro and macro pores. These pores are attributed for more swelling index as it permits direct penetration of the liquid in to the network of polymer by means of fluid diffusion.

(a) **(b)**

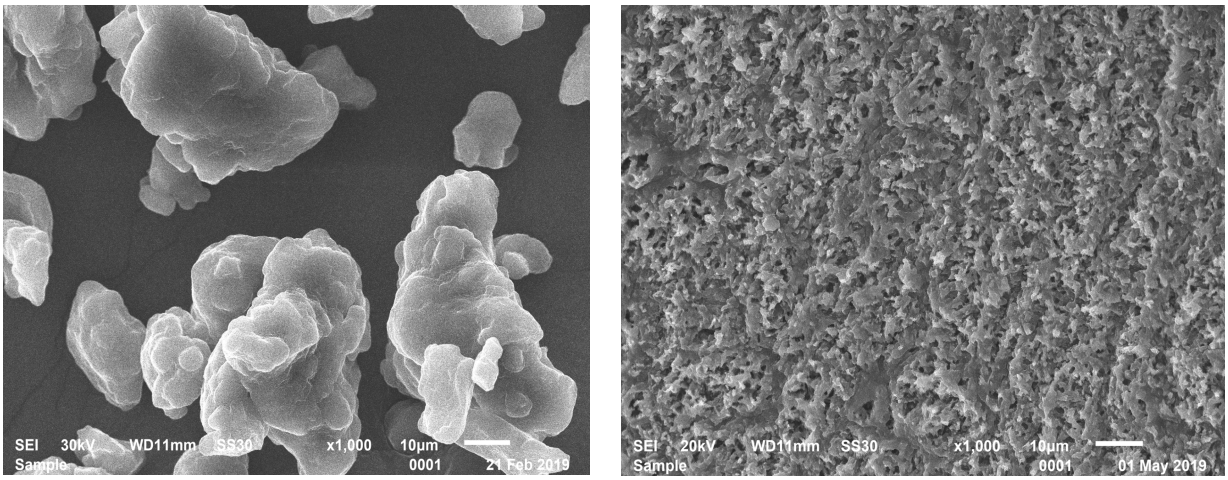

Figure 2.8 SEM (a) CMTKG and (b) synthesized CMTKG-PSA hydrogel

2.4 Conclusions

The superabsorbent hydrogels were fabricated by interpenetrating the natural polymer CMTKG and sodium-acrylate using MBA as a cross-linking agent and KPS as an initiator via free radical mechanism. The synthesis was established by FTIR analysis, TGA examination, and SEM

micrographs studies. The FTIR spectra concluded that PSA were successfully cross-linked onto the CMTKG backbone. TGA analysis confirmed the thermal stability of synthesized hydrogel which was found to be much improved than the biopolymer as at 850°C, the (CMTKG-PSA) SAH recorded more than 40 % of residual mass in comparison to CMTKG with only 18 % of residual mass. SEM studies showed the morphology of (CMTKG-PSA) SAH having lots of interspatial voids and spongy surface.

The effect of various reaction parameters, with respect to the different concentrations of biopolymer, initiator and cross-linker agent, were investigated on swelling behavior of hydrogels. The influence of various solvents, such as standard saline solution, different pH solutions (4, 9, 12), and distilled water on the swelling index of SAH was examined. Out of all the mentioned solvents, the highest swelling percentage was noticed in the distilled water (64800%). This massive swelling index of synthesized CMTKG-PSA hydrogel makes it to be the super desirable candidate for agriculture sector as water conserving agent and soil conditioner. These SAH can further be used as a nutrient carrier vehicle in the field of agriculture.

2.5 References

1. Van der Linden, H.; Westerweel, J. Temperature-Sensitive Hydrogels. *Encyclopedia of Microfluidics and Nanofluidics*; Springer US; 2008: 2006–9.
2. Nangia, S.; Warkar, S.; Katyal, D. A review on environmental applications of chitosan biopolymeric hydrogel based composites. *J. Macromol. Sci. Part A Pure Appl. Chem.* **55**(11–12):747–63; 2018. Doi: 10.1080/10601325.2018.1526041.
3. Hemvichian, K.; Chanthawong, A.; Suwanmala, P. Synthesis and characterization of

superabsorbent polymer prepared by radiation-induced graft copolymerization of acrylamide onto carboxymethyl cellulose for controlled release of agrochemicals. *Radiat. Phys. Chem.* **103**:167–71; 2014. Doi: 10.1016/j.radphyschem.2014.05.064.

4. Bhattacharyya, R.; Ray, S.K.; Mandal, B. A systematic method of synthesizing composite superabsorbent hydrogels from crosslink copolymer for removal of textile dyes from water. *J. Ind. Eng. Chem.* **19**(4):1191–203; 2013. Doi: 10.1016/j.jiec.2012.12.017.
5. Zhou, Y.; Fu, S.; Zhang, L.; *et al.* Superabsorbent nanocomposite hydrogels made of carboxylated cellulose nanofibrils and CMC-g-p(AA-co-AM). *Carbohydr. Polym.* **97**(2):429–35; 2013. Doi: 10.1016/j.carbpol.2013.04.088.
6. Thombare, N.; Jha, U.; Mishra, S.; *et al.* Guar gum as a promising starting material for diverse applications: A review. *Int. J. Biol. Macromol.* **88**:361–72; 2016. Doi: 10.1016/j.ijbiomac.2016.04.001.
7. Wang, W.B.; Wang, A.Q. Preparation, Swelling and Water-Retention Properties of Crosslinked Superabsorbent Hydrogels Based on Guar Gum. *Adv. Mater. Res.* **96**(11):177–82; 2010. Doi: 10.4028/www.scientific.net/AMR.96.177.
8. Kshirsagar, S.; Pandit, A.P. Curcumin Pellets of Carboxymethylated Tamarind Seed Polysaccharide for the Treatment of Inflammatory Bowel Disease. *Drug Deliv. Lett.* **8**(1):29–40; 2017. Doi: 10.2174/2210303107666171106143357.
9. Pal, S.; Sen, G.; Mishra, S.; *et al.* Carboxymethyl tamarind: Synthesis, characterization and its application as novel drug-delivery agent. *J. Appl. Polym. Sci.* **110**:392–400; 2008. Doi: 10.1002/app.28455.
10. H, T.J. Synthesis, characterization, and swelling behavior of superabsorbent hydrogel from sodium salt of partially carboxymethylated tamarind kernel powder-g-PAN. *J. Appl.*

Polym. Sci.; 2013. Doi: doi:10.1002/app.38910.

11. Warkar S.G.; A.P., G. Synthesis, characterization and swelling properties of poly (Acrylamide-cl-carboxymethylguargum) hydrogels. *Int. J. Pharma Bio Sci.* **6**(1):516–29; 2015.
12. Wang, Y.; Wang, J.; Yuan, Z.; *et al.* Chitosan cross-linked poly(acrylic acid) hydrogels: Drug release control and mechanism. *Colloids Surfaces B Biointerfaces* **152**:252–9; 2017. Doi: 10.1016/j.colsurfb.2017.01.008.
13. Flory, P.J. *In Principles of polymer chemistry*. 1953.
14. Wu, L.; Liu, M.; Rui Liang Preparation and properties of a double-coated slow-release NPK compound fertilizer with superabsorbent and water-retention. *Bioresour. Technol.* **99**(3):547–54; 2008. Doi: 10.1016/j.biortech.2006.12.027.
15. Chang, C.; Duan, B.; Cai, J.; *et al.* Superabsorbent hydrogels based on cellulose for smart swelling and controllable delivery. *Eur. Polym. J.* **46**(1):92–100; 2010. Doi: 10.1016/j.eurpolymj.2009.04.033.
16. Zhao, Y.; Kang, J.; Tan, T. Salt-, pH- and temperature-responsive semi-interpenetrating polymer network hydrogel based on poly(aspartic acid) and poly(acrylic acid). *Polymer (Guildf).*; 2006. Doi: 10.1016/j.polymer.2006.08.056.
17. Trivedi, J.H. Synthesis, characterization, and swelling behavior of superabsorbent hydrogel from sodium salt of partially carboxymethylated tamarind kernel powder- g -PAN. *J. Appl. Polym. Sci.* **129**(4):1992–2003; 2013. Doi: 10.1002/app.38910.
18. Reddy, B.V.; Rao, G.R. Vibrational spectra and modified valence force field for N,N'-methylenebisacrylamide. *Indian J. Pure Appl. Phys.* **46**(9):611–6; 2008.

Chapter 3

EVALUATION OF (CMTKG-PSA) CROSS-LINKED SUPERABSORBENT HYDROGELS AS SOIL CONDITIONER

3.1 Introduction

One of the most important inputs in agriculture is water. In rain fed agriculture, the sustainability of crop production majorly depends on availability of water. Even if a drought tolerant trait is introduced, water is not accessible to crops. Irrigation through dams, wells and other ground water sources is still not possible in many areas due to scarcity of groundwater and cost effectiveness. Rain is a free and first source of water but rainfall itself is becoming more and more unpredictable. This variability greatly affects soil which imposes crop production risks, especially on rain fed subsistence cultivation systems on marginal land. Since we know that world faces water and food crises. A growing population means more food to feed. Climate change is causing massive droughts and is expected to get much worse. Top soil erosion makes it harder to grow food and food scarcity leads to high prices which leads to social unrest [1]. To enhance the water utility competency in agriculture, a lot of methods are being implemented. Hydrogels are being explored for soil conditioning and water retention in agriculture because of its special properties[2,3]. All this led to hydrogels as they enhance the growth of the plant, harmless to flora and fauna and have good water intake and retain capacity.

The hydrogels which can absorb water up to 95% of their initial completely dry weight are usually known to be superabsorbent hydrogels (SAH) [4,5]. It helps to retain water in the soil by dispersing the absorbed water slowly, thus soil gets hydrated which capacitates the plant to sustain longer under water stress which consequently enhances the crop production. Henceforth, SAH can act as

a personal underground reservoir which encapsulates all the water that evaporates and helps in crop production in cases of drought [6]. In short, it can supplement rainfall to supply crop water needs [7]. These substances can be called as artificial humus because of the presence of carboxylic groups and their hydrophilicity. In comparison to humus, SAH have a higher density of hydrophilic cation binding groups and contains non aromatic moieties. Since SAH are more pronounced per weight with respect to humus which consequently lowers down the chances of becoming hydrophobic, as humus does become the same in drought conditions [8].

The SAH formed was analyzed for the application in the field of agriculture as a soil conditioner by observing and calculating its effect on physical properties of soil including maximum water holding capacity, porosity, bulk density, particle density and water retention characteristics by planting chickpea seeds and also by using pressure-plate apparatus [9].

3.2 Experimental Section

3.2.1 Materials

CMTKG-PSA superabsorbent hydrogels whose synthesis has been reported in chapter 2. The composition of soil is as follows, Sand 89%, slit & clay 0.7% [10] having particle density 2.625 g/cm^3 ; bulk density 1.32 g/cm^3, was collected from Delhi Technological University.

3.2.2 Bio-degradation studies

Bio-degradation of the fabricated SAH was done through soil burial method [3,11–13] for a period of 38 days. The predetermined quantities of SAH were kept into 50 mesh sieve bag and buried 5-6 cm deep inside the soil while maintaining the moisture in the soil. The samples were taken out at

a particular interval of time and washed thoroughly in order to detach soil. The sample was then further dried and weighed. The degradation percentage was found out on the basis of dry weight of the SAH persisting in the soil after definite time period. The degradation studies were also done by analyzing the changes in the morphology of the SAH's surface (fig. 4(a)(b)).

The percentage determination of left over dry content (DC) of SAH after each sampling period was found out by using the below mentioned formula [9]:

$$\% \text{ DC remaining} = \frac{\text{weight of dry content at particular period}}{\text{weight of initial dry content}} \times 100$$

3.2.3 Maximum water holding capacity determination

For the determination of maximum water holding capacity (MWHC) of soil, definite quantity of fully air dried soil, filtered through 3mm sieve, was made to treat with 0.1%, 0.2% & 0.3% of crushed SAH of particle size : 120-160 mesh, and for comparison, a sample of untreated soil was kept aside as control. To estimate the MWHC of soil, measured amount of the same was taken in a pot with tiny holes at the bottom followed by keeping filter paper in it. These soil samples were kept in the water bath in order to let the soil absorb water to its maximum capacity. After 6h, the samples were removed from the water bath and surplus water was drained out. The net amount of water absorbed (MWHC) by the soil was determined as per the given equation.

MWHC of soil = weight of [whole pot – (wet filter paper + empty pot)]

3.2.4 Determination of particle density, bulk density and porosity of soil

Soil density was determined by taking the representative oven dried soil sample and was filtered through 2mm sieve. Particle density of the control soil was calculated using pycnometer [14].

The determination of bulk density of samples, soil was prepared by mixing powdered SAH having particle size between 120-160 mesh at different doses of 0.1%, 0.2%, and 0.3% w/w were mixed in the soil and taken in beakers which were having holes at the bottom, as explained in MWHC experiment setup. For comparison, control soil was also taken. The samples were then kept under room temperature conditions for a few days to enable drying. These dried samples were finally filtered through 2mm sieve. Standard laboratory method was used for treated soil in determining the bulk density of all control and treated samples [15]. Porosity percentage was calculated with the help of the obtained values for particle and bulk density by using the formula:

$$P\ (\%) = [1 - (BD/PD)] \times 100$$

where, P = porosity, PD = particle density and BD = bulk density

3.2.5 Water retention capacity by plantation method

In an effort to be beneficial to agriculture, especially effective in dry regions, testing of synthesized SAH for water retention was carried out in triplicates by growing chickpea seeds (cicer arietinum) into plants with and without using SAH.

3.2.6 Water retention capacity using pressure-plate apparatus

Pressure plate apparatus (Model: 1600 pressure extractor, Santabarbara, CA, USA) was used to study effect of SAH on water retention capacity of soil at different matric tensions of 0.33 bar (corresponding to field capacity), 1 bar, 5 bar and 15 bar (corresponding to permanent wilting point). The control (untreated soil) and soil treated with 100-160 mesh size SAH at different doses of 0.1, 0.2 and 0.3% was settled in rings made up of rubber which were arranged on ceramic plates. The samples were then allowed to saturate overnight with water. The plates were then set in

pressure chamber applying various tensions until the flow of water ceased completely from the soil. This soil was then transferred into moisture boxes and weighed. These samples were dried in an oven at 100°C for overnight, air cooled and reweighed. The following equation was used to calculate the total amount of water held by soil sample at particular pressure:

$$WC\ (\%\ w/w) = [(\ S_{wet} - S_{dry}\ ) / S_{dry}\ ] \times 100$$

where, WC is the content of soil on weight basis, S_{wet} is the weight of wet soil at a specific pressure, S_{dry} is the weight of dried soil.

3.3 Results and discussions

3.3.1 Bio-degradation studies

In agriculture, synthetic polymeric hydrogels are not preferred because of their non-biodegradable nature which leads to contamination of soil [16]. Here, (CMTKG-PSA) SAH were synthesized by mixing natural polymer with the synthetic polymer so as to upgrade its bio-degradability in comparison to the synthetic hydrogels.

Rate of decomposition in the initial days was rapid followed by slower phase and relatively fast degradation rate. The rate of loss of weight were highest in the first 20 days where about 41 % of the SAH was degraded in the soil whereas about 9 % weight loss was observed from 20 to 38 days. The decomposition of polymers depends on various factors, e.g., oxygen content, pH, temperature, humidity, availability of mineral nutrients, which affects the growth of micro-organisms [17,18]. Rampant decay rate at initial phase can be due to decomposition of organic component of the SAH, CMTKG, which is uniformly blended with the other synthetic components. This decomposition

was supported by soaking up of more soil micro-organisms in the network of swollen SAH while water absorption [3] which promoted the decay rate. This was supported by SEM studies, as depicted in fig. 3.1(a),(b), where rapid phase degradation sample showed eroded and hollow surface morphology.

In the case of post 20 days, rate of decay got heavily reduced due to high water content in the network of SAH which might hinders oxygen from going into the hydrogel network and creating an anaerobic environment [19] that inhibit microbial growth and hence affecting the degradation rate.

(a) **(b)**

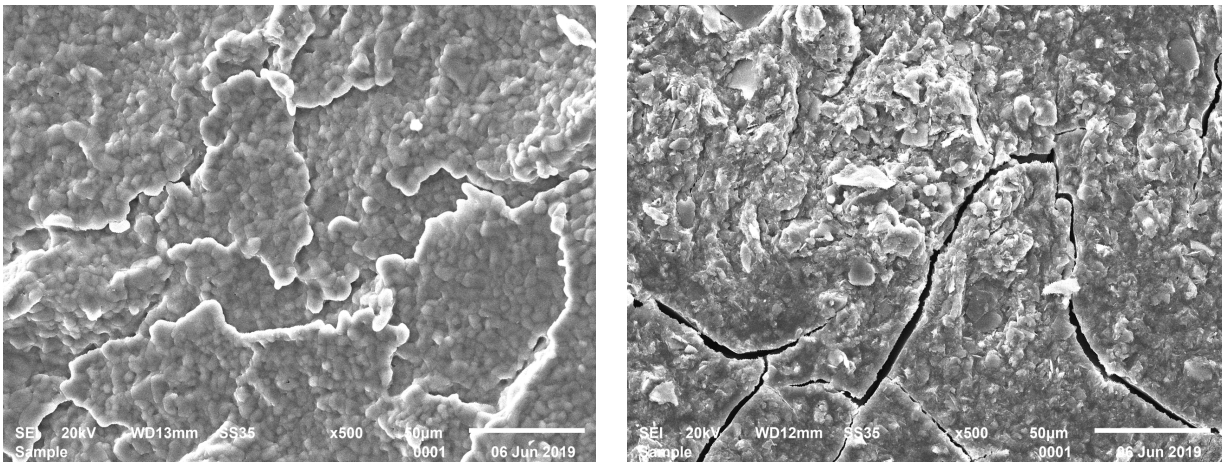

Figure 3.1 Degradation studies of CMTKG-PSA hydrogel by soil burial method (a) Sem morphology after 20 days (b) Sem morphology after 38 days

3.3.2 Maximum water holding capacity of soil

It was established through the experiment that maximum water holding capacity or MWHC of soil significantly enhanced after treatment with (CMTKG-PSA) SAH. It can be seen in fig. 3.2, (CMTKG-PSA) SAH at dosage of 0.1%, 0.2% and 0.3 % was found to be effective in enhancing soil's MWHC.

MWHC of the control (untreated soil) was found to be 43.31 % i.e. 43.31 g of water can be hold by 100 g of dried soil to reach saturation point. Addition of 0.1 % of powdered SAH could enhance MWHC of soil by 10.8 % to push it to 48.01%. Similarly, treatment with 0.2 % and 0.3 % further enhanced MWHC to 53.11% and 58.12 % respectively which was 23.6 % and 34.5 % higher than that of the control. Intriguingly, for increase in SAH quantity by every 0.1 %, approximately 11 % inflation in MWHC was observed. To sum up, this experiment shows that the quantity of SAH mixed with soil is directly proportional to MWHC.

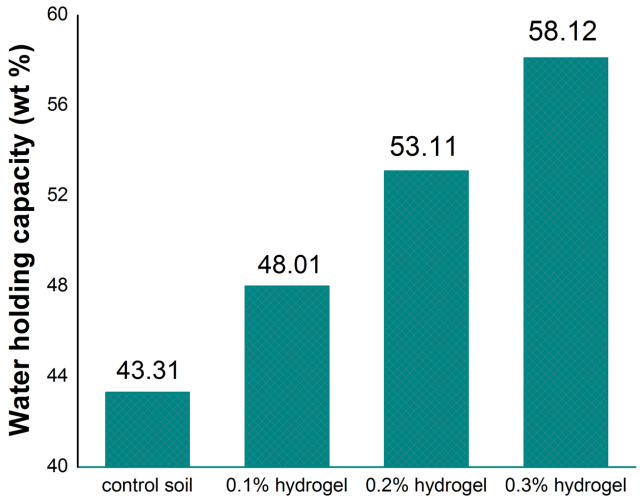

Figure 3.2 Effect of hydrogel treatment on MWHC of soil

3.3.3 Particle density, bulk density and porosity of soil

Particle density (PD) is a peculiar characteristic of any soil, which was found as per standard procedure and was found out to be 2.625 g/cm^3. Using the value of PD, bulk density (BD) of control and distinctively treated soil was found out by following standard protocol (Singh et al.,

2005). Fig. 3.3(a) and (b) depict the trends in BD and porosity of soil prior and post treatment with SAH.

Notable difference was observed in BD of SAH treated soil in contrast to control. In comparison to 1.32 g/cm^3 value of control, BD decreased by 3.0, 5.3 and 6.8 % for 0.1, 0.2 and 0.3 % SAH treated soil, respectively. BD and porosity have inverse relationship with each other. Porosity aids good health of soil by amplifying microbial count and soil aeration. In this experiment, about 50 % of porosity observed for the control soil whereas for treated soils, it improved to 53 %. The improvement in porosity may be due to the voids left in soil by the particles of SAH. There was not much difference between treated and control soil as the amount of SAH added was in the powdered form and hence the difference is notably visible in swollen stage only.

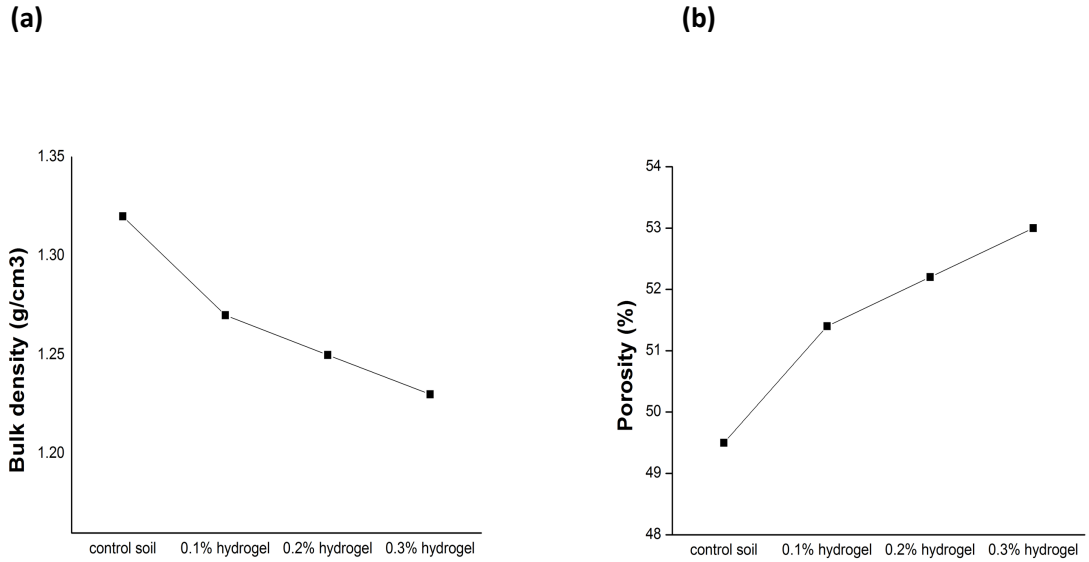

Figure 3.3 Effect of hydrogel treatment on physical properties of soil (a) Bulk density (b) Porosity

3.3.4 Water retention capacity by plantation

The determination of water retention capacity by planting chickpea seeds was conducted in triplicates by mixing SAH (0.5 % (w/w)) with the soil (2 Kg) in one set of pots and while the other set, containing only soil, were kept as control. With 400 mL of water, ten healthy seeds were planted in all the pots. Germination was observed after 7 days in both type of sets. The pattern in growth of the plants was observed and special care was taken so that no pests affected the plants. There was not much difference observed in the growth of the plants in both type of sets for up to 18 days. However, after 18 days the plants in the pots containing untreated soil started wilting, while the plants in the pots containing soil with SAH were fresh. After 41 days, the plants in the pots having soil with SAH started wilting. The plants in soil with SAH were sustained fresh and green up to 41 days without any further addition of water (fig. 3.4). Thus by mixing tiny amount of SAH, the moisture can easily be retained in the soil for as many as 41 days in comparison to just 18 days for untreated soil. Thus these SAH have competent water retention capacity in soil. It is notable to mention that the plants showed similar growth pattern in individual set of each category.

Figure 3.4 Effect of hydrogel treatment on chickpea plants after 41 days

3.3.5 Water retention capacity using pressure-plate apparatus

Water retention under distinct matric potential of soil is a vital criterion which informs about the reachability of water to any plant. This plays crucial role under draught and stress condition and even little enhancement in water retention capacity of soil during pressure condition can boost the health of crops and the possibility of crop survival in case of severe draught.

The synthesized SAH has proven to be a successful utility, aiming increment in water retention property of soil at various pressure conditions as examined by pressure plate apparatus (fig. 3.5). The difference was maximum at zero bar matric tension, where as compared to control (43.31 % WHC i.e. water holding capacity), treated soil exhibited geometric elevation in the water retention, 48.01, 53.11 and 58.12 % WHC for 0.1%, 0.2% and 0.3 % of (CMTKG-PSA) SAH treatment respectively. A similar trend was observed at 0.33 bar tension, where as compared to controls 18.05 %, treated soil showed 25.21, 26.62 and 27.62 % WHC for 0.1, 0.2 and 0.3 % CMTKG-PSA SAH treatment respectively. At high matric tension of 1 bar, 5 bar and 15 bar, similar trend was observed which clearly indicated that SAH treated soil could retain more water. At 15 bar pressure, this difference got reduced and control soil could retain 4.99 % moisture as compared to 5.86 % for 0.1 % SAH, 7.06 % for 0.2 % SAH and 8.68 % for 0.3 % SAH. This reduced moisture retention at very high tension can be ascribed to the pressure exerted by neighboring soil particles which limit swelling and compress out initially absorbed water [20].

Out of the treatments, best result was given by 0.3 % SAH, i.e. 3g SAH per Kg of soil and significantly enhanced availability of water to plants in soil.

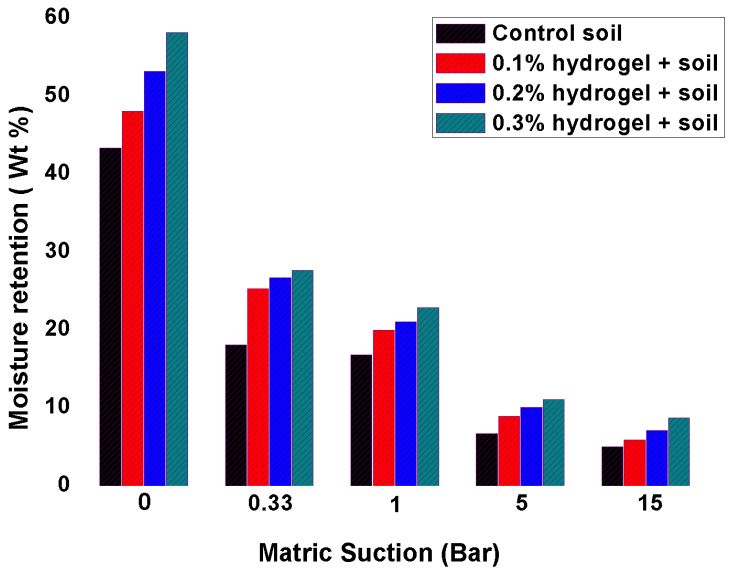

Figure 3.5 Effect of hydrogel treatment on soil's moisture retention at distinct matric potential

3.4 Conclusion

The hydrogel formed was proved out to be bio-degradable using soil burial biodegradation test. The moisture absorption and retention improved notably by adding slight amount of 0.1 to 0.3 % (CMTKG-PSA) SAH into the soil. The maximum water holding capacity of soil was enhanced up to 35% and its porosity up to 7 % of its original. The effects of the hydrogel were also seen on the growth of chickpea plants where by mixing tiny amount of SAH, the moisture can easily be retained in the soil for as many as 41 days in comparison to just 18 days for untreated soil. The incorporation of the synthesized SAH in small dose in the soil showed notably higher moisture percentage retention even at the matric tension of 15 bar. Thus these SAH have competent water retention capacity in soil. Hence, the synthesized (CMTKG-PSA) SAH has the potential to be used

in agriculture sector as water conserving agent and soil conditioner. These SAH can further be used as a nutrient carrier vehicle in the field of agriculture.

3.5 References

1. Wani, S.; Singh, P.; K.B.-A.S. in; *et al.* Climate change and sustainable rain-fed agriculture: challenges and opportunities. *Oar.Icrisat.Org*:221–39; 2009.
2. Xie, L.; Liu, M.; Ni, B.; *et al.* Slow-release nitrogen and boron fertilizer from a functional superabsorbent formulation based on wheat straw and attapulgite. *Chem. Eng. J.* **167**(1):342–8; 2011. Doi: 10.1016/j.cej.2010.12.082.
3. Ni, B.; Liu, M.; Lü, S.; *et al.* Multifunctional Slow-Release Organic−Inorganic Compound Fertilizer. *J. Agric. Food Chem.* **58**(23):12373–8; 2010. Doi: 10.1021/jf1029306.
4. Kuang, J.; Yuk, K.Y.; Huh, K.M. Polysaccharide-based superporous hydrogels with fast swelling and superabsorbent properties. *Carbohydr. Polym.* **83**(1):284–90; 2011. Doi: 10.1016/j.carbpol.2010.07.052.
5. Batista, R.A.; Espitia, P.J.P.; Quintans, J. de S.S.; *et al.* Hydrogel as an alternative structure for food packaging systems. *Carbohydr. Polym.* **205**(October 2018):106–16; 2019. Doi: 10.1016/j.carbpol.2018.10.006.
6. Zhong, K.; Zheng, X.-L.; Mao, X.-Y.; *et al.* Sugarcane bagasse derivative-based superabsorbent containing phosphate rock with water–fertilizer integration. *Carbohydr. Polym.* **90**(2):820–6; 2012. Doi: 10.1016/j.carbpol.2012.06.006.
7. Hemvichian, K.; Chanthawong, A.; Suwanmala, P. Synthesis and characterization of superabsorbent polymer prepared by radiation-induced graft copolymerization of

acrylamide onto carboxymethyl cellulose for controlled release of agrochemicals. *Radiat. Phys. Chem.* **103**:167–71; 2014. Doi: 10.1016/j.radphyschem.2014.05.064.

8. Hüttermann, A.; Orikiriza, L.J.B.; Agaba, H. Application of Superabsorbent Polymers for Improving the Ecological Chemistry of Degraded or Polluted Lands. *CLEAN - Soil, Air, Water* **37**(7):517–26; 2009. Doi: 10.1002/clen.200900048.
9. Thombare, N.; Mishra, S.; Siddiqui, M.Z.; *et al.* Design and development of guar gum based novel, superabsorbent and moisture retaining hydrogels for agricultural applications. *Carbohydr. Polym.* **185**(January):169–78; 2018. Doi: 10.1016/j.carbpol.2018.01.018.
10. Bauder, G.W.G. and J.W. Particle-size Analysis. *Methods of Soil Analysis: Part 1—Physical and Mineralogical Methods*; 1986: 383–411.
11. Sharma, K.; Kumar, V.; Kaith, B.S.; *et al.* A study of the biodegradation behaviour of poly(methacrylic acid/aniline)-grafted gum ghatti by a soil burial method. *RSC Adv.* **4**(49):25637; 2014. Doi: 10.1039/c4ra03765k.
12. Ni, B.; Liu, M.; Lü, S. Multifunctional slow-release urea fertilizer from ethylcellulose and superabsorbent coated formulations. *Chem. Eng. J.* **155**(3):892–8; 2009. Doi: 10.1016/j.cej.2009.08.025.
13. Sharma, K.; Kaith, B.S.; Kumar, V.; *et al.* Synthesis and biodegradation studies of gamma irradiated electrically conductive hydrogels. *Polym. Degrad. Stab.* **107**:166–77; 2014. Doi: 10.1016/j.polymdegradstab.2014.05.014.
14. Klute, A.; Blake, G.R.; Hartge, K.H. Bulk Density. *Methods of Soil Analysis: Part 1—Physical and Mineralogical Methods*, vol. sssabookseries; Soil Science Society of America, American Society of Agronomy; 1986: 363–75.

15. Singh, D.; Chhonkar, P.K.; Dwivedi, B.S. *Manual on soil, plant and water analysis.* Westville Publishing House.; 2005.

16. Stahl, J.D.; Cameron, M.D.; Haselbach, J.; *et al.* Biodegradation of superabsorbent polymers in soil - Springer. *Bio Degrad.* **7**(2):83–8; 2000.

17. Mittal, H.; Jindal, R.; Kaith, B.S.; *et al.* Flocculation and adsorption properties of biodegradable gum-ghatti-grafted poly(acrylamide-co-methacrylic acid) hydrogels. *Carbohydr. Polym.*; 2015. Doi: 10.1016/j.carbpol.2014.09.026.

18. Maiti, M.; Kaith, B.S.; Jindal, R.; *et al.* Synthesis and characterization of corn starch based green composites reinforced with Saccharum spontaneum L graft copolymers prepared under micro-wave and their effect on thermal, physio-chemical and mechanical properties. *Polym. Degrad. Stab.*; 2010. Doi: 10.1016/j.polymdegradstab.2010.05.024.

19. Cen, P.; Xia, L. Production of Cellulase by Solid-State Fermentation. *Advances in Biochemical Enginnering/Biotechnology*, vol. 65; 1999: 69–92.

20. Yangyuoru, M.; Boateng, E.; Adiku, S.; *et al.* Effects of natural and synthetic soil conditioners on soil moisture retention and maize yield. *West African J. Appl. Ecol.* **9**(1):1–8; 2009. Doi: 10.4314/wajae.v9i1.45676.

Chapter 4

CONTROLLED RELEASE AND RELEASE KINETICS STUDIES OF BORON THROUGH THE FUNCTIONAL FORMULATION OF SUPERABSORBENT HYDROGEL

4.1 Introduction

With increasing inhabitants on the surface of the earth, demands for the resurgence of resources are on a very high scale. One of the consequences of this demand is from the areas of arid regions. These regions tend to receive less water than expected, as we witness the wearing out of fluid resources from our earth. Agriculture holds the top priority of problems as a civilization grows around areas rich in agriculture. Adequate water supply is a must for plant growth; however, only water is not sufficient as micronutrients can promote the growth of plants. Therefore, water and micronutrient are two essential necessity of plant growth [1].

Micronutrients are the vital input substances for the continuous growth of crop production and play a significant role in food security [2]. Boron is one such micronutrient critical to the health and growth of all crops. It plays a vital role in a diverse range of plant functions including cell wall formation and stability, maintenance of structural and functional integrity of biological membranes, movement of sugar or energy into growing parts of plants, and pollination and seed set. Adequate boron is also required for effective nitrogen fixation [3–5]. Studies showed that adequate boron nutrition improves the root uptake of phosphorous and potassium. Since it is required in small amounts, traditional fertilizer blends containing boron struggle to achieve uniform nutrient distribution. Despite the need for this critical nutrient, boron is the second most widespread micronutrient deficiency problem worldwide after Zinc [6,7].

Coming up with a solution to provide water along with boron micronutrient to those needy areas, we introduced superabsorbent hydrogels. A superabsorbent hydrogel is a tridimensional crosslinked polymeric network. They are highly absorbent structural units that can imbibe more than three hundred times of its weight in water [8]. Based on their special properties, they have been triumphantly applied in the horticulture and agriculture field to improve the physical properties of soil and reduce irrigation frequency [9,10]. The combination of hydrogels and boron micronutrients could make the products have both water retaining properties and release of Boron. Also, limited literature is available regarding the work dealing with hydrogels as boron vehicle [11]. According to the research gaps and urgent need to supply boron micronutrient to the crops, and to our best information, CMTKG based hydrogel is being utilized for the time as a matrix for the controlled release of boron [12].

This chapter talks about the transformation of Carboxymethyl Tamarind Kernel Gum (CMTKG) based superabsorbent hydrogels by in situ incorporations of boron source and its accomplishment as a carrier vehicle for boron micronutrient for the applications in the field of agriculture.

The objectives of this chapter work were to examine through BSH (Boron loaded superabsorbent hydrogel): (i) the swelling index at different media of pHs, distilled water, and saline solution; (ii) the release studies of boron in water; (iii) the release studies of boron in the soil; (iv) the release kinetics studies of both water and soil.

4.2 Experimental Section

4.2.1 Materials

Acrylic acid (AA, CDH, New Delhi), Boric acid (BA, Merck, Germany), EDTA (Sigma-Aldrich), 0.9 % Azomethine-H (Sigma-Aldrich) solution in 2 % ascorbic acid (Merck, Germany), Ammonium acetate (Sigma-Aldrich), Acetic acid (Sigma-Aldrich), Sodium hydroxide (Fischer Scientific, Mumbai), Potassium persulfate (KPS, Fischer Scientific, Mumbai), N,N'-methylene bis(acrylamide) (MBA, Merck, Germany) were used as received. CMTKG (0.20˚) was graciously gifted by Hindustan Gum and chemicals ltd., Haryana, India. Distilled water was used for the preparation of solutions.

4.2.2 Synthesis of BSH

The *in situ* technique was used for incorporation of boron into CMTKG polymer based superabsorbent hydrogel. All the polymerization and cross-linking reactions took place at 25°C. To start with, a beaker having distilled water (68% w/w) along with CMTKG (0.9% w/w) and sodium acrylate (26% w/w) was kept to stir for an hour on a magnetic stirrer. To this, a prefixed quantity of Boric acid (10% w/w) was added followed by MBA (0.05% w/w), and KPS (0.2% w/w) which was further allowed to stir constantly for another one hour. Afterward, the whole mixture was then poured into the polypropylene tubes which were kept in a hot water bath oven for 2 hours at 60°C. Later on, the polypropylene tubes were cut and BSH was cut into small discs for further use [13]. These discs were first made to dry at room temperature for four days followed by drying at 55°C in a vacuum oven (Fig. 4.1).

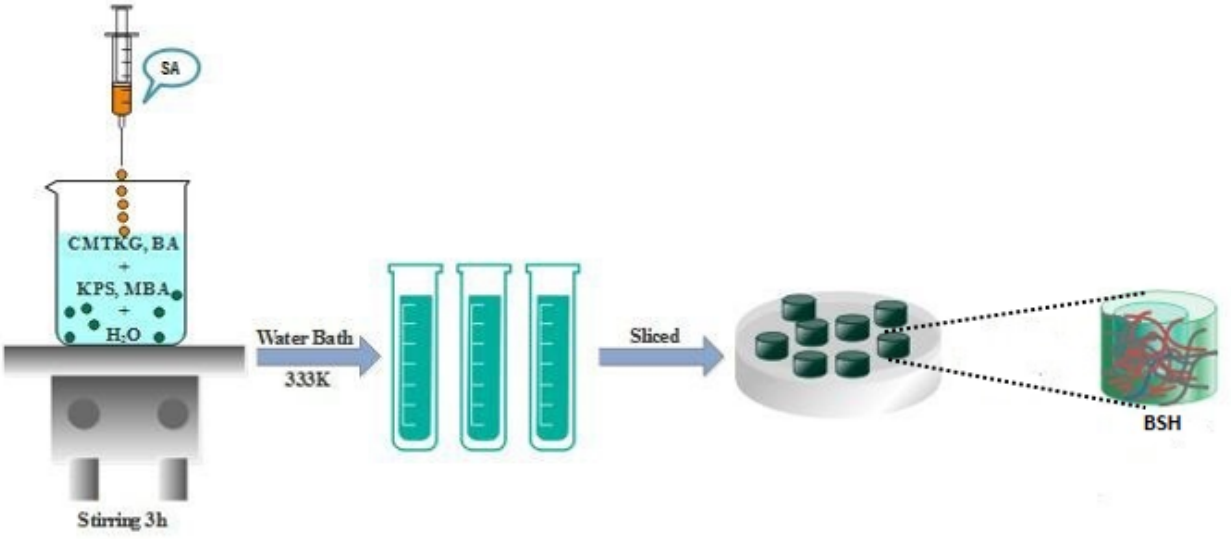

Figure 4.1 Pictorial representation of the synthesis of BSH

4.2.3 Characterization

4.2.3.1 Fourier-transform Infrared (FTIR) spectroscopy

The FTIR (Fourier-transform Infrared) spectra of CMTKG, boric acid and BSH were recorded with the KBr pellet method. FTIR spectrophotometer of Model: PerkinElmer spectrum version 10.5.3 was used and the sample was taken in the solid phase.

4.2.3.2 Scanning electron microscopy (SEM)

The morphological investigation of CMTKG and BSH was performed by Scanning Electron Microscopy (SEM) (Model: JEOL JSM-6610LV).

4.2.3.3 Thermal Analysis

The thermo-gravimetric analysis (TGA) of CMTKG and BSH was performed by the PerkinElmer TGA. The study was carried out with 10°C/min of uniform heating rate and inert N_2 atmosphere (25°C to 900°C).

4.2.4 Swelling studies

Swelling studies of the synthesized BSH were done in triplicates. Completely dried BSH samples (0.2 g) were weighed and soaked in various media such as distilled water, 0.9% NaCl solution (standard saline solution), and pH solutions of 12, 9, and 4 (all the solutions were made by adding NaOH or HCl in dilute form).

After a prefixed time interval, once wiping off the surface water using a filter paper, the swollen BSH were weighed.

The calculation of the swelling index was done using the following equation [14].

$$\text{Swelling Index} = (W_{sg} - W_{dg}) / W_{dg}$$

Where, W_{sg} = weight of equilibrium swollen BSH

W_{dg} = initial weight of the dried BSH

4.2.5 Application of BSH as a boron micronutrient carrier

The BSH synthesized was examined for the agricultural application in order to study the controlled release of the boron micronutrient. It was established by calculating and studying the release behavior pattern along with the kinetics of BSH in water and as well in the soil for 72 hours and 80 days, respectively. The composition of soil showed particle density 2.625 g/cm^3, bulk density

1.32 g/cm^3, and carried slit & clay 0.7%, sand 89%, which was gathered from Delhi Technological University, New Delhi, India.

4.2.5.1 Release study of boron in water

A precisely weighed BSH was taken in nylon sieve bags (0.2 g, particle size: 150-200 mesh) and put into beakers carrying 1 L of water. At a regular interval of time namely, 0.5, 1, 3, 6, 9, 12, 24, 36, 48, and 72 hours, 2 mL of solution was taken out. To this 2 mL solution, 0.5 mL of buffer solution (comprising EDTA, ammonium acetate, and acetic acid), and 0.5 mL of azomethine-H solution were added uniformly. It was then allowed to rest in a dark chamber for almost 30 min so as to attain total boron complexation [15]. This prepared sample solution, with the help of UV-Vis spectrophotometer (Systronics UVVIS spectrophotometer-117), was then analyzed for Boron concentration. The results were then compiled with respect to time in the form of a graph. All the release data were collected in triplicates.

4.2.5.2 Release study of boron in soil

In the plastic pots containing 0.2 kg soil (20 mesh), each non-woven bag carrying an accurately weighed BSH (200 mg, particle size: 150-200 mesh) were buried 5 cm below the surface of the soil. Throughout the study, samplings were done periodically (1, 3, 5, 10, 15, 20, 30, 40, and 80 days) while maintaining the moisture of the soil. The soil samples were taken out, post removing the non-woven bags, one by one at definite incubated time intervals. These soil samples then dried in an oven at 100°C overnight and weighed. 10 g of each soil samples were treated with 20 ml of distilled water along with 0.25 g of activated charcoal and filtered through Whatman No. 42 filter paper once it was boiled for 5 min on a hot plate [16]. For UV-vis measurements, the above-extracted

solution along with buffer solution, and azomethine-H solution were used. All the release data of boron concentrations were collected in triplicates.

4.2.5.3 Release kinetic studies of BSH in water and soil

Several mathematical models including the Korsmeyer-Peppas Model have been reported over the period of time for estimating the release of an active agent from superabsorbent hydrogel as a function of time.

Boron release data, in case of water studies as well as in case of soil studies, were fitted to different forms of mathematical kinetic models for understanding boron-slow release mechanism namely, Korsmeyer-Peppas model [17], first-order equation [18], and Higuchi model [19,20], Olson model [21]. All these models' data are tabulated in Table 1 and Table 2. The coefficient of determination (R^2) was kept as the grounds for differentiating the data for the best fit model. The model having the highest R^2 value is considered as the best fit model.

4.3 Results and discussions

4.3.1 Synthesis of BSH

In an effort to fabricate BSH, CMTKG based cross-linked network (SH) was used to incorporate boron via the *in-situ* mechanism, in the form of boric acid. The hypothetical incorporation of boric acid in the three-dimensional network of SH is illustrated through fig. 4.2.

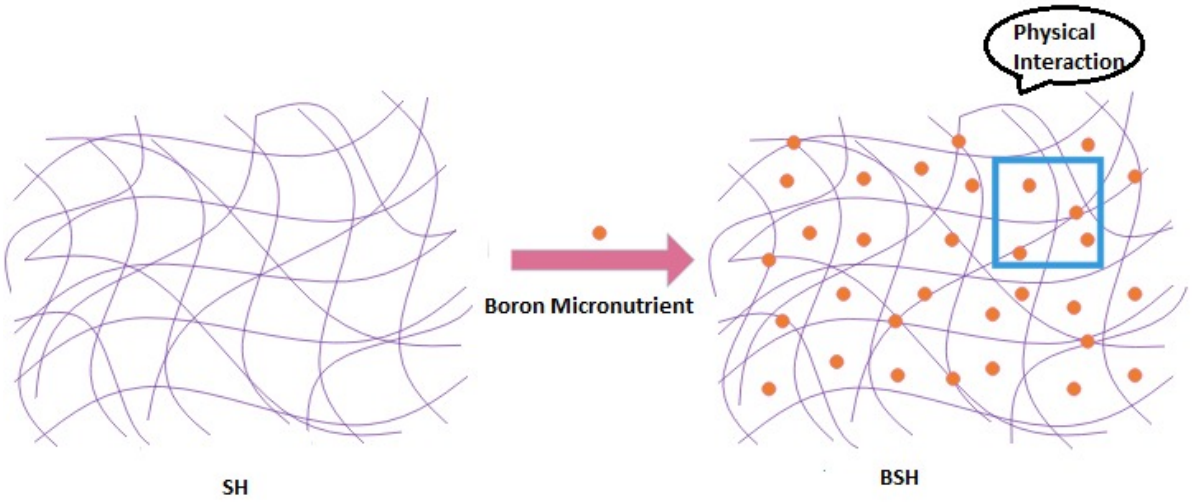

Figure 4.2 Pictorial representation of the formation of BSH from SH

4.3.2 Characterization

4.3.2.1 FTIR spectroscopy

FTIR spectra of CMTKG, Boric acid and BSH are shown in fig. 4.3. CMTKG showed symmetric vibrations (1415 cm^{-1}) and asymmetric vibrations (1631 cm^{-1}) for $-COO^-$ group. It also showed significant and broad band (3428 cm^{-1}) for -OH stretching. In BSH FTIR spectrum, -OH stretching vibration was at around 3418 cm^{-1} while symmetric vibrations and asymmetric vibrations for $-COO^-$ group around 1410 cm^{-1} and 1568 cm^{-1}, respectively [22]. Also, sharp peak (1568 cm^{-1}) was observed for the C=O bond related to SA whereas, CMTKG skeleton validated by the peaks shown at 627 cm^{-1} and 1039 cm^{-1}. The cross-linked took place between CMTKG and SA by MBA can be attributed to the broad band at 627 cm^{-1} (O=C-N bond) and a peak at 1317 cm^{-1} (C-N bond) [23]. It is significant to mention that no notable peak was observed in the FTIR spectra of BSH related to boric acid as noticeable from the absence of any peak shifts related to boric acid. Interpreting

this behavior, it can be inferred that only weak interactions (physical interactions) took place between CMTKG based cross-linked network and boron micronutrient.

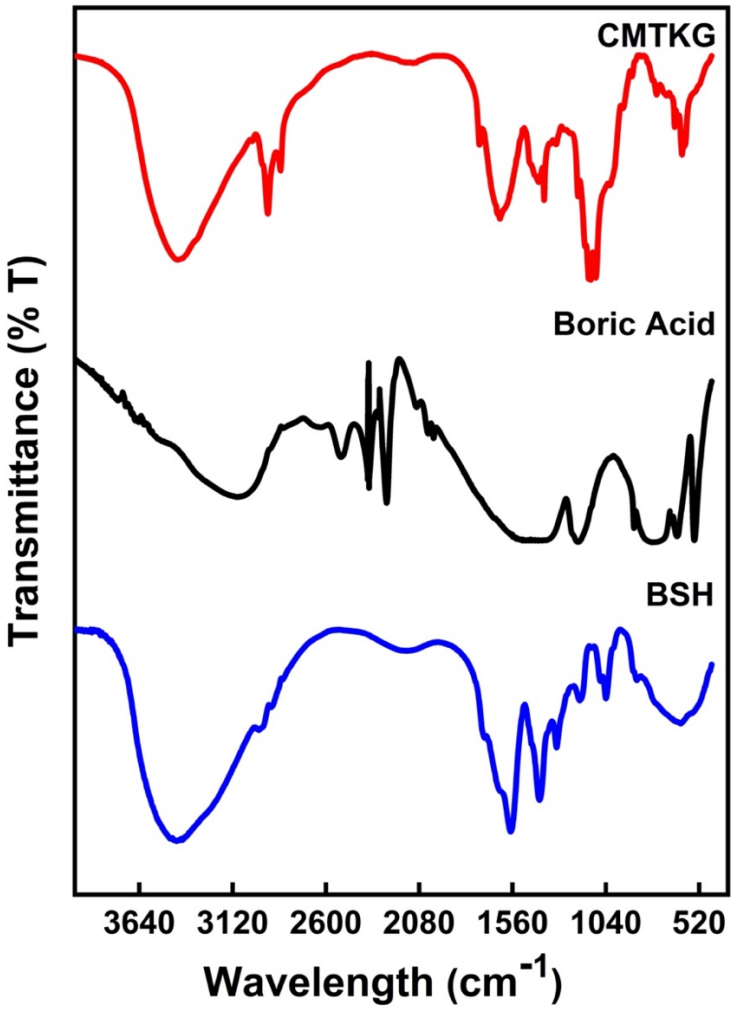

Figure 4.3 FTIR of CMTKG, Boric acid and, BSH

4.3.2.2 Scanning electron microscopy (SEM)

The morphological examination of CMTKG and BSH was done to see the morphological alterations in BSH as an effect of boron incorporation. SEM micrographs of CMTKG, is shown in fig. 4.4 (a). For a comparative study, SEM of BSH has also been shown in fig. 4.4 (b). This analysis

of CMTKG showed rough, non-porous and compact surface while BSH showed spongy surface, distinct boundaries, and interspatial voids. Although, the morphology of BSH seemed to have influenced by the addition of boron in the form of slightly fractured appearance of BSH. The reason being is that the intercalation of boron into the CMTKG based cross-linked network's matrix [24].

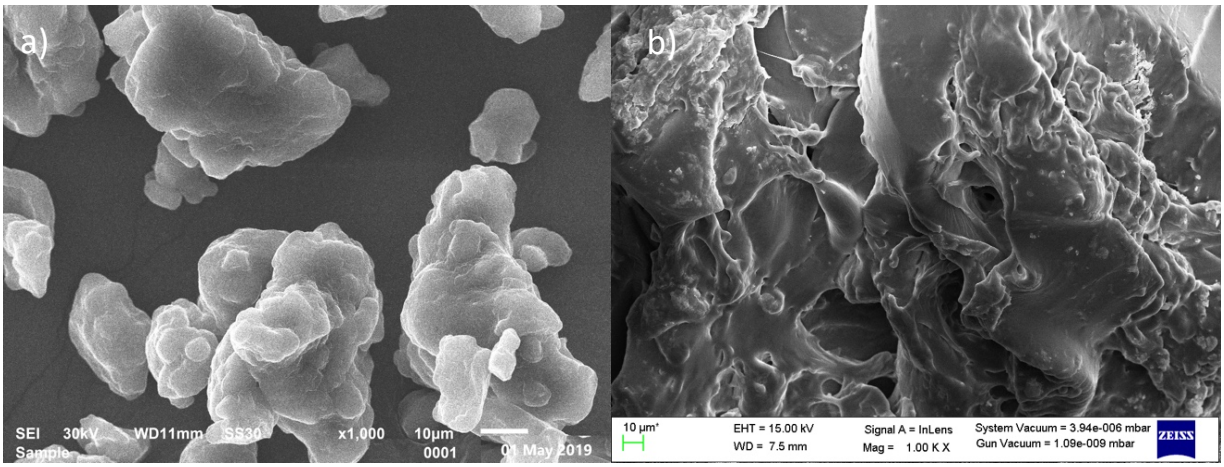

Figure 4.4 SEM micrographs of (a) CMTKG and (b) BSH

4.3.2.3 Thermal Analysis

Fig. 4.5 showed thermogravimetric analysis (TGA) thermograms of CMTKG and BSH which was done in order to establish its thermal stability. Weight loss pattern for CMTKG was observed in three different zones. The first zone showed a weight loss of 13.31 % for 30°C -240 °C which is simply due the removal of moisture present in CMTKG polymer. The second zone (240°C-602°C) observed prominent weight loss of 47.38 % due to the breakdown of CMTKG's polymeric backbone which was followed by the 602°C-900°C (third zone) with weight loss of 21.49 % [25].

However, in case of BSH, weight loss was found in four distinct zones. The weight loss of 19.38 %, at an initial zone of 30°C -295°C, is due to moisture removal from the polymeric network of

BSH. The second zone of 295°C-465°C showed a major weight loss of 24.95 % which was due to the degradation of the polymeric backbone [26]. Weight loss of 11.86 % was observed for the third zone (465°C-698°C). The reason for this weight loss may be the degradation of crosslinker and cross-linked bonds between hydroxyl groups of the polymer backbone present in the network of BSH. This was lastly followed up with 11.37 % weight loss by the fourth zone of complete combustion from 698°C to 900°C. It can be clearly seen that 50 % of CMTKG degraded at 365°C whereas for BSH, 50 % degradation was observed at 481°C . Moreover, the residual mass of BSH came out to be more than 32 % in comparison to the residual mass of CMTKG (17.82 %), henceforth, it can be concluded that BSH is more thermally stable than CMTKG, even at 900°C.

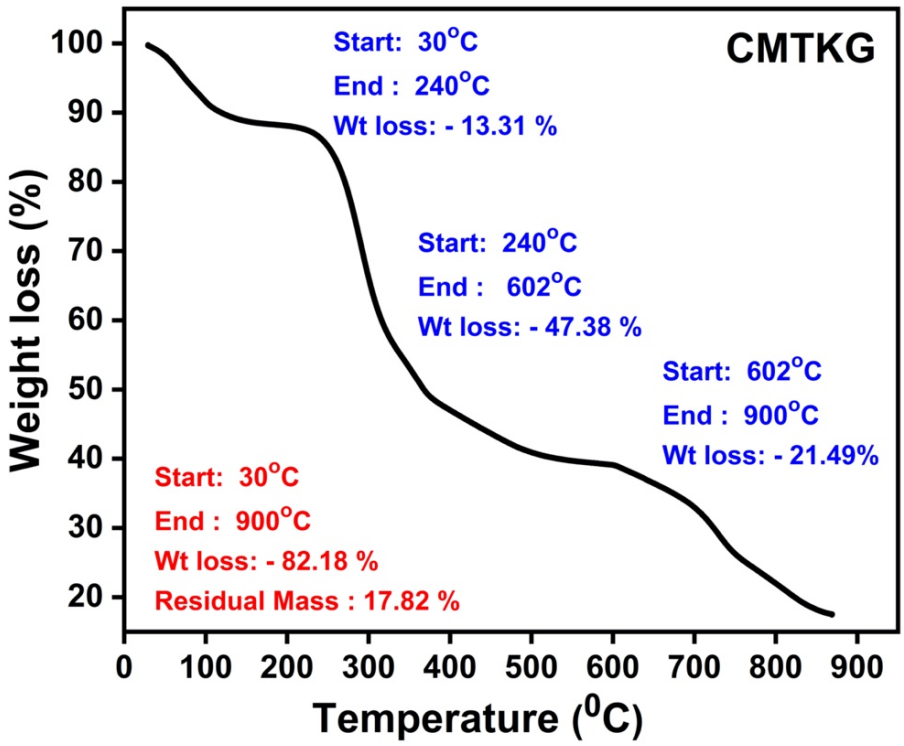

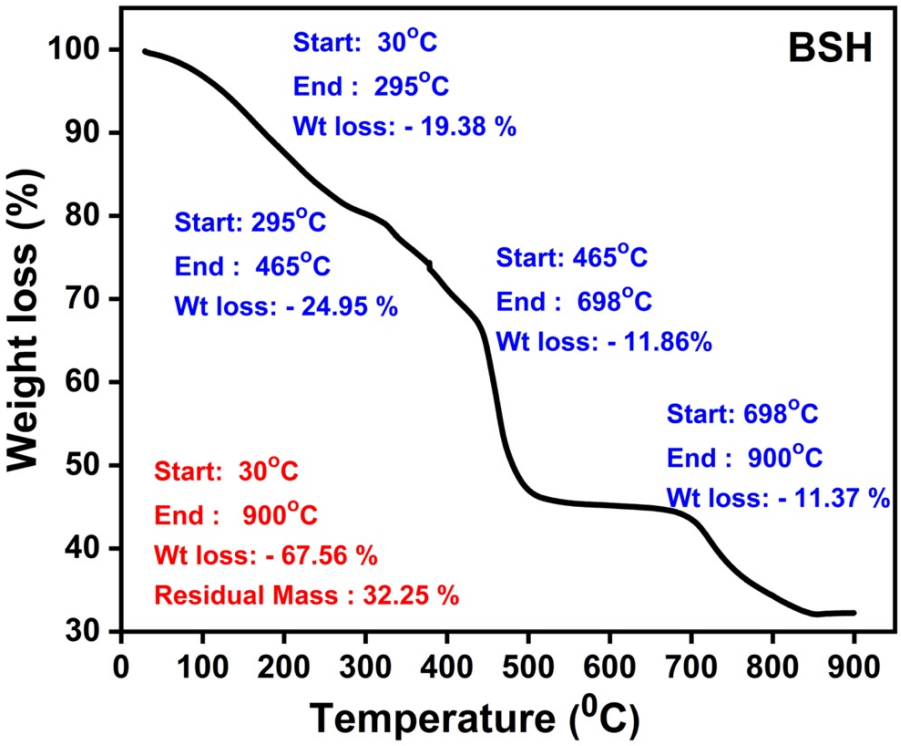

Figure 4.5 TGA thermogram of (a) CMTKG (b) BSH

4.3.3 Swelling studies

Swelling studies of BSH showed its immense range to swell by soaking water into its polymeric porous framework. The swelling index of BSH for various solvents such as standard saline solution (0.9 % NaCl), pH 12, 9 and 4, and distilled water all have been compiled in fig. 4.6. BSH took 42 h in order to attain swelling equilibrium and out of all used solvents, the highest swelling index of 466 g/g, was shown by distilled water.

For solutions at diverse pHs media, the water absorption capacity reduced significantly from pH 12-4. At pH 12, 402 g/g swelling index was observed by BSH which at pH 9 declined to 310 g/g and it got further lessened to 83 g/g at pH 4. The spaces present in the polymeric network of BSH might have broadened in alkaline conditions because of amplification in electrostatic repulsions

produced by the carboxylate (COO^-) anions in BSH [27]. However, the least swelling was observed for acidic medium, the reason being is that the protonation of COO^- anions decreases the anionic-anionic repulsion which results in the shrinkage of polymeric framework of BSH. Whereas, water absorbency of BSH was found to be fallen off significantly in 0.9% NaCl (49 g/g) solution case. This can be attributed to the existence of high ionic concentration which produced disparity in the surroundings of inner and outer phases of osmotic pressure and consequently entry of free water got obstructed inside the tri-dimensional network of BSH [28].

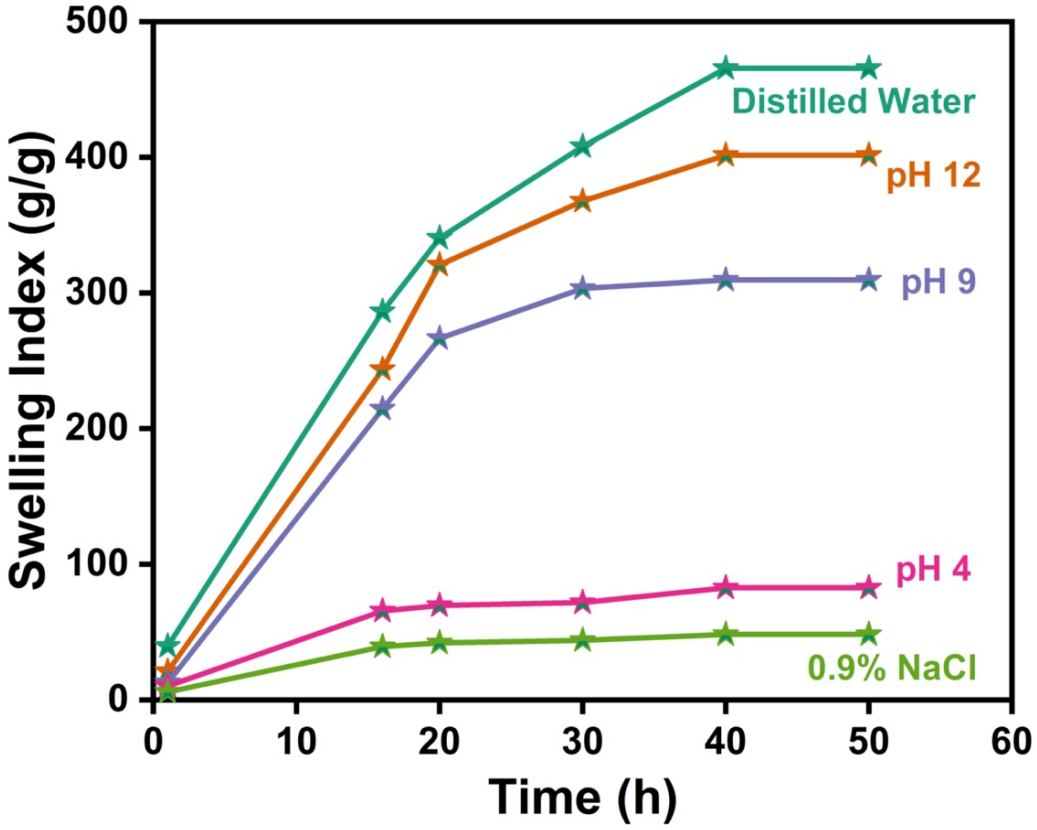

Figure 4.6 Swelling studies of BSH

4.3.4 Agricultural applications of BSH

Boron plays a key role in a diverse range of plant functions including maintenance of functional and structural integrity of biological membranes, cell wall formation, and pollination to name a few. Despite the importance and need of boron, boron is still the second most widespread micronutrient deficiency problem. In this work, BSH was synthesized in order to supply boron to the plants. Fig. 4.7 depicts the release rate of boron with respect to time whereas fig. 4.8 depicts the release kinetics of BSH.

4.3.4.1 Release study of boron in water and soil

The recurrent release of boron from BSH in water is shown in fig. 4.7(a). This study was done for the time span of 72 h where a linear trend was noticed to be followed in releasing boron from BSH. To start with 60 min, the boron release percentage was observed to be 14.1 %. However, the release percentage got amplified with time and in 72 h, the release percentage notably hiked up to 66.5 %.

In the case of soil also, the recurrent release was noticed to see the release of boron from BSH as depicted in fig. 4.7(b). This study was done for the time span of 80 days. In this case, also, a linear trend was observed in releasing boron from BSH. In soil, BSH exhibited 21.07 % for the 5^{th} day to further 40.77 % for the 30^{th} day, which significantly augmented on the 80^{th} day to 76.17 %. This slow release of boron in the soil can be discussed through three phases as visible in fig. 4.7(b). Initially, the release happened because of the wetting time of BSH while later on, diffusion of boron occurred from the outer layers of BSH and consequently, boron diffused through inner layers by setting equilibrium with the outer matrix of BSH. Hence, it can be concluded, in the case of soil also, the BSH showcased a moderate increase in the pattern of releasing boron.

a)

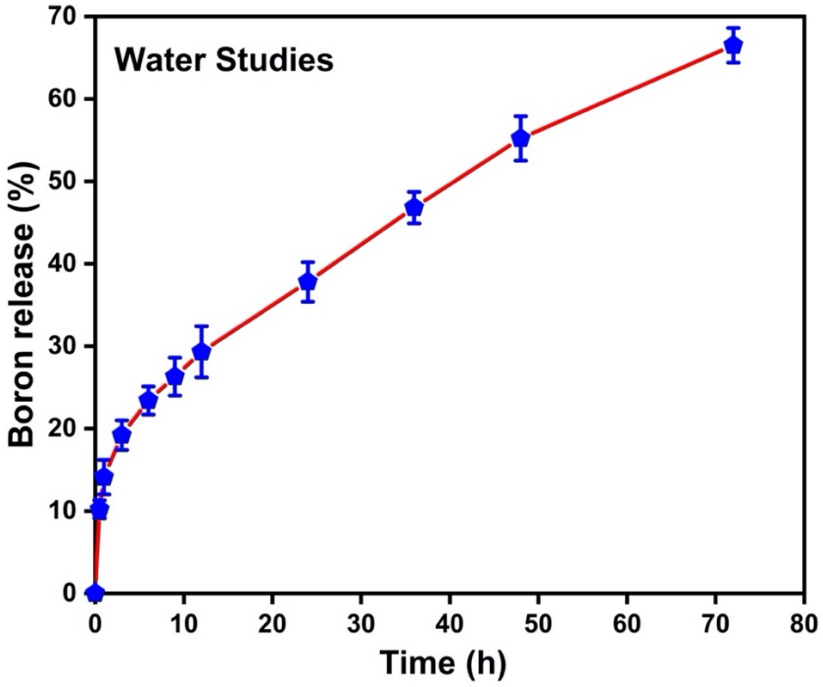

b)

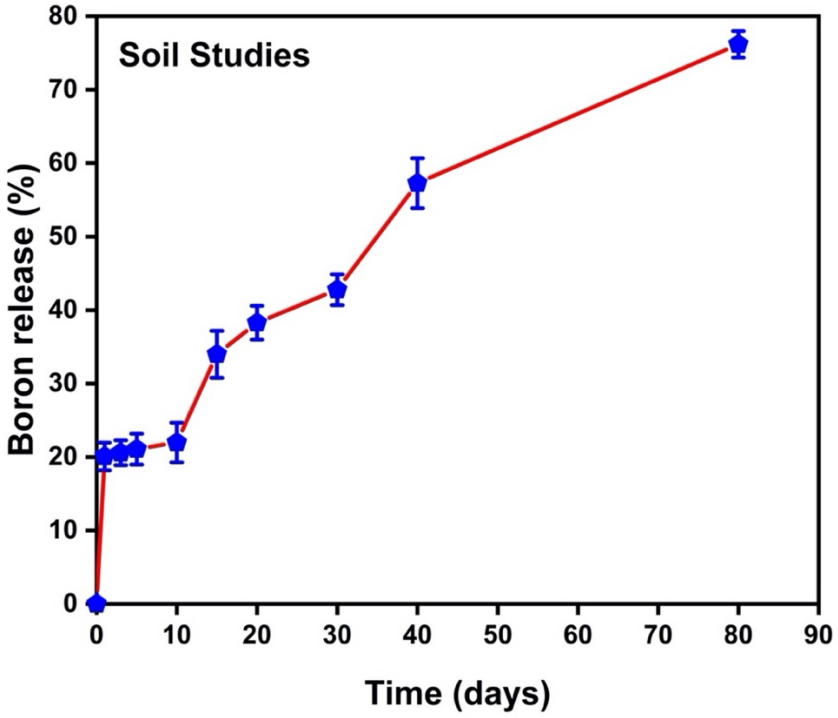

Figure 4.7 Cumulative release percentage of Boron with respect to time (a) in water (b) in soil

4.3.4.2 Release kinetics study of boron in water and soil

In order to elucidate the kinetics of boron release from the BSH, release data were carefully examined as per the various kinetic equations. The release data for water observed with the coefficient of determination values (R^2) nearer to one and hence it followed the Korsmeyer-Peppas model. However, for the release of boron, BSH followed the Higuchi model, with 0.94 as R^2, in the case of soil (Table 4.1).

Table 4.1 Mathematical Models used for the released kinetics from BSH

Model	Proposed Mechanism	Equation	Water		Soil		Ref.
			n	R^2	n	R^2	
Korsmeyer-Peppas	a. Fickian Diffusion (n<0.5) b. Non-Fickian Diffusion (0.89≥n≥0.45) c. Super case II	$\frac{M_t}{M_\infty} = kt^n$ k=kinetic constant n=diffusion exponent	0.35	0.99	0.31	0.88	[17]
First Order	Rate is dependent on the concentration of one reactant only	$\log\left(1 - \frac{M_t}{M_0}\right) = k_1 \cdot \frac{t}{2 \cdot 303}$	-	0.89	-	0.82	[18]

		K_1=release rate constant					
Higuchi	Fickian Diffusion	$\frac{M_t}{M_\infty} = k_H t^{\frac{1}{2}}$ k_H= kinetic constant	-	0.98	-	0.94	[19,20]

As per the value of R^2 given in Table 4.1, in case of water, the Korsmeyer-Peppas model was observed to be the best fit model which narrated the release kinetic behavior of boron from BSH (fig. 4.8(a)). Boron release in the water had 0.99 as R^2, and 0.35 as diffusion exponent value (n) which distinctly demonstrated solely Fickian diffusion taking place which happens via the simple method of diffusion through the hydrogel polymeric network [29].

However, the release of boron from BSH in soil showed its maximum R^2 to be 0.94 and that too for the Higuchi model (fig. 4.8(b)). This clearly indicated that the release mechanism was through Fickian diffusion, which suggested that boron could be considered to be diffused through the hydrogel framework network plainly by diffusion processes [19].

The predicted time (in days), as per the Olson equation [21] to release 50 %, 95 %, and 99 %, i.e. (T_{50}, T_{95}, and, T_{99}), of boron from developed BSH formulation, are listed along with other parameters in Table 4.2. Boron release in soil from BSH had higher T_{50}, T_{95}, and, T_{99} values, 38.08, 164.84, and, 274.72 days respectively, than the release of boron in water (1.29, 5.60, and, 9.33 days

in the same order). This difference can be attributed to the fact that in case of water, water is a limiting factor for release whereas, in soil, soil moisture is responsible for the release.

a)

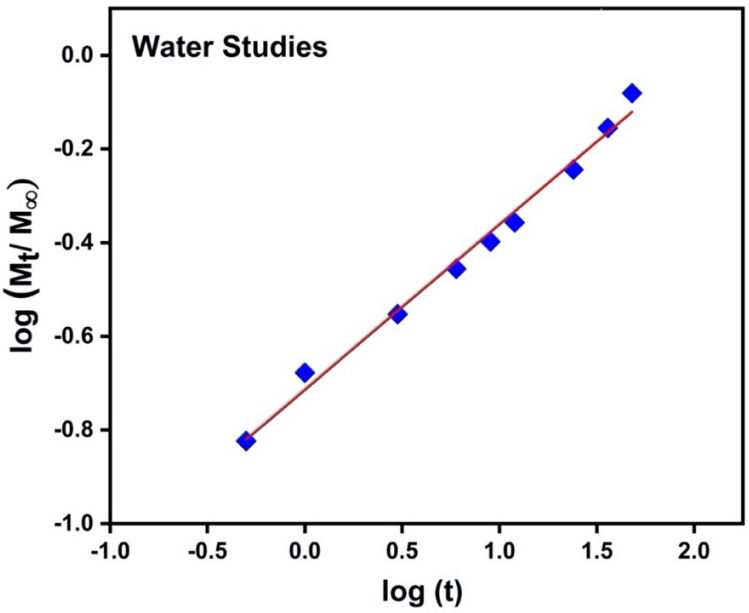

b)

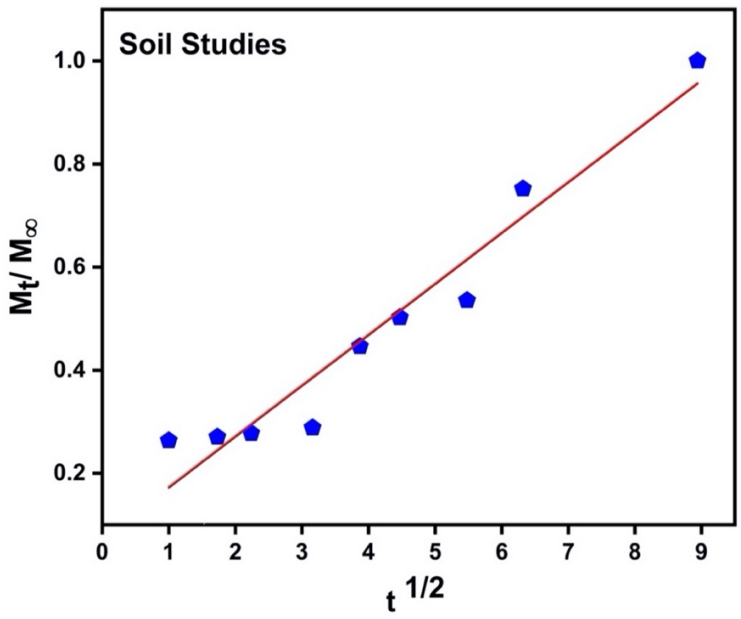

Figure 4.8 Release kinetics of Boron as per (a) Korsmeyer-Peppas model in water (b) Higuchi model in soil

Table 4.2 Relative time period (days) for the released amount of boron from BSH

	Olson equation	**R^2**	**k**	**T_{50}**	**T_{95}**	**T_{99}**
Water	$y = 17.618e^{0.527x}$	0.80	0.0224	1.29	5.60	9.33
Soil	$y = 21.813e^{0.018x}$	0.88	0.0183	38.08	164.84	274.72

4.4 Conclusions

Novel BSH was synthesized by doping boron into the CMTKG's cross-linked network by using *the in-situ* technique. The effect of different solutions like pH 4, 9, 12, distilled water, and standard saline solution, on the water capacity of BSH was studied. The highest swelling index was shown in the case of distilled water, up to 466 g/g. Release and kinetics studies of boron were observed in water and, as well as in soil and studied with respect to time. It is significant to note that in soil, BSH exhibited 21.07 % boron release for the 5^{th} day which notably enhanced to 76.17 % on the 80^{th} day. Release kinetic studies were also analyzed in both water and soil in which the Korsmeyer-

Peppas model fitted the best, in case of water, as its R^2 values were nearer to one. However, in the case of soil, the Higuchi model was found out to be the best fit. It also revealed that the release of boron from BSH, in water, was highly independent of the structure of the polymeric network as it followed the Fickian diffusion mechanism. The half-life (T_{50}), T_{95}, and, T_{99} values have also been determined using the Olson model, which clearly showed the boron release in soil (38.08, 164.84, and, 274.72 days, respectively) had higher values than the release of boron in water (1.29, 5.60, and, 9.33 days in the same order).

These attractive qualities of BSH make it a powerful competitor in the field of horticulture as a water-rationing operator as well as above all as a boron micronutrient transporter.

4.5 References

1. Zhong, K.; Lin, Z.T.; Zheng, X.L.; *et al.* Starch derivative-based superabsorbent with integration of water-retaining and controlled-release fertilizers. *Carbohydr. Polym.* **92**(2):1367–76; 2013. Doi: 10.1016/j.carbpol.2012.10.030.
2. Xie, L.; Liu, M.; Ni, B.; *et al.* Slow-release nitrogen and boron fertilizer from a functional superabsorbent formulation based on wheat straw and attapulgite. *Chem. Eng. J.* **167**(1):342–8; 2011. Doi: 10.1016/j.cej.2010.12.082.
3. Shorrocks, V.M. The occurrence and correction of boron deficiency. *Plant Soil* **193**(2):121–48; 1997. Doi: 10.1023/A:1004216126069.
4. Marschner, H. *Mineral nutrition of higher plants*. 2nd ed. 1995.
5. Gupta, U.; Solanki, H.A. Impact of boron deficiency on plant growth. *Int. J. Bioassays* **2**(07):1048–50; 2013.

6. Brown, P.H.; Bellaloui, N.; Wimmer, M.A.; *et al.* Boron in Plant Biology. *Plant Biol.* **4**(2):205–23; 2002. Doi: 10.1055/s-2002-25740.

7. Cakmak, I.; Römheld, V. Boron deficiency-induced impairments of cellular functions in plants. *Plant Soil* **193**(2):71–83; 1997. Doi: 10.1023/A:1004259808322.

8. Thombare, N.; Mishra, S.; Siddiqui, M.Z.; *et al.* Design and development of guar gum based novel , superabsorbent and moisture retaining hydrogels for agricultural applications. *Carbohydr. Polym.* **185**(2018):169–78; 2018.

9. Mo, C.; Shu-quan, Z.; Hua-Min, L.; *et al.* Synthesis of poly(acrylic acid)/sodium humate superabsorbent composite for agricultural use. *J. Appl. Polym. Sci.* **102**(6):5137–43; 2006. Doi: 10.1002/app.24661.

10. Abedi-Koupai, J.; Sohrab, F.; Swarbrick, G. Evaluation of hydrogel application on soil water retention characteristics. *J. Plant Nutr.* **31**(2):317–31; 2008. Doi: 10.1080/01904160701853928.

11. Bortolin, A.; Serafim, A.R.; Aouada, F.A.; *et al.* Macro- and Micronutrient Simultaneous Slow Release from Highly Swellable Nanocomposite Hydrogels. *J. Agric. Food Chem.* **64**(16):3133–40; 2016. Doi: 10.1021/acs.jafc.6b00190.

12. Khushbu; Warkar, S.G. Potential applications and various aspects of polyfunctional macromolecule- carboxymethyl tamarind kernel gum. *Eur. Polym. J.* **140**(July):110042; 2020. Doi: 10.1016/j.eurpolymj.2020.110042.

13. Khushbu; Warkar, S.G.; Kumar, A. Synthesis and assessment of carboxymethyl tamarind kernel gum based novel superabsorbent hydrogels for agricultural applications. *Polymer (Guildf).* **182**(September):121823; 2019. Doi: 10.1016/j.polymer.2019.121823.

14. Warkar S.G.; A.P., G. Synthesis, characterization and swelling properties of poly

(Acrylamide-cl-carboxymethylguargum) hydrogels. *Int. J. Pharma Bio Sci.* **6**(1):516–29; 2015.

15. Wolf, B. Improvements in the azomethine-H method for the determination of boron. *Commun. Soil Sci. Plant Anal.* **5**(1):39–44; 1974. Doi: 10.1080/00103627409366478.

16. Singh, D.; Chhonkar, P.K.; Dwivedi, B.S. *Manual on soil, plant and water analysis.* Westville Publishing House.; 2005.

17. Korsmeyer, R.W.; Von Meerwall, E.; Peppas, N.A. Solute and penetrant diffusion in swellable polymers. II. Verification of theoretical models. *J. Polym. Sci. Part B Polym. Phys.* **24**(2):409–34; 1986. Doi: 10.1002/polb.1986.090240215.

18. Serra, L.; Doménech, J.; Biomaterials, N.P.-; *et al.* Drug transport mechanisms and release kinetics from molecularly designed poly (acrylic acid-g-ethylene glycol) hydrogels. *Biomaterials* **27**:5440–51; 2006.

19. Siepmann, J.; Peppas, N.A. Higuchi equation: Derivation, applications, use and misuse. *Int. J. Pharm.* **418**(1):6–12; 2011. Doi: 10.1016/j.ijpharm.2011.03.051.

20. Higuchi, T. Mechanism of sustained-action medication. Theoretical analysis of rate of release of solid drugs dispersed in solid matrices. *J. Pharm. Sci.* **52**(12):1145–9; 1963. Doi: 10.1002/jps.2600521210.

21. Olson, J.S. Energy Storage and the Balance of Producers and Decomposers in Ecological Systems. *Ecology* **44**(2):322–31; 1963. Doi: 10.2307/1932179.

22. Trivedi, J.H. Synthesis, characterization, and swelling behavior of superabsorbent hydrogel from sodium salt of partially carboxymethylated tamarind kernel powder- g - PAN. *J. Appl. Polym. Sci.* **129**(4):1992–2003; 2013. Doi: 10.1002/app.38910.

23. Reddy, B.V.; Rao, G.R. Vibrational spectra and modified valence force field for N,N'-

methylenebisacrylamide. *Indian J. Pure Appl. Phys.* **46**(9):611–6; 2008.

24. Sarkar, D.J.; Singh, A.; Mandal, P.; *et al.* Synthesis and Characterization of Poly (CMC-g-cl-PAam/Zeolite) Superabsorbent Composites for Controlled Delivery of Zinc Micronutrient: Swelling and Release Behavior. *Polym. - Plast. Technol. Eng.* **54**(4):357–67; 2015. Doi: 10.1080/03602559.2014.958773.

25. Pal, S.; Sen, G.; Mishra, S.; *et al.* Carboxymethyl tamarind: Synthesis, characterization and its application as novel drug-delivery agent. *J. Appl. Polym. Sci.* **110**(1):392–400; 2008. Doi: 10.1002/app.28455.

26. Dias, R.J.; Havaldar, V.D.; Mali, K.K.; *et al.* sustained delivery of aceclofenac Interpenetrating networks of carboxymethyl tamarind gum and chitosan for sustained delivery of aceclofenac (October); 2017. Doi: 10.12991/mpj.2017.20.

27. Chang, C.; Duan, B.; Cai, J.; *et al.* Superabsorbent hydrogels based on cellulose for smart swelling and controllable delivery. *Eur. Polym. J.* **46**(1):92–100; 2010. Doi: 10.1016/j.eurpolymj.2009.04.033.

28. Zhao, Y.; Kang, J.; Tan, T. Salt-, pH- and temperature-responsive semi-interpenetrating polymer network hydrogel based on poly(aspartic acid) and poly(acrylic acid). *Polymer (Guildf).*; 2006. Doi: 10.1016/j.polymer.2006.08.056.

29. Ritger, P.; Release, N.P. A simple equation for description of solute release I. Fickian and non-fickian release from non-swellable devices in the form of slabs, spheres, cylinders or discs. *J. Control. Release* **5**:23–6; 1987.

Chapter 5

ZINC MICRONUTRIENT LOADED SUPERABSORBENT HYDROGELS: CONTROLLED RELEASE AND RELEASE KINETICS STUDIES FOR AGRICULTURAL APPLICATIONS

5.1 Introduction

The demand for the resurgence of industrial agriculture all around the world is increasing with the expansion of the global population, so as to keep up the pace with the growing inhabitants on earth. For achieving high agricultural productivity, an adequate supply of water and micronutrients is very important. Moreover, the supply of micronutrients is very critical because limits of their minimum availability and toxicity in the soil are narrower as compared to major nutrients, and hence, they play a vital role in securing the productivity of crops by influencing their quality and yield. Therefore, specific micronutrients should be made available to plants in a controlled fashion so as to attain an ideal performance. Conventionally, nutrients are applied to put a frequent and heavy dose of fertilizers to the crop. There are several drawbacks in the conventional means of micronutrient applications such as high labor cost, difficulty in control release, low nutrient efficiency, and environmental pollution [1,2]. Different technological and scientific strategies have been developed over the years in order to overcome these hurdles, such as controlled or slow-release systems. Various materials have been tested for this goal, among which superabsorbent hydrogels with the added advantage of moisture retention, protrude as a promising matrix to supply agricultural nutrients [3].

Superabsorbent hydrogels are the tri-dimensional cross-linked structures that can imbibe more than 300 times its weight in water [4]. It has fetched a lot of consideration in this context because of its

controlled or slow-release properties [5]. They have been found effective in enhancing the physical properties of soil like water holding capacity, bulk density, porosity and hence proved their potential in being an excellent aid for drought-prone areas [6–11]. Their utility as the carrier of fertilizers for their controlled release has also been reported [12–15] but there is little published work on the slow or controlled release of micronutrients from superabsorbent hydrogels.

Zinc is an essential micronutrient for crops as it plays a vital role in many physiological functions of plants. Zinc deficiency can affect plants by increasing crop maturity period, stunting its growth, decreasing the number of tillers, small leaves and chlorosis, spikelet sterility, and inferior quality of products [16]. Hence, zinc plays a notable role in plant metabolism by affecting the activities of carbonic anhydrase, hydrogenase, synthesis of cytochrome, and stabilization of ribosomal fractions [17] which further affects the integrity of cellular membranes, pollen formation, and protein synthesis and auxin synthesis in plants [18]. Zinc deficiency causes “Khaira” disease in rice grown in the calcareous soil of north India. Despite the need for this critical micronutrient, zinc is found to be the most deficient micronutrient in the soil. Hence, it has become imperative to do needful research in this direction. Also, very limited literature is available as utilization of hydrogels for nourishing the soil with zinc [5]. Keeping in view the research gaps and need to ensure steady supply of zinc micronutrient to the crops, to the best of our knowledge, CMTKG based hydrogel is being used for the first time as a matrix for controlled release of zinc [19].

This study discusses the modification of Carboxymethyl Tamarind Kernel Gum (CMTKG) based superabsorbent hydrogels by *in situ* incorporation of zinc source and its performance as a zinc micronutrient carrier vehicle for agricultural applications. The objectives of this study were to assess: (i) the swelling index of zinc loaded superabsorbent hydrogel (ZSAH) at various pHs

solutions, saline solution and distilled water; (ii) the release studies of zinc from ZSAH in water; (iii) the release studies of zinc from ZSAH in the soil; (iv) the release kinetic studies of ZSAH in both, water and soil.

5.2 Experimental Section

5.2.1 Materials

CMTKG (0.20˚) was gifted by Hindustan Gum and Chemicals Ltd., Haryana, India. Acrylic acid (AA, CDH, New Delhi), Zinc Chloride (ZC, Merck, Germany), Potassium persulfate (KPS, Fischer Scientific, Mumbai), Sodium hydroxide (Fischer Scientific, Mumbai), N,N'-methylene bis(acrylamide) (MBA, Merck, Germany) were used as received. Distilled water was used for the preparation of solutions. Sodium acrylate was further prepared by mixing desired ratios of above mentioned acrylic acid (7 mL) and sodium hydroxide pellets (4 gm).

5.2.2 Synthesis of ZSAH

Zinc was loaded by *in situ* incorporation technique to the CMTKG based superabsorbent hydrogel. All the polymerization and cross-linking reactions took place at 25°C. In brief, CMTKG (0.9% w/w) was weighed and put in a beaker having distilled water and sodium acrylate (26% w/w). To this, a measured quantity of Zinc Chloride (5% w/w) was added and stirred for one hour. Afterward, a fixed amount of KPS (0.2% w/w) and MBA (0.05% w/w) were added and further stirred constantly for another one hour. After that, the whole mixture was transferred to the polyethylene tubes which were kept at 60°C in a hot water bath for 2 hours. Later on, the polyethylene tubes were released vertically to get the desired ZSAH, and then ZSAH was cut into

small discs for further use. These discs were initially dried at room temperature for three days and afterward at 50°C in a vacuum oven till constant is achieved [20].

5.2.3 Swelling studies

Swelling studies of the synthesized ZSAH were done by the gravimetric method. Completely dried ZSAH samples (0.19 g) were weighed and immersed in solutions of pH 12, 9, and 4 (all the solutions were made by adding HCl or NaOH in dilute form), 0.9% NaCl solution (standard saline solution) and distilled water.

After a regular time interval, the swollen ZSAH were weighed post wiping off the surface water with the help of a filter paper. All experiments were done in triplicate.

The following equation [21] was used in calculating the swelling indexes.

$$\text{Swelling Index} = (W_{sh} - W_{dh}) / W_{dh}$$

where, W_{sh} = weight of equilibrium swollen ZSAH

W_{dh} = initial weight of the dried ZSAH

5.2.4 Characterization

5.2.4.1 Fourier-transform Infrared (FTIR) spectroscopy

KBr pellet method was used for recording the FTIR (Fourier-transform Infrared) spectra of CMTKG, ZC, and ZSAH. It was done in the solid phase by using an FTIR spectrophotometer (Model: PerkinElmer spectrum version 10.5.3).

5.2.4.2 Scanning electron microscopy (SEM)

Analysis of CMTKG and ZSAH's surface morphology was done by SEM (Model: JEOL JSM-6610LV).

5.2.4.3 Thermal Analysis

PerkinElmer TGA was used for carrying out the thermo-gravimetric analysis (TGA) of CMTKG and ZSAH. For this purpose, 10°C/min of uniform heating rate and N_2 atmosphere from 25°C to 900°C were used.

5.2.5 Application of ZSAH as a zinc micronutrient carrier

The ZSAH synthesized was examined for the application in the sphere of agriculture for the controlled release of zinc micronutrient. It was established by studying and calculating the release behavior pattern along with the kinetics of ZSAH in water and as well in the soil for 72 hours and 80 days, respectively. The composition of soil carried slit & clay 0.7%, Sand 89% and showed bulk density 1.32 g/cm^3, particle density 2.625 g/cm^3, which was collected from Delhi Technological University, New Delhi, India.

5.2.5.1 Release study of zinc in water

An accurately weighed ZSAH (200 mg, particle size: 100-150 mesh) was put into beakers containing 1 L of water under constant stirring. 2 ml of solution was taken out after a regular interval of time namely, 1, 2, 3, 4, 5, 6, 7, 8, 9, 10, 11, 12, 24, 48 and 72 hours. The sample solution was then analyzed for zinc concentration with the help of AAS (Spectrum ZXPRESS 8000). The results were then compiled with respect to time. The experiments were carried out in triplicates.

5.2.5.2 Release study of zinc in soil

An accurately weighed ZSAH (200 mg, particle size: 100-150 mesh) was taken in nylon sieve bags (Chiffon woven fabric: 200 mesh) and each was kept in soil (0.2 Kg) in pots. Throughout the study, the moisture of soil was being maintained and samplings were done periodically (1, 3, 5, 10, 15, 20, 30, 40, and 80 days). The soil samples were taken out post uniform mixing (after removing nylon bag) one by one at pre-fixed time intervals. These samples were dried in an oven at 100°C overnight and weighed. 10 g of each soil samples were treated with 20 ml of DTPA (Diethylenetriamine pentaacetate) and shaken for 2 h. The supernatant solution was then filtered using Whatman filter paper-42 and analyzed in AAS. The experiments were carried out in triplicates.

5.2.5.3 Release kinetic studies of ZSAH in water and soil

Various models including the Korsmeyer-Peppas Model have been reported over time for estimating the release of a mobile agent from hydrogel as a function of time.

Zinc release data, in water as well as in soil, were fitted to different forms of kinetic models in order to understand zinc release mechanism namely, the Korsmeyer-Peppas model [22], Higuchi model [23], first-order equation [24], and Olson model [25]. All these models are framed in Table 5.1. The model having the highest coefficient of determination (R^2) value has been considered as the best fit model.

5.3 Results and discussions

5.3.1 Synthesis of ZSAH

In an endeavor to fabricate ZSAH, zinc, in the form of ZC, was incorporated into the CMTKG cross-linked network (SAH) via *in-situ* mechanism. The hypothetical representation incorporation of ZC ions in the three-dimensional network of SAH is illustrated through fig 5.1 whereas fig 5.2 is the schematic representation for the synthesis of ZSAH.

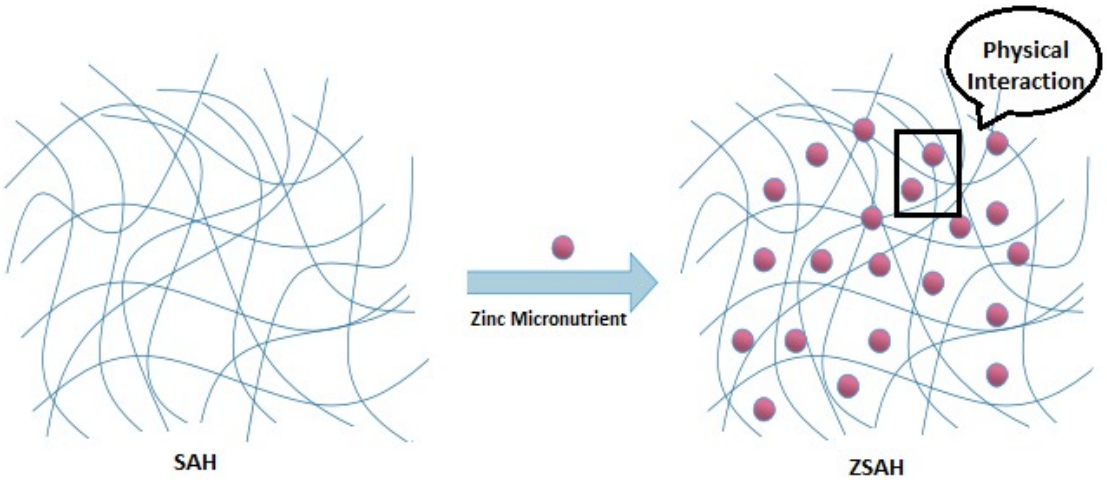

Figure 5.1 Pictorial representation of the formation of ZSAH

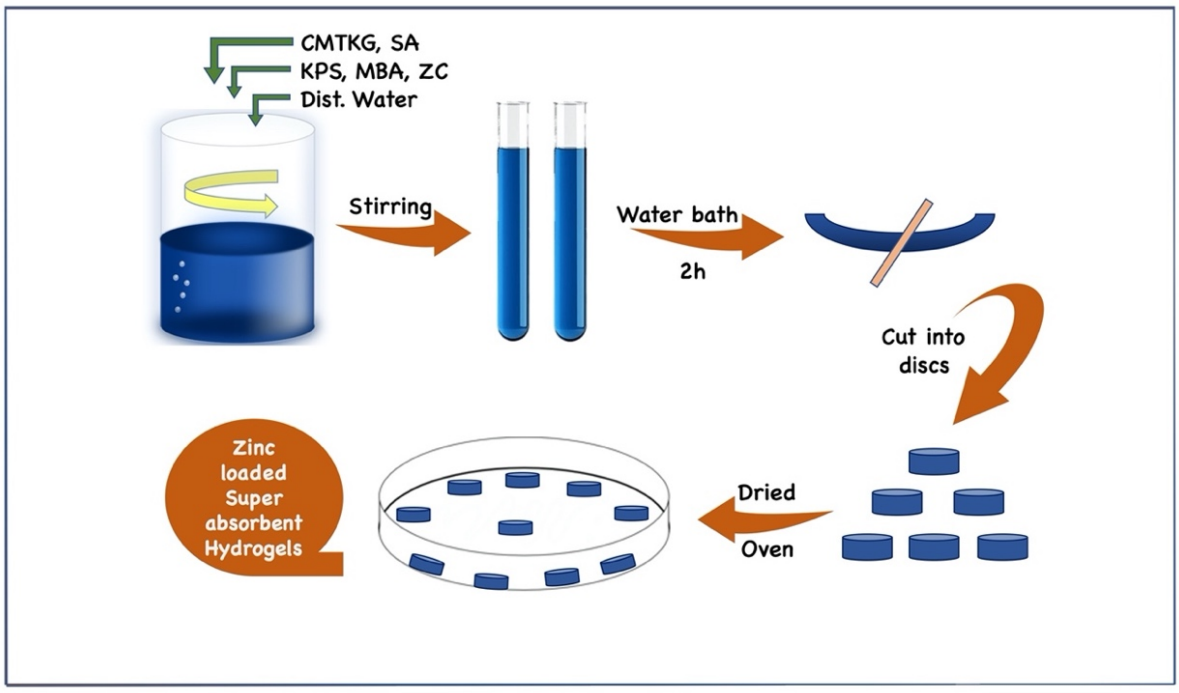

Figure 5.2 Schematic representation for the synthesis of ZSAH

5.3.2 Swelling studies

Swelling studies of ZSAH showed its immense capacity to swell by absorbing water into its porous framework. The swelling index of ZSAH for various solvents viz., 0.9 % NaCl (standard saline solution), pH 12, 9 and 4, and distilled water have been compiled in fig. 5.3. ZSAH took 40 h in order to attain swelling equilibrium, where, amongst out of all used swelling media, the highest swelling index was observed by the distilled water (410 g/g).

For solutions of diverse pH, the water absorption capacity amplified significantly from pH 4-12. At pH 4, 90 g/g swelling index was observed by ZSAH which at pH 9 increased to 257 g/g and it got further increased to 334 g/g at pH 12. The lowest swelling was observed for acidic medium, the reason being improper ionization of the crosslinked network which resulted in a collapsed state of ZSAH. However, the spaces present in the network of ZSAH might have widened in case of alkaline conditions because of elevation in electrostatic repulsions produced by the carboxylate (COO^-) anions in ZSAH [26]. Whereas, water absorbency of ZSAH was found to be dropped substantially in 0.9% NaCl solution case (30 g/g) which can be attributed to the existence of high ionic concentration which produced disparity in the surroundings of inner and outer phases of osmotic pressure and consequently entry of free water got obstructed inside the tridimensional network of ZSAH [27].

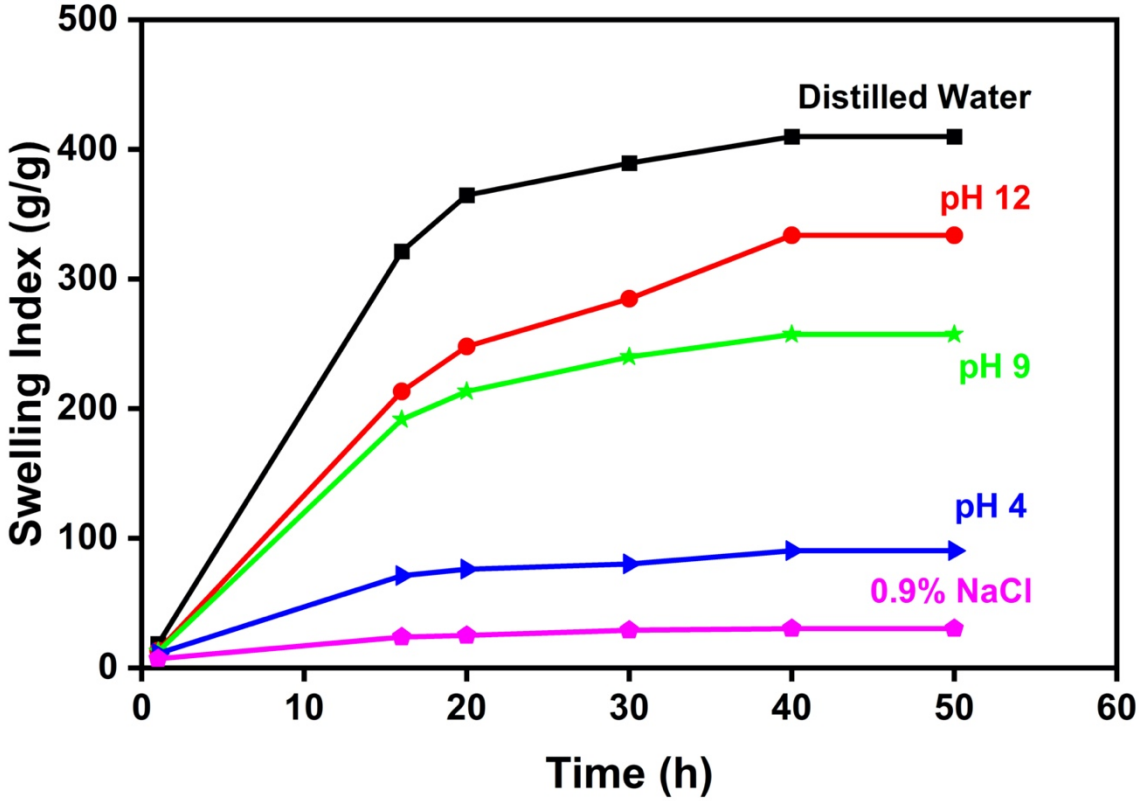

Figure 5.3 Swelling studies of ZSAH

5.3.3 Characterization

5.3.3.1 FTIR spectroscopy

FTIR spectra of CMTKG, $ZnCl_2$ and ZSAH are shown in fig. 5.4. CMTKG showed a broad band for -OH stretching vibrations at 3428 cm^{-1}. The asymmetric and symmetric vibrations for $-COO^-$ moiety was shown at 1631 cm^{-1} and 1415 cm^{-1}, respectively [28]. In ZSAH spectrum, a broad band (3418 cm^{-1}) is associated with -OH stretching vibration whereas, around 1568 cm^{-1} and 1410 cm^{-1}, shows asymmetric and symmetric vibrations, respectively for $-COO^-$ moiety. A sharp transmittance peak around 1568 cm^{-1} was observed for C=O stretching vibration of SA while the

peak (1317 cm^{-1}) and a broad band (627 cm^{-1}) was linked with C-N and O=C-N groups of MBA [29]. The appearance of bands at 627 cm^{-1} and 1039 cm^{-1} can be associated with the CMTKG skeleton. It is notable mentioning that no significant peak was observed in the FTIR spectra of ZSAH as evident from the absence of any peak related to $ZnCl_2$. Considering this behavior, it can be concluded that only physical interactions (weak interactions) took place between zinc micronutrient and CMTKG cross-linked network. This further proved that the reversible retention of zinc micronutrient in the hydrogel matrix is unlikely to occur [5].

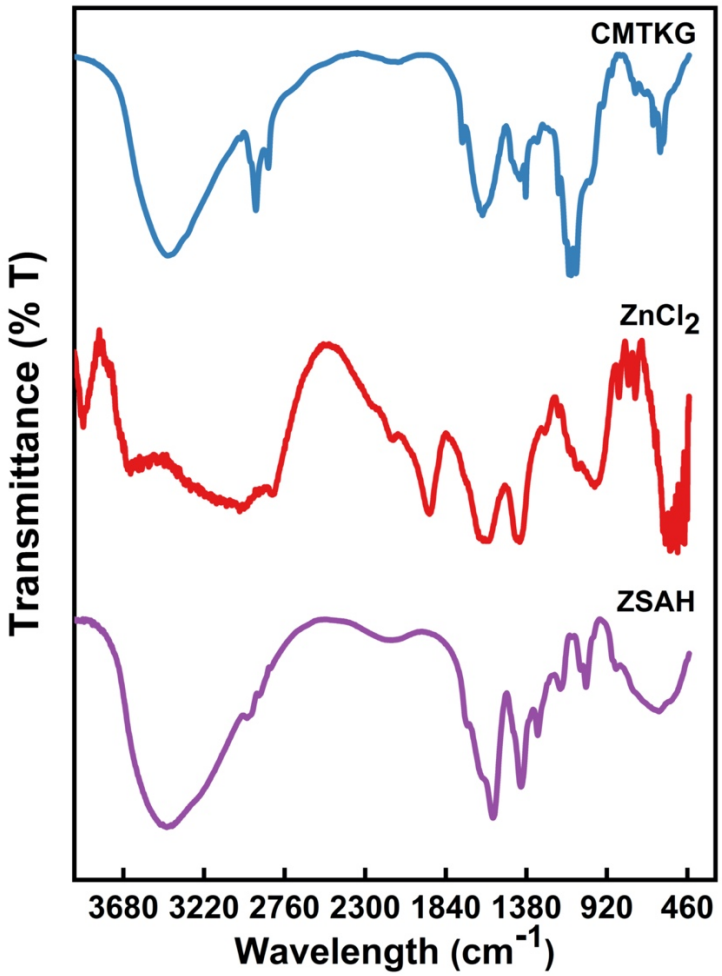

Figure 5.4 FTIR of CMTKG, $ZnCl_2$ and ZSAH

5.3.3.2 Scanning electron microscopy (SEM)

SEM micrographs of CMTKG (a, b) and ZSAH (c, d), at different magnifications, are shown in fig. 5.5. The morphological investigation of the ZSAH has been done so as to see the morphological changes in ZSAH as an effect of zinc incorporation. For a comparative study, SEM of CMTKG has also been shown in fig. 5.6. This analysis of CMTKG showed non-porous, rough and compact surface whereas ZSAH showed spongy surface, interspatial voids, and distinct boundaries. However, the addition of zinc seemed to influence the morphology in the form of aggregated fractured appearance of ZSAH. This can be attributed to the intercalation of zinc into the matrix of cross-linked network of CMTKG [5].

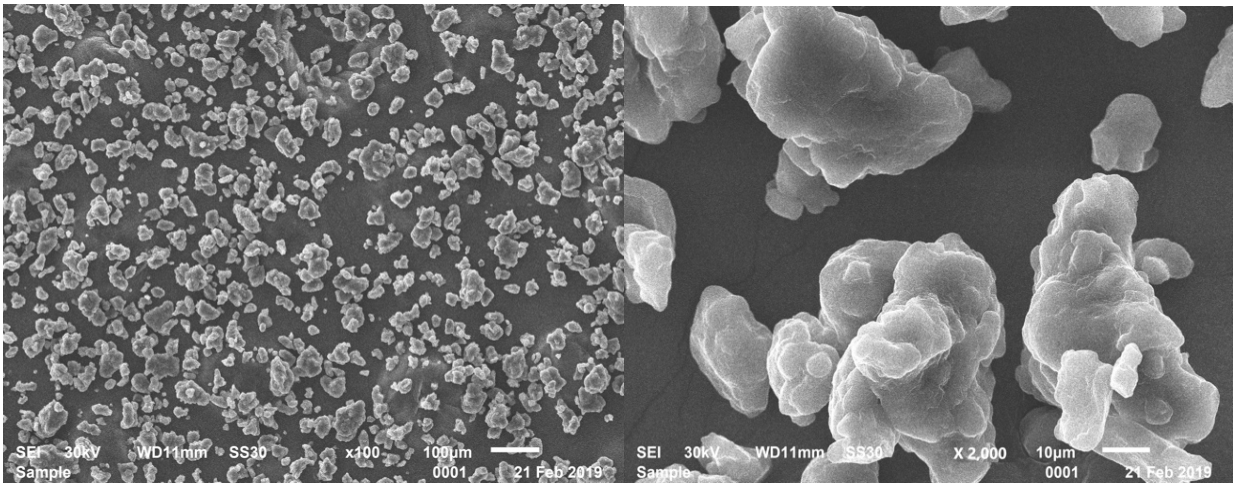

(a) (b)

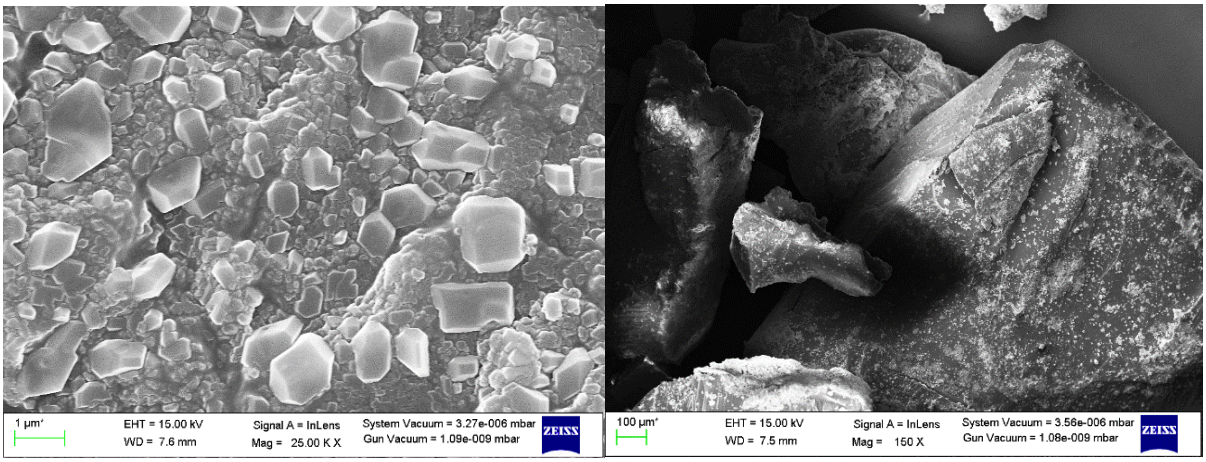

(c) (d)

Figure 5.5 SEM micrographs of (a), (b) CMTKG and (c), (d) ZSAH

5.3.3.3 Thermal Analysis

To confirm the thermal stability of the CMTKG and ZSAH, thermogravimetric analysis (TGA) was done. Fig. 5.7 showed TGA thermograms of CMTKG (fig. 5.6(a)) and ZSAH (fig. 5.7(b)). Weight loss was found in three distinct zones in the case of CMTKG. The very first zone (30°C-240°C) showed weight loss of 13.31 % due to the removal of moisture content from CMTKG whereas, degradation of polymeric backbone could be attributed to the major weight loss of 47.38 % for the second zone (240°C-602°C) followed by the third and the final weight loss (21.49 %) in the range of 602°C-900°C [30].

However in the case of ZSAH, the weight loss pattern was found out in four zones, the weight loss of 15.34 %, at an initial zone of 30°C-262°C, is due to the removal of moisture from the cross-linked network of ZSAH. The second zone of 262°C-379°C showed a weight loss of 5.65 % which was for degradation of cross-linked bonds between hydroxyl groups of the polymer backbone and crosslinker present in the network of ZSAH. Major weight loss of 24.97 % was observed for the

third zone (379°C-494°C) which can be attributed to the degradation of the main polymeric backbone namely, carboxymethyl and hydroxyl group of CMTKG [31]. This was lastly followed by the fourth zone of complete combustion from 494°C to 900°C with 18.53 % weight loss. It can be clearly seen that 50 % of ZSAH degraded at 598°C while for CMTKG, 50 % of degradation observed at 365°C. It may also be noted here that the residual mass left was also found out to be more than 35 % which was far more than the residual mass left in the case of CMTKG (18 %). Hence, one may conclude ZSAH to be highly thermally stable than CMTKG.

a)

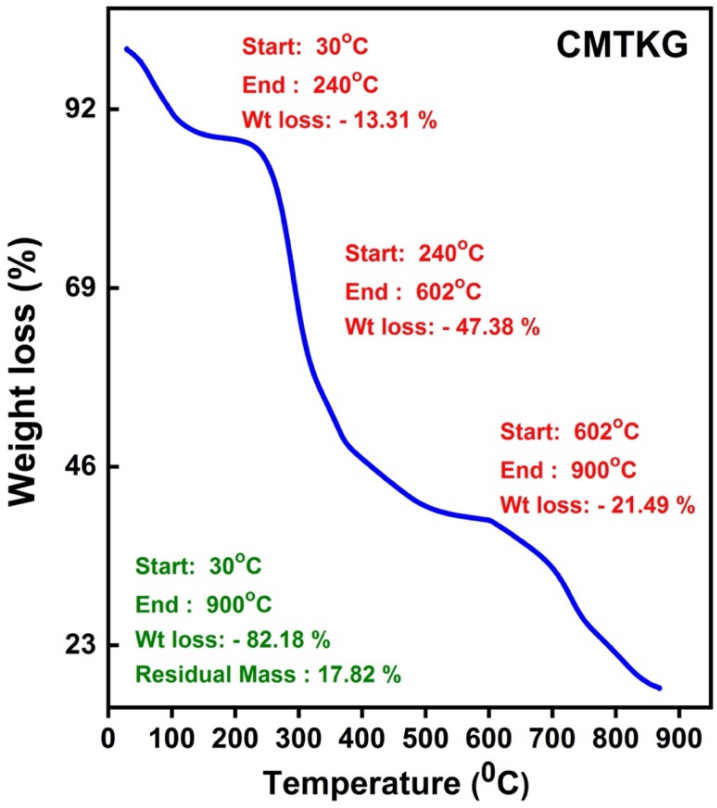

b)

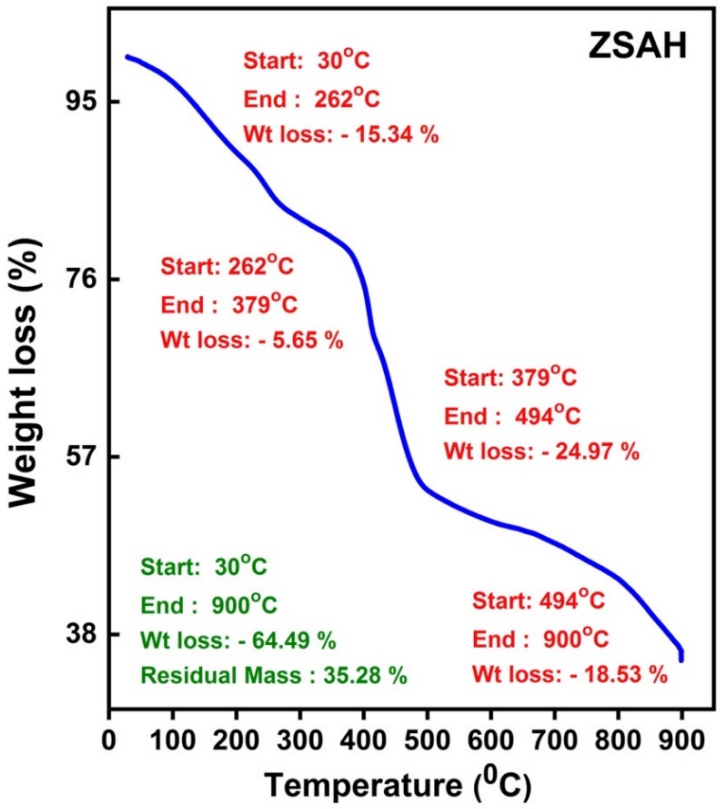

Figure 5.6 TGA thermogram of (a) CMTKG and (b) ZSAH

5.3.4 Agricultural applications of ZSAH

Zinc is primarily the utmost essential micronutrient for plants but even then earth is still suffering from the valuable micronutrients and zinc being the number one on the most deficient micronutrient. In this work, ZSAH was fabricated in order to provide zinc to the plants. Fig. 5.7 depicts the release rate of zinc with respect to time while fig. 5.8 depicts the release kinetics of ZSAH.

5.3.4.1 Release study of zinc in water and soil

The periodic release of zinc from ZSAH in water is shown in fig. 5.7(a). This study was done for the duration of 72 h, the release of zinc was observed to follow a linear trend. Initially at the time period of 30 mins., zinc release percentage was found out to be just 12.2 %. With time, the release percentage got steeply increased and in 72 h, the release percentage reached up to 54.2 %.

In the case of soil also, the periodic release was analyzed to see the release of zinc from ZSAH which is depicted in fig. 5.7(b). This study was done for the duration of 80 days. In this case also, a linear trend was shown by ZSAH in releasing zinc. In soil, ZSAH exhibited 59.28 % for the 10^{th} day which notably enhanced to 83.68 % on the 80^{th} day. Hence, in the case of soil also, ZSAH showed a gradual increase in releasing zinc. It is significant to mention that the obtained result from the cumulative release of zinc through ZSAH in water was found out to be greater in comparison to the release of zinc in soil. For a time period of 72 h, the release was found to be 54.2 % in water in contrast to just 42.28 % in soil. The controlled release of zinc in the soil could be explained through three phases as seen in fig. 5.7(b). At first, the release occurred as a result of the wetting time of ZSAH whereas later on, zinc happened to release from the external layers of ZSAH due to the diffusion mechanism followed by, zinc diffused through inward layers by setting equilibrium with the external network of ZSAH. Thus, it can be inferred, in the soil case also, the ZSAH displayed a moderate increment in the pattern of releasing zinc.

a)

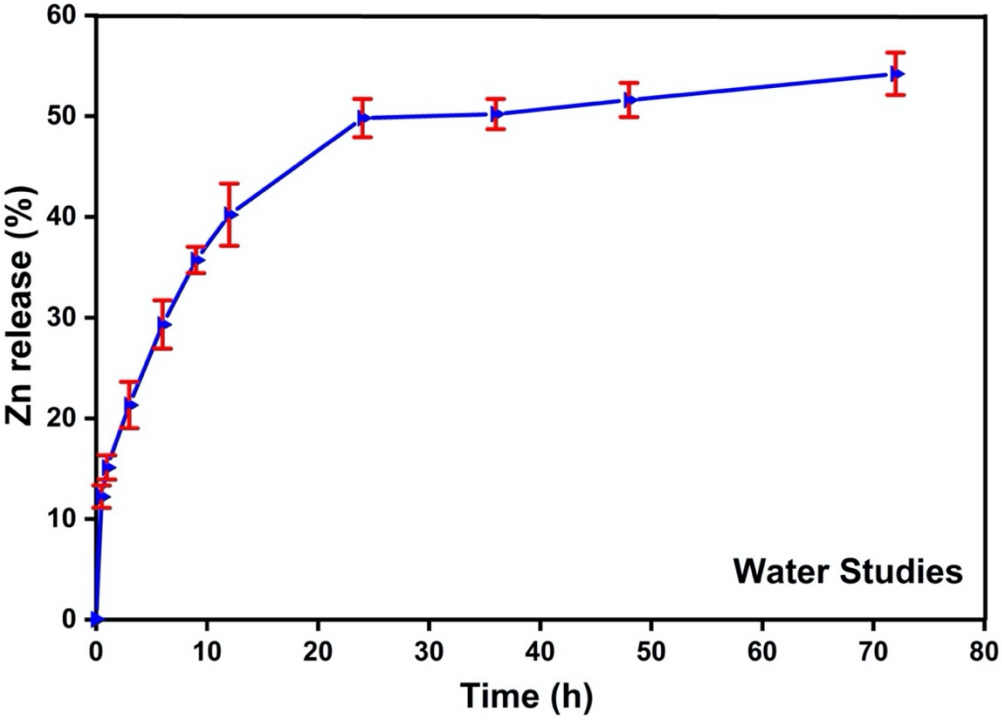

b)

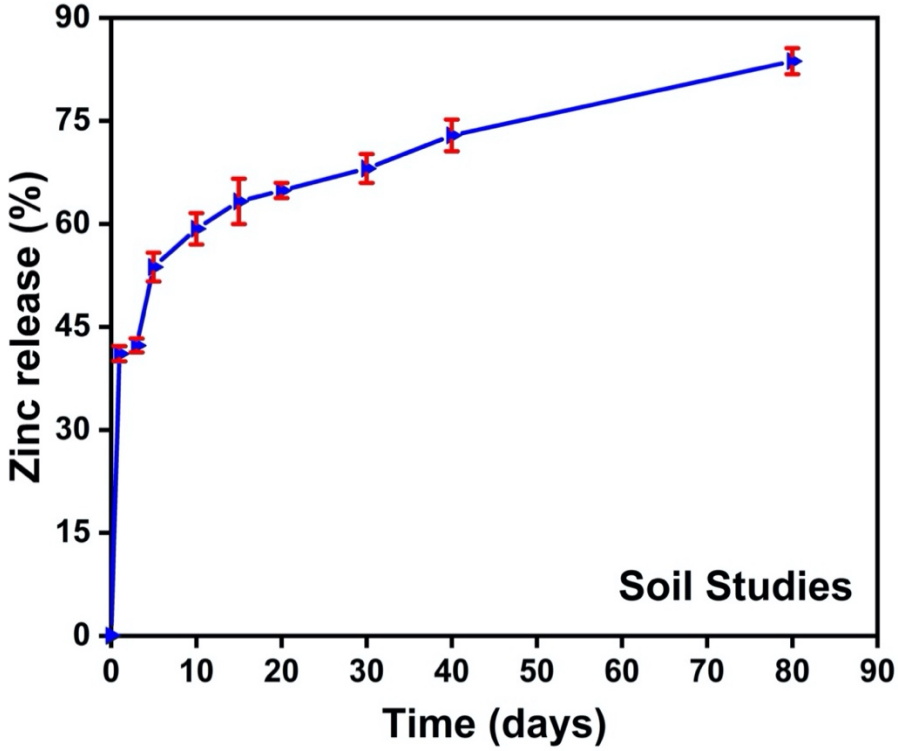

Figure 5.7 Cumulative release percentage of zinc with respect to time (a) in water (b) in soil

5.3.4.2 Release kinetics study of zinc in water and soil

Release data were examined as per the various kinetic equations to describe the kinetics of zinc micronutrient release from the ZSAH matrix. All the release data showed the coefficient of determination values (R^2) nearer to one for the Korsmeyer-Peppas model and hence ZSAH followed the Korsmeyer-Peppas model (Table 5.1).

Table 5.1 Mathematical Models used for the released kinetics from ZSAH

Model	**Mechanism Proposed in the Model**	**Equation**	**Water**		**Soil**		**Ref.**
			n	**R^2**	**n**	**R^2**	
Korsmeyer-Peppas	d. Fickian Diffusion (n<0.45) e. Non-Fickian Diffusion (0.89≥n≥0.45) f. Super case II (n>0.89)	$\frac{M_t}{M_\infty} = kt^n$ k=kinetic constant n=diffusion exponent	0.32	0.97	0.16	0.99	[22]
Higuchi	Fickian Diffusion	$\frac{M_t}{M_\infty} = k_H t^{\frac{1}{2}}$ k_H= kinetic constant	-	0.88	-	0.91	[23]

First Order	Rate is dependent on the concentration of one reactant only	$\log\left(1 - \frac{M_t}{M_0}\right) = k_1 \cdot \frac{t}{2 \cdot 303}$ K_1=release rate constant	-	0.89	-	0.81	[24]

As per the value of R^2 given in Table 1, the Korsmeyer-Peppas model was suggested to be the best fit model which statistically narrated the release kinetic behavior of zinc from ZSAH. Zinc release in the water had 0.32 as diffusion exponent value (n) and 0.97 as R^2, which clearly suggested Fickian diffusion that happens due to the simple diffusion method through the network of hydrogel (fig. 5.8(a)).

Interestingly, the release of zinc from ZSAH in soil showed its n value to be 0.16 and 0.99 as R^2 (fig. 5.8(b)). This clearly demonstrates that the release mechanism was solely Fickian diffusion, which implies that zinc micronutrient is considered to be diffused through the framework of the hydrogel network simply by diffusion processes [32].

The anticipated time (in days), according to the Olson equation [25] to release 50 %, 95 %, and 99 %, that is (T_{50}, T_{95}, and, T_{99}), of zinc from developed ZSAH, are recorded alongside with different parameters in Table 5.2. Zinc release in soil from ZSAH had a higher half-life (T_{50}), and T_{95}, T_{99} values, 86.63, and, 375, 625 days respectively than the release of zinc in water (1.69, 7.33, and, 12.22 days in a similar fashion). This distinction can be ascribed to the fact that the water is a

constraining component for the release in water, though in the soil, it can be attributed to the presence of moisture.

a)

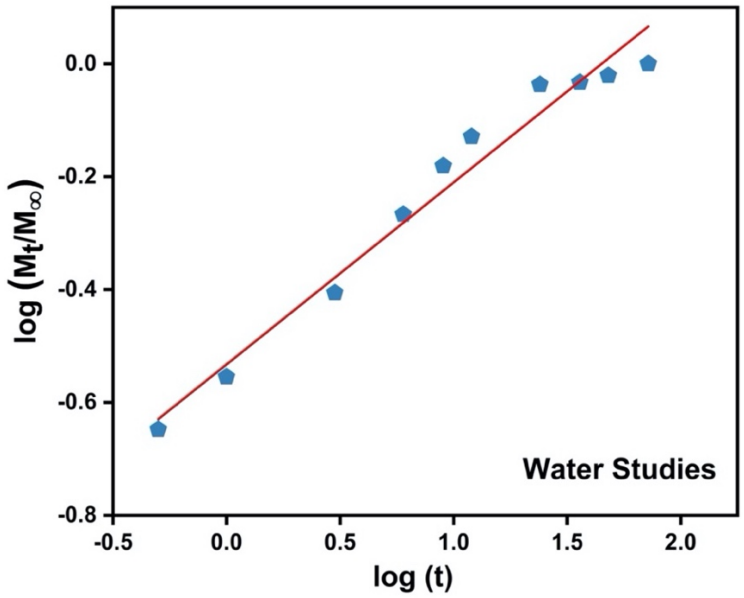

b)

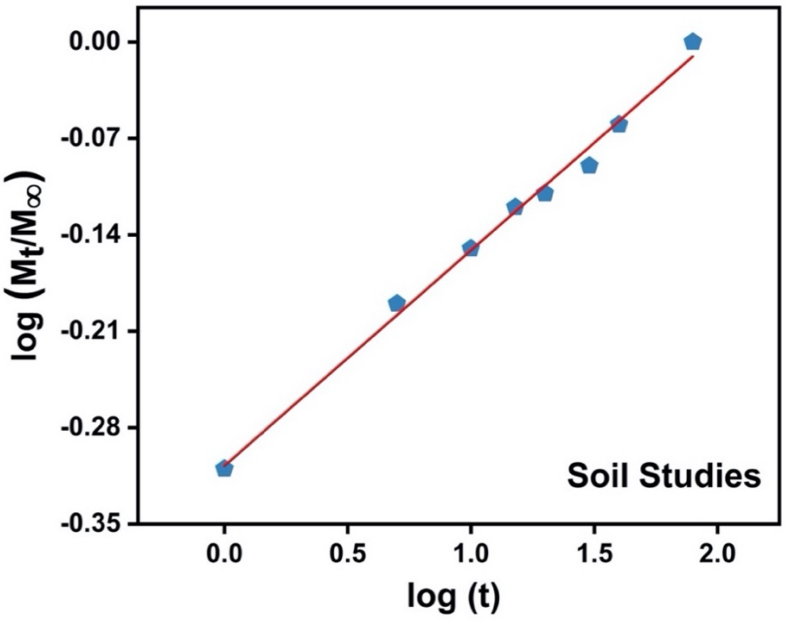

Figure 5.8 Release kinetics of Zinc by Korsmeyer-Peppas model (a) in water (b) in soil

Table 5.2 Relative time period (days) for the released quantity of zinc from ZSAH

Media	**Olson model equation**	**k**	**T_{50} (days)**	**T_{95} (days)**	**T_{99} (days)**
Water	$y = 22.391e^{0.401x}$	0.017	1.69	7.33	12.22
Soil	$y = 49.749e^{0.008x}$	0.008	86.63	375	625

5.4 Conclusions

Novel ZSAH was synthesized by using *the in-situ* technique, where zinc was doped into the CMTKG cross-linked network. The effect of various swelling media viz. distilled water, pH 4, 9, 12, and standard saline solution, on the water absorption capacity of ZSAH were studied. The highest swelling index was observed up to 410 g/g, in the case of distilled water. Release studies of zinc were tested in water and as well as in soil with respect to time. It is significant to note that in soil, ZSAH exhibited 59.28 % zinc release for the 10^{th} day which notably enhanced to 83.68 %

on the 80th day. Release kinetic studies were also analyzed in both water and soil in which the Korsmeyer-Peppas model fitted the best as its R^2 values were nearer to one. It also revealed that the release of zinc from ZSAH, in the soil as well as in water, was highly independent of the structure of the polymeric network as it followed the Fickian diffusion mechanism. The half-life (T_{50}), T_{95}, and, T_{99} values have been calculated by utilizing the Olson's single exponential model, which unmistakably demonstrated the zinc release in soil (86.63, 375, and, 625 days, respectively) had higher amount than the release of zinc in water (1.69, 7.33, and, 12.22 days in a similar manner).

These desirable characteristics of ZSAH make it a potent candidate in the field of agriculture not only as a water-conserving agent but most importantly as a zinc micronutrient vehicle.

5.5 References

1. Li, J.; Zhuang, X.; Font, O.; *et al.* Synthesis of merlinoite from Chinese coal fly ashes and its potential utilization as slow release K-fertilizer. *J. Hazard. Mater.* **265**:242–52; 2014. Doi: 10.1016/j.jhazmat.2013.11.063.
2. Bortolin, A.; Serafim, A.R.; Aouada, F.A.; *et al.* Macro- and Micronutrient Simultaneous Slow Release from Highly Swellable Nanocomposite Hydrogels. *J. Agric. Food Chem.* **64**(16):3133–40; 2016. Doi: 10.1021/acs.jafc.6b00190.
3. Azeem, B.; Kushaari, K.; Man, Z.B.; *et al.* Review on materials & methods to produce controlled release coated urea fertilizer. *J. Control. Release* **181**:11–21; 2014. Doi: 10.1016/j.jconrel.2014.02.020.
4. Thombare, N.; Mishra, S.; Siddiqui, M.Z.; *et al.* Design and development of guar gum

based novel, superabsorbent and moisture retaining hydrogels for agricultural applications. *Carbohydr. Polym.* **185**(January):169–78; 2018. Doi: 10.1016/j.carbpol.2018.01.018.

5. Sarkar, D.J.; Singh, A.; Mandal, P.; *et al.* Synthesis and Characterization of Poly (CMC-g-cl-PAam/Zeolite) Superabsorbent Composites for Controlled Delivery of Zinc Micronutrient: Swelling and Release Behavior. *Polym. - Plast. Technol. Eng.* **54**(4):357–67; 2015. Doi: 10.1080/03602559.2014.958773.
6. El-Hady, O.; And, S.A.-S.-I.J. of A.; 2006, U. Conditioning effect of composts and acrylamide hydrogels on a sandy calcareous soil. II-Physico-bio-chemical properties of the soil. *Int. J. Agric. Biol.* **8**(6):876–84; 2006.
7. Bhardwaj, A.K.; Warrington, D. Water Retention and Hydraulic Conductivity of Cross-Linked Polyacrylamides in Sandy Soils Climate change mitigation and adaptation strategies for salt affected soils View project להבנת השפעת המימשק האורגני על פוריות הקרקע .*Soil Sci. Soc. Am. J.* **71**(2):406–12; 2007. Doi: 10.2136/sssaj2006.0138. טווח ארוך מחקר
8. Johnson, M.S.; Leah, R.T. Effects of superabsorbent polyacrylamides on efficiency of water use by crop seedlings. *J. Sci. Food Agric.* **52**(3):431–4; 1990. Doi: 10.1002/jsfa.2740520316.
9. Johnson, M.S. Effect of soluble salts on water absorption by gel-forming soil conditioners. *J. Sci. Food Agric.* **35**(10):1063–6; 1984. Doi: 10.1002/jsfa.2740351004.
10. Kumar, R.; Parmar, B.; Kumar, A.; *et al.* Performance of a new superabsorbent polymer on seedling and post planting growth and Water use pattern of chrysanthemum grown under controlled environment. *Acta Hortic.* **742**:43–50; 2007. Doi: 10.17660/ActaHortic.2007.742.5.

11. Anupama, K.; Jat, M.; Management, B.P.-J. of W.; *et al.* Performance of a new superabsorbent polymer on crop and water productivity of summer mung bean (Phaseolus radiatus). *J. Water Manag.* **13**:1–5; 2005.

12. Rudzinski, W.E.; Dave, A.M.; Vaishnav, U.H.; *et al.* Hydrogels as controlled release devices in agriculture. *Des. Monomers Polym.* **5**(1):39–65; 2002. Doi: 10.1163/156855502760151580.

13. Bettini, R.; Catellani, P.; Santi, P.; *et al.* Translocation of drug particles in HPMC matrix gel layer: effect of drug solubility and influence on release rate. *J. Control. Release* **70**(3):383–91; 2001.

14. Shavit, U.; Shaviv, A.; Shalit, G.; *et al.* Release characteristics of a new controlled release fertilizer. *J. Control. Release* **43**:131–8; 1997.

15. Jamnongkan, T.; Kaewpirom, S. *Controlled-Release Fertilizer Based on Chitosan Hydrogel: Phosphorus Release Kinetics*. vol. 1. 2010.

16. Hafeez, B.; Khanif, Y.M.; Saleem, M. Role of Zinc in Plant Nutrition- A Review. *Am. J. Exp. Agric.* **3**(2):374–91; 2013.

17. Tisdale, S.L.; Nelson, W.L.; Beaton, J.D. Soil fertility and fertilizers. *Soil fertility and fertilizers.*; Collier Macmillan Publishers; 1985: 382–91.

18. Marschner, H. *Mineral nutrition of higher plants*. 1995.

19. Khushbu; Warkar, S.G. Potential applications and various aspects of polyfunctional macromolecule- carboxymethyl tamarind kernel gum. *Eur. Polym. J.* **140**(July):110042; 2020. Doi: 10.1016/j.eurpolymj.2020.110042.

20. Khushbu; Warkar, S.G.; Kumar, A. Synthesis and assessment of carboxymethyl tamarind kernel gum based novel superabsorbent hydrogels for agricultural applications. *Polymer*

(Guildf). **182**(September):121823; 2019. Doi: 10.1016/j.polymer.2019.121823.

21. Warkar S.G.; A.P., G. Synthesis, characterization and swelling properties of poly (Acrylamide-cl-carboxymethylguargum) hydrogels. *Int. J. Pharma Bio Sci.* **6**(1):516–29; 2015.

22. Korsmeyer, R.W.; Von Meerwall, E.; Peppas, N.A. Solute and penetrant diffusion in swellable polymers. II. Verification of theoretical models. *J. Polym. Sci. Part B Polym. Phys.* **24**(2):409–34; 1986. Doi: 10.1002/polb.1986.090240215.

23. Higuchi, T. Mechanism of sustained-action medication. Theoretical analysis of rate of release of solid drugs dispersed in solid matrices. *J. Pharm. Sci.* **52**(12):1145–9; 1963. Doi: 10.1002/jps.2600521210.

24. Serra, L.; Doménech, J.; Biomaterials, N.P.-; *et al.* Drug transport mechanisms and release kinetics from molecularly designed poly (acrylic acid-g-ethylene glycol) hydrogels. *Biomaterials* **27**:5440–51; 2006.

25. Olson, J.S. Energy Storage and the Balance of Producers and Decomposers in Ecological Systems. *Ecology* **44**(2):322–31; 1963. Doi: 10.2307/1932179.

26. Chang, C.; Duan, B.; Cai, J.; *et al.* Superabsorbent hydrogels based on cellulose for smart swelling and controllable delivery. *Eur. Polym. J.* **46**(1):92–100; 2010. Doi: 10.1016/j.eurpolymj.2009.04.033.

27. Zhao, Y.; Kang, J.; Tan, T. Salt-, pH- and temperature-responsive semi-interpenetrating polymer network hydrogel based on poly(aspartic acid) and poly(acrylic acid). *Polymer (Guildf).*; 2006. Doi: 10.1016/j.polymer.2006.08.056.

28. Trivedi, J.H. Synthesis, characterization, and swelling behavior of superabsorbent hydrogel from sodium salt of partially carboxymethylated tamarind kernel powder- g -

PAN. *J. Appl. Polym. Sci.* **129**(4):1992–2003; 2013. Doi: 10.1002/app.38910.

29. Reddy, B.V.; Rao, G.R. Vibrational spectra and modified valence force field for N,N'-methylenebisacrylamide. *Indian J. Pure Appl. Phys.* **46**(9):611–6; 2008.

30. Pal, S.; Sen, G.; Mishra, S.; *et al.* Carboxymethyl tamarind: Synthesis, characterization and its application as novel drug-delivery agent. *J. Appl. Polym. Sci.* **110**:392–400; 2008. Doi: 10.1002/app.28455.

31. Dias, R.J.; Havaldar, V.D.; Mali, K.K.; *et al.* sustained delivery of aceclofenac Interpenetrating networks of carboxymethyl tamarind gum and chitosan for sustained delivery of aceclofenac (October); 2017. Doi: 10.12991/mpj.2017.20.

32. Ritger, P.; Release, N.P. A simple equation for description of solute release I. Fickian and non-fickian release from non-swellable devices in the form of slabs, spheres, cylinders or discs. *J. Control. Release* **5**:23–6; 1987.

CHAPTER 6

CONCLUSIONS AND FUTURE SCOPE OF THE WORK DONE

6.1 Summary and conclusion

In this thesis, the novel superabsorbent hydrogels were fabricated by interpenetrating the natural polymer CMTKG and sodium-acrylate using MBA as a cross-linking agent and KPS as an initiator via free radical mechanism, have been reported. The synthesis was established by FTIR analysis, TGA examination, and SEM micrographs studies. The effect of various reaction parameters, with respect to the different concentrations of biopolymer, initiator and cross-linker agent, were investigated on swelling behavior of hydrogels. The influence of various solvents, such as standard saline solution, different pH solutions (4, 9, 12), and distilled water on the swelling index of SAH was examined. Out of all the mentioned solvents, the highest swelling percentage was noticed in the distilled water (64800%). This massive swelling index of synthesized CMTKG-PSA hydrogel makes it to be the super desirable candidate for agriculture sector as water conserving agent and soil conditioner.

The hydrogel formed was proved out to be bio-degradable using soil burial biodegradation test. The moisture absorption and retention improved notably by adding slight amount of 0.1 to 0.3 % (CMTKG-PSA) SAH into the soil. The maximum water holding capacity of soil was enhanced up to 35% and its porosity up to 7 % of its original. The effects of the hydrogel were also seen on the growth of chickpea plants where by mixing tiny amount of SAH, the moisture can easily be retained in the soil for as many as 41 days in comparison to just 18 days for untreated soil. The incorporation of the synthesized SAH in small dose in the soil showed notably higher moisture

percentage retention even at the matric tension of 15 bar. Thus these SAH have competent water retention capacity in soil. Hence, the synthesized (CMTKG-PSA) SAH has the potential to be used in agriculture sector as water conserving agent and soil conditioner.

Novel BSH was synthesized by doping boron into the SH by using *the in-situ* technique. The effect of different solutions like pH 4, 9, 12, distilled water, and standard saline solution, on the water capacity of BSH was studied. The highest swelling index was shown in the case of distilled water, up to 466 g/g. Release and kinetics studies of boron were observed in water and, as well as in soil and studied with respect to time. It is significant to note that in soil, BSH exhibited 21.07 % boron release for the 5^{th} day which notably enhanced to 76.17 % on the 80^{th} day. Release kinetic studies were also analyzed in both water and soil in which the Korsmeyer-Peppas model fitted the best (exhibiting Fickian diffusion mechanism) , in case of water, as its R^2 values were nearer to one. However, in the case of soil, the Higuchi model was found out to be the best fit. It also revealed that the release of boron from BSH, in water, was highly independent of the structure of the polymeric network as it followed the Fickian diffusion mechanism. The half-life (T_{50}), T_{95}, and, T_{99} values have also been determined using the Olson model, which clearly showed the boron release in soil (38.08, 164.84, and, 274.72 days, respectively) had higher values than the release of boron in water (1.29, 5.60, and, 9.33 days in the same order). These attractive qualities of BSH make it a powerful competitor in the field of horticulture as a water-rationing operator as well as above all as a boron micronutrient transporter.

Novel ZSAH was synthesized by using *the in-situ* technique, where zinc was doped into the SAH. The effect of various swelling media viz. distilled water, pH 4, 9, 12, and standard saline solution, on the water absorption capacity of ZSAH were studied. The highest swelling index was observed

up to 410 g/g, in the case of distilled water. Release studies of zinc were tested in water and as well as in soil with respect to time. It is significant to note that in soil, ZSAH exhibited 59.28 % zinc release for the 10^{th} day which notably enhanced to 83.68 % on the 80^{th} day. Release kinetic studies were also analyzed in both water and soil in which the Korsmeyer-Peppas model fitted the best as its R^2 values were nearer to one. It also revealed that the release of zinc from ZSAH, in the soil as well as in water, was highly independent of the structure of the polymeric network as it followed the Fickian diffusion mechanism. The half-life (T_{50}), T_{95}, and, T_{99} values have been calculated by utilizing the Olson's single exponential model, which unmistakably demonstrated the zinc release in soil (86.63, 375, and, 625 days, respectively) had higher amount than the release of zinc in water (1.69, 7.33, and, 12.22 days in a similar manner). These desirable characteristics of ZSAH make it a potent candidate in the field of agriculture not only as a water-conserving agent but most importantly as a zinc micronutrient vehicle.

Overall, the synthesized CMTKG based hydrogels can be a promising material as soil conditioners and matrix for nutrient delivery in agricultural applications.

6.2 Future Scope

The present research work indicates that the CMTKG and its cross-linked derivatives can be effectively used in agricultural applications. Fairly durable as well as degradable, transparent, and super absorbent CMTKG-PSA hydrogels can be further explored in high-value fields as pharmaceuticals, surgical gels, wound healing gels, eye lenses, baby diapers, sanitary pads, etc. Though in agricultural applications, it has shown potential under pot experiments, it needs to be evaluated on a larger scale, i.e. field level and actual benefit in the crop yield, etc. needs to be

evaluated. Further, in the agriculture sector, CMTKG hydrogels can be promising material as soil water-retaining additives and can also be used for the controlled release of pesticides, micro, and macro-nutrient fertilizers. The synthesis procedures can be scaled up or improved for commercial production of these materials, which needs dedicated research intuition into it.